8-2009

Reconfigurable RF Front End Components for Multi-Radio Platform Applications

Chunna Zhang
University of Tennessee - Knoxville

To the Graduate Council:

I am submitting herewith a dissertation written by Chunna Zhang entitled "Reconfigurable RF Front End Components for Multi-Radio Platform Applications." I have examined the final electronic copy of this dissertation for form and content and recommend that it be accepted in partial fulfillment of the requirements for the degree of Doctor of Philosophy, with a major in Electrical Engineering.

Aly E. Fathy, Major Professor

We have read this dissertation and recommend its acceptance:

Benjamin J. Blalock, Marshall O. Pace, Thomas T. Meek

Accepted for the Council:

Carolyn R. Hodges

Vice Provost and Dean of the Graduate School

(Original signatures are on file with official student records.)

To the Graduate Council:

I am submitting herewith a dissertation written by Chunna Zhang entitled "Reconfigurable RF Front End components for multi-radio platform applications." I have examined the final electronic copy of this dissertation for form and content and recommend that it be accepted in partial fulfillment of the requirements for the degree of Doctor of Philosophy, with a major in Electrical Engineering.

Aly E. Fathy, Major Professor

We have read this dissertation
and recommend its acceptance:

Benjamin J. Blalock

Marshall O. Pace

Thomas T. Meek

Accepted for the Council:

Carolyn R. Hodges

Vice Provost and Dean of the Graduate School

(Original signatures are on file with official student records)

Reconfigurable RF Front End Components for Multi-Radio Platform Applications

A Dissertation

Presented for the

Doctor of Philosophy

Degree

The University of Tennessee, Knoxville

Chunna Zhang

August 2009

Dedication

To my families: Weirui Zhang, Fengqin Liu, Chunlei Zhang and Suheng chen

Acknowledgments

I would like to thank my major advisor Dr. Aly E. Fathy for invaluable guidance during my Ph.D. education. Not only great suggestions, discussions about research work, but also all the great opportunities that he provided, including working on reconfigurable antenna work sponsored by Intel, working as an intern at RFMD, and joining many top level conferences in my field, such as IMS and AP.

I would like to thank my committee members: Dr. Benjamin J. Blalock, Dr. Marshall Pace, and Dr. Thomas T. Meek for their endless encouragement and helpful advice about my proposal and dissertation.

This dissertation includes two parts: The reconfigurable antennas research and design work was sponsored by Intel Corporation with three years grant. The reconfigurable power amplifier research and design work was sponsored by RF Micro Device with two internships, IC and module fabrication. I would like to thank these two companies sponsor and support to let me complete this work. Specially thanks to Fred Schindler, Steve Richard, Doug Teeter, Vijay K. Nair, Samir El-Ghazaly, Helen K. Pan, Scott Smith, Ming Ji, Charles Wang, Rob Knicaid, Robert Kloczkowski, Ken White, Ginny Lacquio and Wilfer Hernandez.

I would like to thank Dr. Syed Islam for his help and support of the reconfigurable power amplifier design on silicon process, which provided a good experience to finish the reconfigurable power amplifier design I finished in my dissertation now.

I would like to thank all my lab colleagues, especially Songnan Yang and Songwoo Lee, for their help and close cooperation in the past few years.

I would like to thank Shara Galloway for her great job on grammar checking of this work.

I would like to thank my parents: Weirui Zhang and Fengqin Liu, my sister Chunlei Zhang, my brother-in-law Suheng Chen and all my friends for their love, encouragement and support

Abstract

The multi-service requirements of the 3G and 4G communication systems, and their backward compatibility requirements, create challenges for the antenna and RF front-end designs with multi-band and wide-band techniques. These challenges include: multiple filters, which are lossy, bulky, and expensive, are needed in the system; device board size limitation and the associated isolation problems caused by the limited space and crowd circuits; and the insertion loss issues created by the single-pole-multi-through antenna switch.

As will be shown, reconfigurable antennas can perform portions of the filter functions, which can help solve the multiple filters problem. Additionally, reconfigurable RF circuits can decrease the circuit size and output ports, which can help solve board size limitation, and isolation and antenna switch insertion loss issues.

To validate the idea that reconfigurable antennas and reconfigurable RF circuits are a viable option for multi-service communication system, a reconfigurable patch antenna, a reconfigurable monopole antenna, and a reconfigurable power amplifier (PA) have been developed. All designs adapt state-of-the-art techniques.

For the reconfigurable antenna designs, an experiment demonstrating its advantages, such as jamming signal resistance, has been performed. Reconfigurable antennas provide a better out-of-operating-band noise performance than the multi-band antennas design, decreasing the need for filters in the system. A full investigation of reconfigurable antennas, including the single service reconfigurable antenna, the mixed signal service reconfigurable antenna, and the multi-band reconfigurable antenna, has been completed. The design challenges, which include switches investigation, switches integration, and service grouping techniques, have been discussed.

In the reconfigurable PA portion, a reconfigurable PA structure has first been demonstrated, and includes a reconfigurable output matching network (MN) and a reconfigurable die design. To validate the proposed reconfigurable PA structure, a reconfigurable PA for a 3G cell phone system has been designed with a multi-chip module technique. The reconfigurable PA structure can significantly decrease the real-estate, cost, and complexity of the PA design. Further, by decreasing the number of output ports, the number of poles for the antenna switch will be decreased as well, leading to an insertion loss decrease.

Table of Contents

List of Tables

List of Figures

Chapter 1 INTRODUCTION

1.1 Introduction

Customer demand is a major impetus for wireless communication developments. To date, three distinct generations of mobile cellular networks have existed. They started from an analog voice communication system (first generation) to a system (third generation) providing Email, web browsing, GPS, real-time financial information, social networking, and multimedia mail services. The handsets of the third generation (3G) are highly integrated systems. They provide multiple functions and services over a wide frequency range. The handsets contain state-of-the-art technologies to handle the strict requirements of the current third generation (3G) systems. They also need to provide a backward compatibility and seamless switching to lower generation services. Now, the handsets are being pushed even further to comply with the future fourth-generation (4G) systems under development.

On the other hand, the consumers typically do not care about the techniques of mobile phones. They desire services that can fulfill their needs. Consumers are also concerned with the size and price of the equipment. The complication of the multi-radio system and the continual persistent for smaller size phones has presented a challenge for wireless circuit designers.

In this chapter, we shall first examine drivers that propel us to look for new and groundbreaking solutions for a key system in these mobile devices—the RF front end. The RF front end, generally speaking, includes a receiver and a transmitter. The receiver includes a Low Noise Amplifier (LNA) and a down converter. The transmitter includes the power amplifier, an up converter. There also have some filters, duplexers, and RF switches in both the receiver and the transmitter.

1.2 Multi-standards of the wireless communication system shaping the front end design

The first-generation (1G) of wireless telephone technology utilized the analog telecommunications standards introduced in the 1980s and continued until being replaced by the second generation (2G) digital telecommunications. The primary difference between the 1G and 2G technologies is that the radio signals are analog signals in the 1G network, but are digital signals in the 2G networks. Commercial examples of the 2G system are the Global System for Mobile Communications (GSM), the North American version of the CDMA Standard (IS-95), and the Personal Digital cellular phone (PDC) [1, 2].

Table 1-1 Frequency bands from IMT-2000 [3]

Frequency Band (MHz)	Bandwidth (MHz)
806-960	154
1710-1885	175
1885-2025	140
2110-2200	90
2500-2690	190

The transition from the 2G to the 3G was a large technical jump. The major difference between the 2G and the 3G technologies can be found in the types of internet services provided. 3G systems support higher data rates and wider bandwidths standards which in turn provide Email, web browsing, GPS and real-time financial information services. Between the 2G and 3G systems, there is a two and half generation (2.5G) which uses a portion of the existing 2G infrastructures and can provide mobile internet service similar to a 3G. However, the 3G provides a wider bandwidth which can lead to additional new services.

To reduce implementation complexity and cost, the ideal case is a single global communication spectrum utilized in the 3G system. However, because different standards have been used in the 2 and 2.5G in various countries, and because there are multiple competing standards, it is hard to reach an agreement to use one standard across the entire world. Table 1-1 shows the frequency bands for a 3G from an International Mobile Telecommunications-2000 (IMT-2000). The bands are in two major spectrum ranges: 806MHz to 960MHz and 1.7GHz to 2.2GHz [3].

For 2.5G and 3G communication systems, two distinct domains exist. One is the wireless group and the other is the internet group, as shown in Figure 1.1. These two domains are connected by the network devices (gateways) which provide the protocol, control, and other necessary translation functions [1]. Because of the bandwidth difference between the two domains, and because the wireless group is connected to the internet via the gateway, the wireless device can not provide the full spectrum of internet services currently in the 2.5G and 3G.

By changing the architecture, the gateway issue can be avoided. In a fourth generation (4G) communication system, a higher system bandwidth is a desirable characteristic. At the ITU World

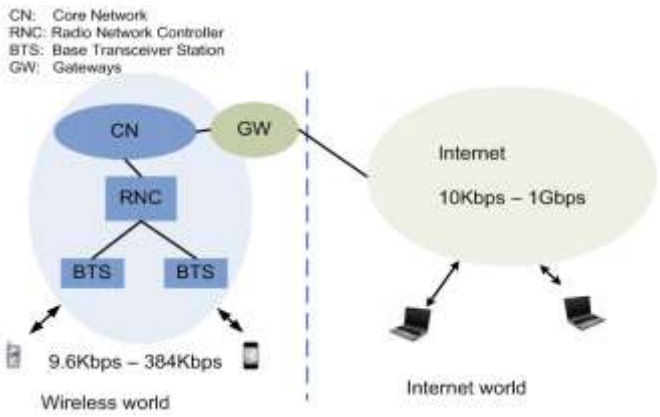

Figure 1.1 Two divided world [2]

Radio communication conference in 2007, additional radio spectrum was added for the 4G. These additional bands are located at 400MHz to 700MHz, 2.3GHz, 2.5GHz, and 3.5GHz. Detailed information is listed in Table 1-2 [3].

The multi-mode requirements of the 3G and 4G communication systems, and their backward compatibility requirements, create a challenge for the RF front end design, as previously mentioned. This means the RF front end has to handle multiple standards in one device. An example of this is the mobile phone application. In a 3G system, for example, a typical cell phone design needs to cover 7 services, which are shown in Table 1-3 [4]. For the 4G communication system, consumers expect a faster speed and a wider bandwidth. Additional services can be introduced into the system such as UWB, WiMax, etc. Another example of a 4G is the laptop application [5, 6]. More than 6 radios are expected to be in the laptop by 2009, as shown in Figure 1.2. Each of these modules may support more than one frequency band of the same services (as shown in Table 1-4) [5, 6].

1.3 Conclusion:

Future wireless receiver technologies tend to have strict requirements and need to provide a backward compatibility and seamless switching to lower generation services. The effort to develop highly complicated multi-radio systems and the continual persistent derives for size shrinking has become a challenge for wireless circuit designers. Meanwhile, because varying standards have been used in different countries, and because of the many competing standards, it is hard to reach an agreement to use one worldwide standard.

Table 1-2 Frequency Bands were added for 4G services from WRC-07 [3]

Frequency Band (MHz)	Bandwidth (MHz)
450-470	20
780-862 ITU Reg. 1	72
698-806 ITU Reg. 2	108
698-806 ITU Reg. 3	108
2300-2400	100
3400-3600	200

Table 1-3 some of the 3G cell phone system services [4]

System	GSM	EDGE	WCDMA
Common frequency bands	US Cellular UL:824-849MHz DL:869-894MHz	US Cellular UL:824-849MHz DL:869-894MHz	US Cellular(Band 5) UL:824-849MHz DL:869-894MHz
	EGSM UL:880-915 DL:925-960MHz	EGSM UL:880-915 DL:925-960MHz	
	DCS UL:1710-1785MHz DL:1805-1880 MHz	DCS UL:1710-1785MHz DL:1805-1880 MHz	
	PCS UL:1850-1910MHz DL:1930-1990MHz	PCS UL:1850-1910MHz DL:1930-1990MHz	PCS (Band 2) UL:1850-1910MHz DL:1930-1990MHz
			IMT2000 (Band 1) UL:1920-1980MHz DL:2110-2170 MHz
Ourput power	33dBm (Low Band) 30dBm (High Band)	33dBm (Low Band) 30dBm (High Band)	24dBm (class 3)

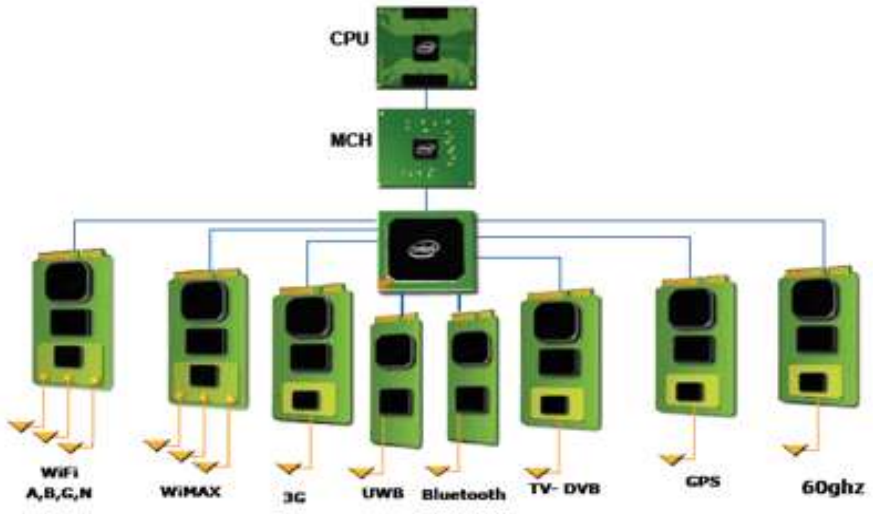

Figure 1.2 System diagram of a Multi-Radio laptop [5, 6]

Table 1-4 wireless services provided by the future laptop [6]

Wireless Services	Frequency Bands
WiFi	IEEE 802.11b/g/n : 2.4GHz~2.48GHz IEEE 802.11a/n : 5.15GHz~5.85GHz
WiMax	IEEE 802.16: 2.3-2.4GHz, 2.5-2.7GHz, 3.2-3.8GHz, 5.15-5.85GHz
3G	GSM 850 :0.824~0.894GHz, GSM 900 : 0.88~0.96GHz DCS 1800 : 1.71~1.88GHz, PCS 1900 : 1.85~1.99GHz UMTS : 1.92~2.17GHz
Bluetooth	IEEE 802.15.1 : 2.4GHz~2.48GHz
GPS	1.575GHz
UWB	3-10GHz

The need for multi-standards which stemmed from the various wireless generation developments and their backward compatibility requirements creates a challenge for the RF front end design. 4G and beyond systems, for example, would require a wider bandwidth and faster data rates than the 3G systems. This means the RF front ends have to handle multiple standards and multi-modes in one device. A summary of various RF Front-End developments will be highlighted in the next chapter.

Chapter 2 MULTI-SERVICE RF FRONT-END DESIGN TOPOLOGIES

2.1 Introduction

In Chapter 1, we discussed the challenges faced in the search for improvements in the increased complexity of the front end for 3G and beyond communication devices. We presented various activities towards adding services and functions in the next generation wireless system, which will open the door for a voice, multi-media, high-speed data transmission, and reception combined service. For example, 3G multimode handsets are typically capable of operating two to five UMTS bands, as well as backward-compatibility with 2G systems.

Primarily, the challenges of a wireless terminal design in a multi-service system include:

- Faster speed
- Wider bandwidth
- Additional services are required
- Multiple standards are covered
- Adequate isolation between the different blocks is necessary

In short, the demanding requirements for multiple services/standards in one system have impacted the wireless devices' design topologies.

In this chapter, different evolving topologies will first be discussed. Next, the diverse challenges involved in a multi-service RF front-end design, with traditional architectures, will be examined in section 2.3.

2.2 Variable developed topologies for multi-service wireless communication systems

The different blocks comprising the RF front-end and the techniques used to design the components in the RF front-end will be discussed in this section. The techniques are chosen based on the requirements of the system and the selected design topologies. Examples of several existing topologies for RF front-end designs will be introduced.

2.2.1 Different techniques for components in RF front end

Figure 2.1 [7] is an example of a RF front-end. Typically, the receiver includes an LNA, a down converter, and part of the transceiver—up-converter. These components are designed using either BiCMOS (a process where bipolar junction transistors and CMOS are integrated into a single device), or SI bipolar processes on the same die. The up and down converters have similar

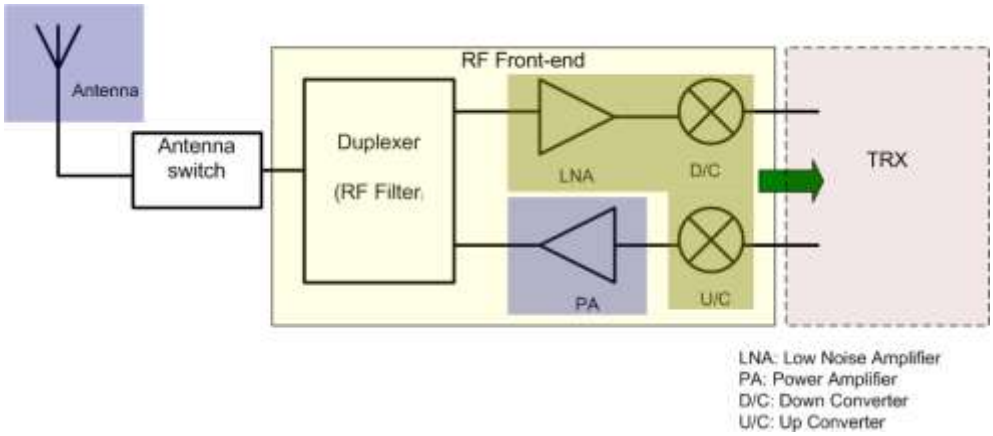

Figure 2.1 A RF transceiver configuration example [7]

structures. The primary difference is they operate at either an up-link or down-link frequency band. The up and down converters include VCOs, mixers, and various automatic gain control (AGC) amplifiers. The transmitter is comprised of the up-converter and the power amplifier, but the power amplifier is difficult to integrate onto the silicon substrate. Therefore, most PA designs for cell phones are built on Gallium Arsenide (GaAs) process because of its high-current density capabilities and acceptable linearity performance at high frequencies.

A detailed illustration of the RF front-end components is shown in Figure 2.2 [8]. A list of commonly used technologies for RF front end components is provided in Table 2-1.

Meanwhile, an antenna is conveniently not considered part of the front-end design to simplify the design steps and phases. The antenna is typically considered a separate component by the system engineer. However, as will be shown in the following chapters, by analyzing the antenna design and the RF front-end design together, the antenna can achieve a portion of the filter function as well. This will assist in decreasing the number of the filters necessitated, as well as relaxing the stringent requirements for the filters in the system.

2.2.2 RF front end design topologies in the 2G, 2.5G and 3G communication systems [2-6]

With the development of wireless communication systems, the RF front-end design topologies have significantly changed, based on expansions in their functionary requirements. Three major topologies will be introduced, specifically, the discrete RF front end topology, the hybrid design, and the mixed hybrid-and-discrete design.

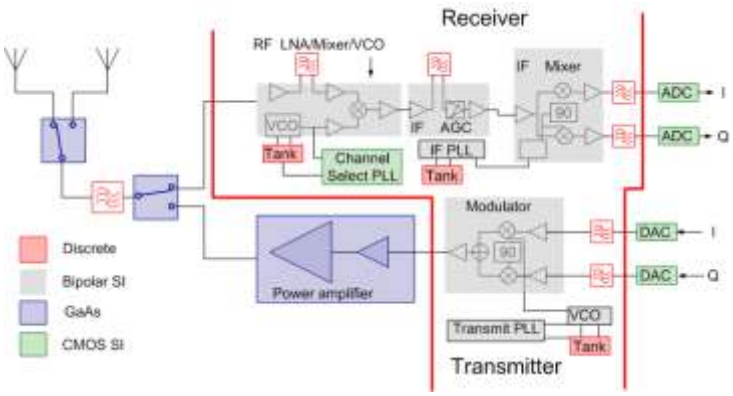

Figure 2.2 A RF transceiver block diagram example [8]

Table 2-1 A list of commonly used technologies for RF front-end components

Si Bipolar	IF amplifiers, AGC, Mixer, LNA, VCO, RF gain blocks, I/Q modulators, transmit PLL
GaAs	RF switches, PAs
Discrete	All tank circuits and RF filters
CMOS SI	ADCs, DACs, Channel Select PLL

2.2.2.1 The Discrete RF front end design topology

It is estimated that among the different 2G standards, over 80% of the global mobile market uses a global system for mobile communications (GSM) [2]. Additionally, most 2G GSM networks operate in the 900 MHz or 1800 MHz bands. For such systems, which have only one or two frequency bands, each RF front-end design can be tailored for predefined, specific requirements. Such tailored designs can provide flexibility to pursue the performance metrics, such as output power, linearity, and DC power consumptions, in different cell phone models.

To improve the data rate of GSM systems, a new standard is necessary. It is directed to Enhanced Data rates for GSM Evolution (EDGE) standards. The new standard is supported by GSM carriers, which is considered a 2.5G wireless communication system. Due to the backwards compatibility requirements, the RF front-end needs to support two extra frequency bands, allocated at 800MHz and 1.7GHz. These quad-band cellular handsets are still widely used.

The disadvantages of the discrete RF front-end design topology become apparent with the increasing number of frequency bands that are frequently added. The disadvantages include a bigger real-estate area needed on the Printed Circuit Board (PCB) and the associated cost of the

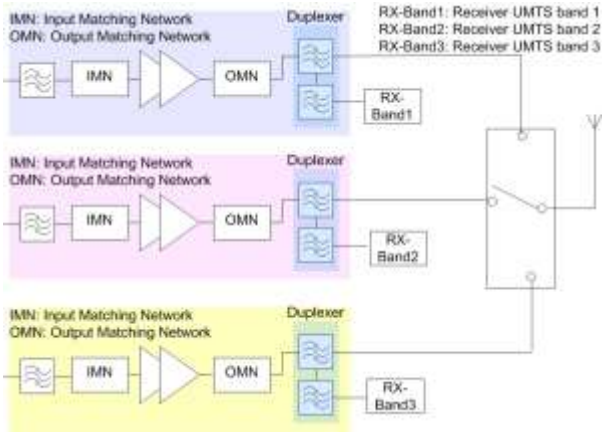

Figure 2.3 An example of a discrete RF front-end schematic [3]

needed components. These disadvantages have become drastically unaffordable in a 3G and beyond wireless communication devices for implementation purposes. Figure 2.3 [3] shows a discrete RF front-end design which supports three UMTS bands. As can be seen, three times the area and components are needed in the system.

2.2.2.2 The hybrid and mixed RF front end design topology

For a model that encompasses design complexity, cost, and area targets, the hybrid RF front-end design topology, or the mixed hybrid and discrete RF front-end design topology, is currently used to design the devices for the 2.5G and 3G wireless communication systems.

The concept diagram for a hybrid RF front-end design topology is shown in Figure 2.4 [3]. The area and cost are decreased by integrating multiple dies into one package. However, this topology still requires a discrete signal path for different modes and frequency bands. Multiple duplexers and a single pole multi-throw 'SPMT' antenna switch are still necessary, as well.

An example of a mixed technology implementation is the commercial quad-band PAs for a 3G wireless communication system. Hybrid topology is used for the quad-band 2.5G application design and discrete topology is used for the UMTS band design. Note the use of a duplexer for the UMTS band, according to its specifications. In such a design, a single pole, nine-through switch is needed, as shown in Figure 2.5.

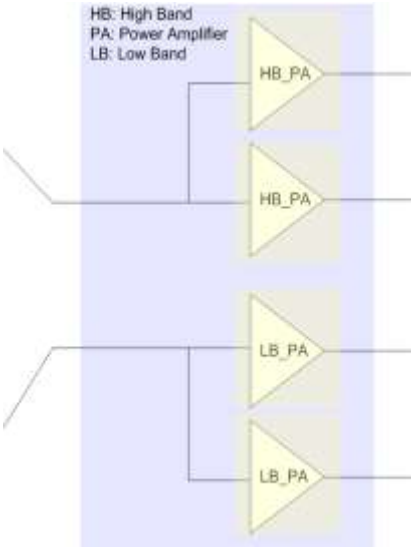

Figure 2.4 An example of a hybrid RF front-end schematic [3]

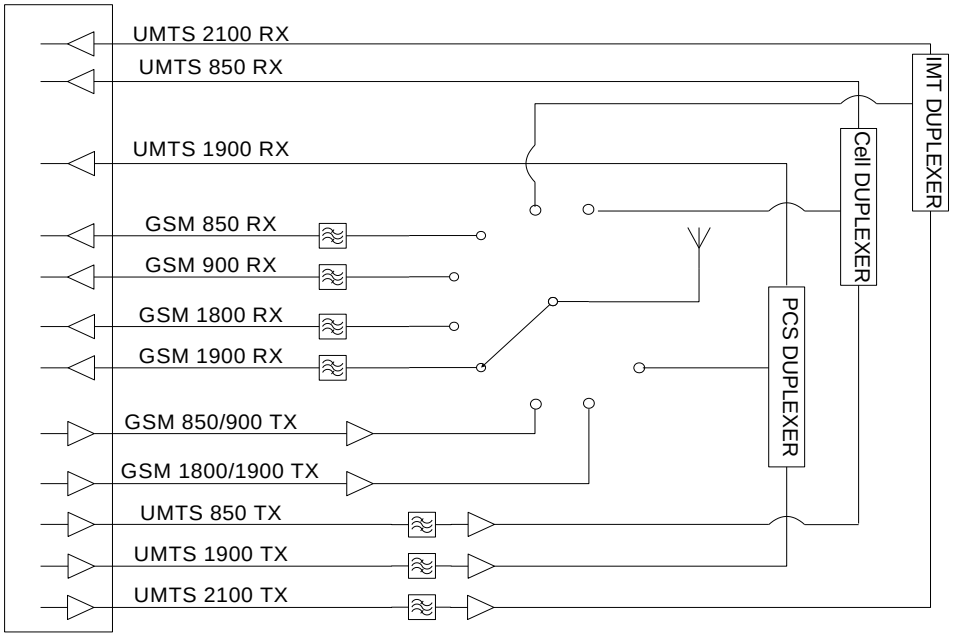

Figure 2.5 a 3G cell phone system example [4]

2.3 Wireless terminal design challenges in a multi-service system

As previously mentioned in section 2.2, mobile devices are evolving into "All-In-One" devices. Unquestionably, using individual designs to implement all the services is not a feasible option due to the devices' size and cost constraints. Additionally, because of the coupling, the isolation performance of the single designs in a multi-service system is difficult to actualize. One example that can be used to convey these problems is a multi-service application in a laptop environment [5, 6]. It is expected that more than six radio channels will be required to work simultaneously in the future platforms to perform all necessary multi-functions. To quantify this isolation problem, several state-of-the art laptop computers with 6 radios have been measured. The average isolation between the radios is listed in Table 2-2 [6]. Four distinct colors represent the antenna isolation requirements, ranging from a low < 25dB to a high > 55dB.

At the same time, the measurement isolation performance between the two services is assessed. The assessments are listed in Table 2-2. For example, the measured isolation between the WiFi and Wimax (Worldwide Inter-operability for Microwave Access) is only 17.3 dB, but the requirement is over 55dB, as indicated in red. The isolation between 3G and WiMax is 22.5dB which is on the border line of the required isolation of 25dB. It also can be noted from Table 2-2 that for more than half of the cases, the antennas' isolation is below the requirement, thus the corresponding radio performance will be severely impaired. The primary cause is their close spacing and proximity. The problem would be exasperated if further services are added.

Table 2-2 Antenna isolation requirements for radios simultaneously operating [5, 6]

Antenna Isolation (dB)	WiMax	WiFi	3G	GPS	BlueTooth (BT)	UWB
WiMax	19.0	17.3	22.5	25.9	18.2	25.9
WiFi	20.7	16.7	25.3	29.4	19.8	21.6
3G	27.6	26.0	27.7	29.1	28.1	23.1
Bluetooth-BT	17.6	19.7	27.2	29.6		
UWB	17.6	19.7	27.2	29.6		

>55dB	40dB-55dB	25dB-40dB	<25dB

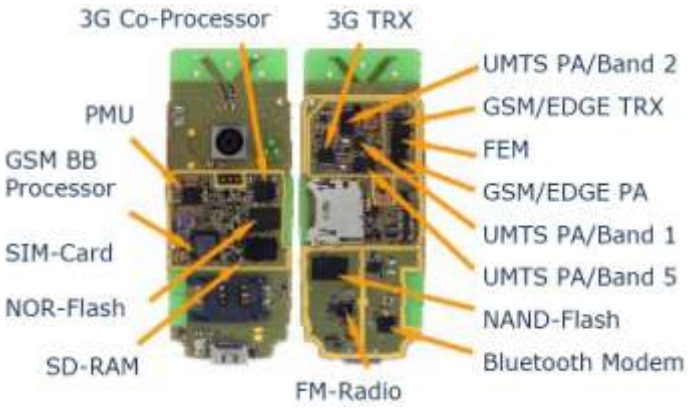

Figure 2.6 Future mobile phone content limited by board space [9]

RF front-end designs yield the same problem. Figure 2.6 [9] depicts the circuits in a 3G cell phone system that are closely packed. The 3G cell phone, which is shown in Figure 2.6, supports seven services. The side-by-side single service designs degrade the multi-service system isolation performance. To resolve this problem, multiple high Q filters are introduced into the system, typically Surface Acoustic Wave (SAW) or Bulk Acoustic Wave (BAW) filters. These filters are typically lossy, bulky, and expensive.

Meanwhile, to switch the function among all the single service designs, a single pole multi-through switch needs to be utilized before the antenna. The more services in the system, the more poles the switch should have. For example, a single-pole nine-through switch is needed in a 3G cell phone system, as has been shown in Figure 2.5. Unfortunately, with the increasing number of the switch's poles, insertion loss will increase and its isolation will decrease. Due to these design challenges, a converged RF front-end topology is the developing trend for the 3G and beyond wireless communication devices.

2.4 The converged RF front end design topology

Ideally, a RF front-end design for a multi-frequency and multi-mode wireless communication system requires the same or comparable area and components as needed for a 2G wireless communication system. The concept diagram of the converged RF front-end design topology is shown in Figure 2.7 [3]. By reducing the number of amplifiers, redundant packaging, die, inductors, and capacitors in the matching network, duplexers, and poles of the antenna switches, the design targets of less area and a lower cost can be attained.

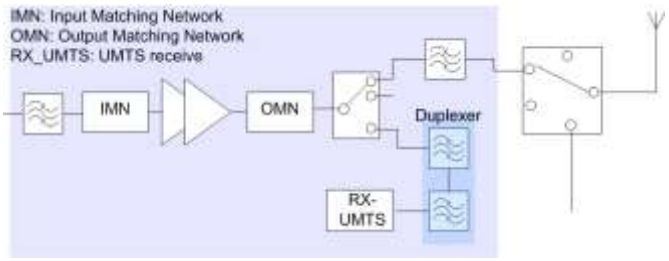

Figure 2.7 An example of a converged RF front-end schematic [3]

In practice, however, challenges and technology limitations exist to producing such a design, and will be addressed in the following chapters.

2.5 Conclusions

There are different RF front end topologies with their design based on the targeted application. For example, the discrete RF front-end topology is well-suited for single Band UMTS applications. However, the discrete RF front-end topology is obviously not the optimal choice for 3G multi-frequency and multi-mode devices. The hybrid RF front-end topology integrates multiple dies to cover the different bands and could be enhanced further by using discrete components (i.e. mixed hybrid). The mixed hybrid is a result of the transition from a discrete RF front-end topology to the converged RF front-end topology. This is the emerging trend for 3G and beyond wireless communication device designs.

Chapter 3 CIRCUITS AND ANTENNAS RECONFIGURABILITY TOWARDS CONVERGED RF FRONT END

3.1 Introduction

Different standards have been developed in the past few decades for the various communication services in use today. Many of these services, discussed in Chapter 1, will coexist in the 3G and beyond communication systems, presenting a challenge for hardwire realization. Multiple reasons have caused the coexistence of many standards within one system, including, but not limited to:

- Varying standards have been developed in different countries during the process of developing their own wireless communication systems.
- New standards developed from old versions also vary.
- Different standards are developed to support the diverse interests of the end user.
- The majority of standards are not compatible.
- Standards are adapted to varying frequency bands.
- Political constraints in different countries did not assist in the alignment of standards.

As a result, the unification of standards for needed services in future communication systems is not an easily attainable target. This is a challenge engineers will have to face in the upcoming years. Due to the aforementioned reasons, the trend to develop a converged RF front-end topology, discussed in chapter 2, has led to the conclusion that reconfigurable circuits and antennas are a viable topology.

In this chapter, the advantages of the reconfigurable RF front-end will be discussed in section 3.2. With full utilization, the RF front-end's advantages can effectively solve the many problems of multi-service systems. Research efforts are currently underway on both reconfigurable antennas and RF front-ends with the ultimate goal of realizing a fully reconfigurable RF front-end. This could mean one signal chain with reconfigurable components, such as reconfigurable LNAs, VCOs, and PAs. However, multiple design challenges still need to be addressed and resolved.

A complete reconfigurable topology implementation has not yet been realized, but many partial reconfigurable RF front-end topologies that can alleviate the difficulties involved in a multi-service system design have been investigated and will be introduced in section 3.3.

Preliminary results regarding RF front-end reconfigurable component designs are encouraging. In this chapter, several reconfigurable designs, specifically LNAs, mixers, and VCOs, will be also discussed in detail in section 3.3, followed by a summary of the beginning reconfigurable LNA and VCO designs developed in our group. These examples assist in understanding the process leading to reconfigurable PA and antenna designs that are the focus of our investigation in the following chapters.

3.2 Advantages of the reconfigurable circuits and antennas in a multi-service wireless communication system

The existence of multiple standards has disadvantages, including:

1) Manufactures invest a large amount of funds and efforts to optimize devices and systems to address the different services and standards.
2) The need to buy expensive equipment for base stations and receivers. The base stations have become increasingly complex, and are expensive to maintain with consistently required upgrades.
3) Users still do not receive a high quality of service and have to pay additional costs for specific services or access to services in different countries.
4) Overall cost has become high with exceedingly large development costs.

Several existing systems in the market support frequency bands operating with similar standards that use basic re-configurability to address the aforementioned disadvantages. However, this basic re-configurability includes similar procedures and channel coding for the frequency bands that have similar standards and depends on switching the different blocks. Our goal is to extend this concept to combine multiple standards into a single hybrid system. The proposed system would integrate the different standards, and its implementation would require a complete system optimization rather than switching the various blocks. The goal of this effort is:

1) Better performance.
2) Lower development and manufacturing costs.
3) Lower power consumption.
4) Size and weight reduction.

Achieving these aggressive goals will require extensive system analysis and optimization rather than a block-by-block, single-function optimization. Currently, researchers are investigating technical ways to solve these challenging and contradictory requirements. These challenging and contradictory requirements include:

1) Filters with stringent requirements are needed, which increase the cost and insertion loss of the system.
2) The increase in the insertion loss of the filters has led to higher demand and restrictions on the PA and LNA performance.
3) Redundant components, such as LNAs, PAs and VCOs, exist in one system which increase the device size and cost, but at the same time, decrease the inter-space between components. The decrease in overall size has caused significant isolation and performance degradation.
4) Strong coupling and poor isolation between the various components would require the use of additional filters in the system.

In the following sections, the impact of using reconfigurable antennas and RF front-ends on overall performance will be demonstrated.

3.2.1 Reconfigurable antennas' out of band noise rejection performance

Reconfigurable antennas, when compared to multi-band or wide-band antennas, have a better out-of-band noise rejection performance, which can help perform a portion of the filter's function in a multi-service system. Thus, the filter's stringent requirements are reduced in a multi-band system.

To demonstrate the advantages, such as jamming signal resistance, of reconfigurable antennas, a commercial GPS receiver was exposed to an external jamming signal, as shown in Figure 3.1.

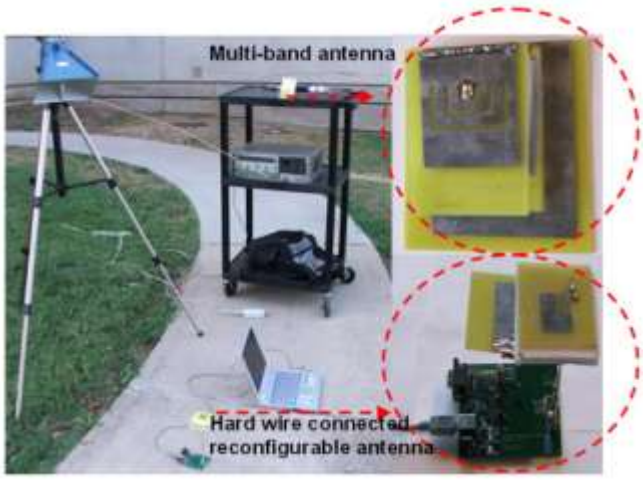

Figure 3.1 Noise rejection performance test bench setup

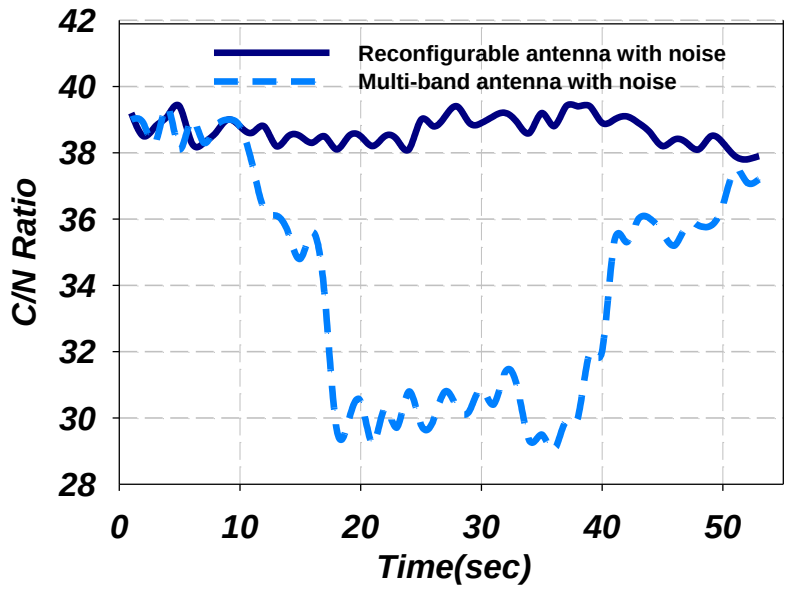

Figure 3.2 Carrier noise ratio

In the first trial, the receiver was connected to a multi-band antenna. In the second trial, the receiver was connected to a previously developed, hard-wire connected reconfigurable antenna. The multi-band antenna utilized operates on both the Global Positioning System (GPS) and the WLAN-2.4GHz bands, while the reconfigurable antenna is controlled to operate on the GPS band only and not to support WLAN service. Both antennas have identical gain and similar carrier-to-noise ratios (C/N) across the GPS band. The jamming signal was centered at approximately 2.4 GHz and has a 20 dBm power level. It was directed to the GPS receiver system to emulate a transmitted signal from a WLAN access point. No pronounced degradation was noticed while using the reconfigurable antenna, but an over 8 dB C/N ratio drop was measured when using the multi-band antenna, as shown in Figure 3.2, although a SAW filter is on the receiver board. This is not a typical case as a 20dBm WLAN signal interrupts a GPS receiver, but it was employed here to prove the point that a multi-band antenna has an unsatisfactory out-of-band-noise rejection when compared to a reconfigurable antenna. Thus, multi-band antennas require additional expensive and lossy filters in order to negate the out-of-band noise. Conversely, reconfigurable antennas have inherently satisfactory band-pass characteristics and commendable out-of-band rejection, eliminating the need for additional expensive filters. It is essential for a comparison of these two antenna alternatives to include the price of any required filters.

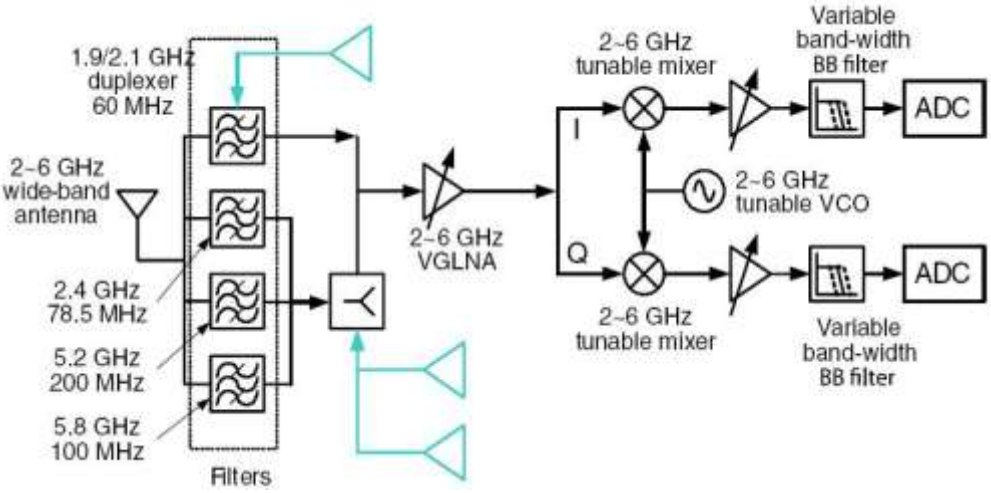

Figure 3.3 Reconfigurable receivers for four-band applications [10]

3.2.2 Redundant component reduction in a multi-service system with reconfigurable components design

An additional forward-thinking method to apply the reconfigurable component's concept is to eliminate redundant components, thus overcoming the device size and cost limitations. This concept has previously been implemented. For example, in [10], the authors investigated a reconfigurable receiver for the WCDMA, 802.11a, 802.11 b(g) and Wibro standards. The researchers utilized a reconfigurable LNA and mixers, as shown in Figure 3.3. The entire receiver has only one I/Q signal chain, dramatically decreasing the receiver size and eliminating redundant components.

For the successful implementation of a multi-standard receiver, a reconfigurable receiver architecture and component design technique is essential. In [10], the adaptable receiver architecture and reconfigurable RF design technique, using a switchable passive network, were proposed. A reconfigurable mixer and VCO were designed utilizing a flexible matching network and flexible LC tank, respectively. The measured results of each component have proven the usefulness of the switchable passive network [10].

3.3 The design evolution leading to a full reconfigurable RF front end

The use of only one signal chain in the RF front-end for all non-simultaneous operating services that the device supports is ideal. However, this creates multiple design challenges that need to be resolved in the design of each component. Examples of the design complexities will be

discussed in detail during the process of designing the reconfigurable antennas and PAs in Chapter 4 and Chapter 5. As researchers are still solving the design problems, many preliminary reconfigurable RF front-end structures have been investigated to negate the system's stringent requirements. Generally, the reconfigurable RF front-ends are strongly dependent on the RF front-end architecture. In the following sections, background information about the RF front-end architectures will be introduced, followed by the presentation of several of the existing reconfigurable RF front-ends for multi-service wireless communication system that have been recently developed.

3.3.1 Transceiver architectures

A transceiver includes a receiver and a transmitter. The receiver acquires the signal from the communication channel and demodulates the signal to the base-band. The transmitter modulates the base-band signal to the carrier frequency and transmits the signal to the communication channel. The base band blocks are primarily digital circuits and the RF front-end blocks are analog circuits. Although current efforts are directed towards digital blocks recognizing RF front-ends, the process is still in the infancy stage.

Generally, on the receiver side, the signal, which is received by the antenna, will pass the LNA first. The amplified signal is then demodulated to the base-band and converted to digital format by the Analog-to-Digital converter (ADC). This basic process, however, does not necessarily have to be performed in this manner. Three receiver architectures exist. They are the heterodyne (IF receiver), homodyne (zero-IF receiver), and combined (low IF receiver). A comparison of the three architectures is given in Table 3-1 [11].

On the transmitter side, the digital signal from the baseband is converted to an analog signal by the Digital-to-Analog converter (DAC). The analog signal is then modulated by the carrier frequency and amplified by the PA. Next, the signal is transmitted to the communication channel by an antenna. Typically, there are two transmitter architectures used for the transmission. They are the heterodyne-up converter, and the direct-up converter. A comparison between the two architectures is provided in Table 3-2 [11].

Table 3-1 A comparison among the three receiver architectures

Receiver	Advantages	Disadvantages
Heterodyne (IF receiver)	Classic design. Relatively simple design. Have higher sensitivity. Better selectivity and inter-modulation behavior.	Requires an image reject filter (IRF) with stringent specifications. IRF is placed off chip, with bad integration. Multiple filters and oscillators
Homodyne (zero-IF receiver)	No IF Processing. Easier integration. Less number of filters. Lower cost and board size. Lowest requirements for ADC.	Sensitive to matching, and to phase and amplitude error in the quadrate oscillator. Parasitic base band signal created by crosstalk of mixer RF and LO input.
Combined (low IF receiver)	Less components compared to IF receiver. Less crosstalk issues compared to zero-IF receiver.	More components compared to zero-IF receiver.

Table 3-2 A comparison between the two transmitter architectures

Transmitter	Advantages	Disadvantages
Heterodyne up converter	Classic design, widely used. Only a high frequency filter is needed.	Single stage heterodyne-up converter is hard to realize. Low integrability with a multi-stage heterodyne design.
Direct up converter	Better integration, no image rejection problem.	Crosstalk between LO and RF of the mixer degrade the system performance. Local oscillator may have self modulation problem.

3.3.2 Methods for reconfigurable RF front end topology

Three distinct methods can be utilized for re-configurability. The first method is to develop various chains of transmitters and receivers, and connect them in parallel. Each chain is designed in accordance with a given set of standards and tailored for a specific service. They are activated one chain at a time using a multi-pole, single-throw switching scheme between the chains and antenna. The second approach is similar to the first, except that only a minimal number of common blocks are shared, given that all blocks fulfill the requirements of the varying standards. Meanwhile, the third approach is to develop fully reconfigurable blocks. Each block can be reconfigured to provide more than one function and standard.

Ref. [12] has reported a fully integrated, zero IF transceiver for GSM/DCS/PCS applications, and is an example of the first re-configurability approach . The schematic diagram of this design is shown in Figure 3.4. The integrated components in the design are indicated by the blue squares. As can be seen, there are three sets of LNAs and up/down converters in the system and each can selected via a switch. However, in the transmitter section, the PAs are not included in the design.

In the second approach, the majority of components in the different signal chains have similar, or the same requirements, for various standards. Therefore, one component can be designed to support multiple standards.

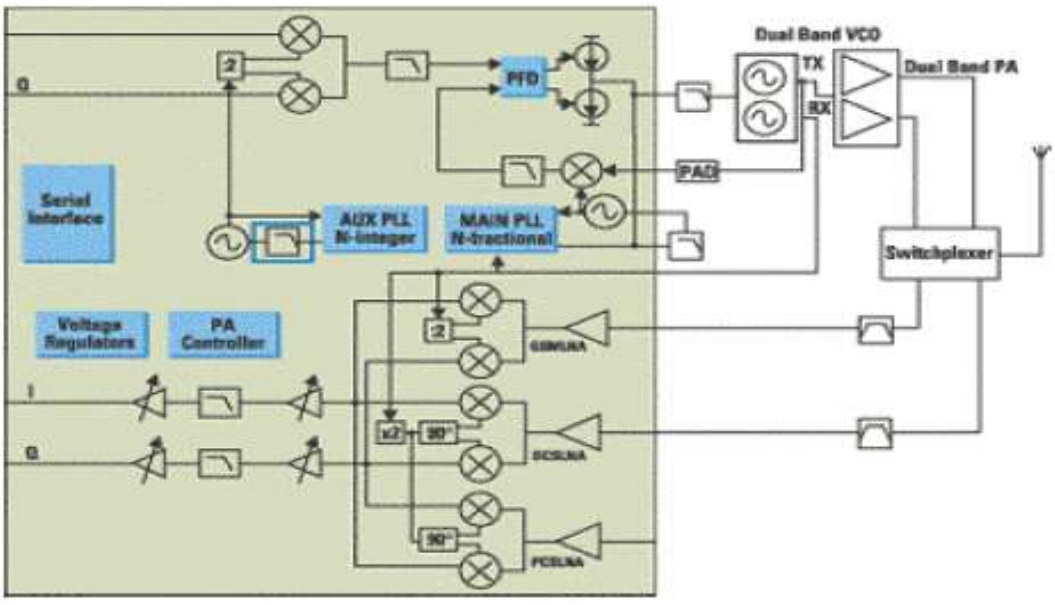

Figure 3.4 A Fully integrated zero IF transceiver for GSM/DCS/PCS applications [12]

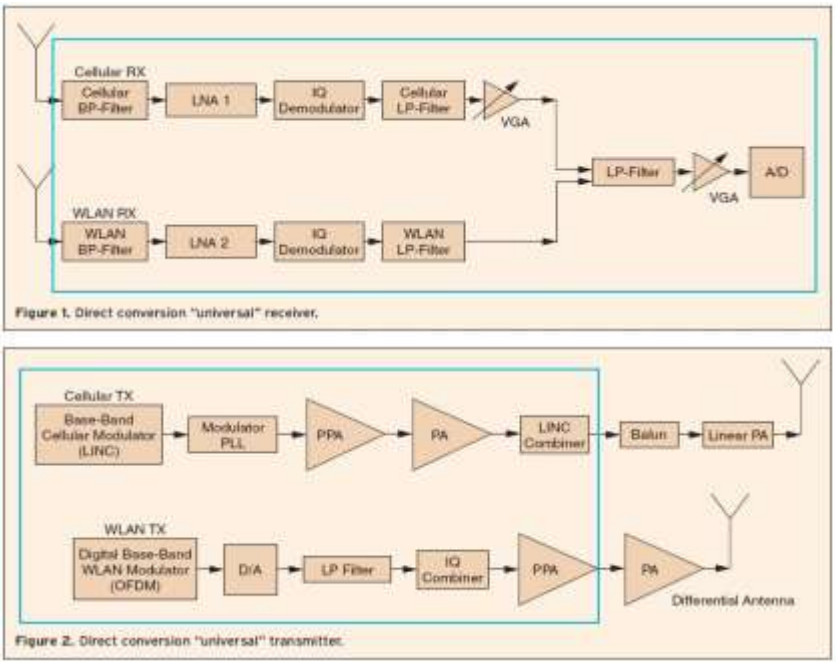

Figure 3.5 Two signal chains for cell phone and WLAN simultaneous operating system [13]

For the third approach, fully reconfigurable components are developed. The components can be used for multiple standards that are similar, or completely different. The number of signal chains is decided by the number of required, simultaneous operating services. For example, if only one service is needed, only one signal chain is required, but if two services are operating in tandem, two signal chains are required. In each of the two chains, several services that are not in operation at that time can be supported. In [13], two signal chains, each with reconfigurable components, were designed. One is supports services for cell phones, such as GSM, DCS and PCS. The other chain supports services for laptops, such as WLAN and Bluetooth, as shown in Figure 3.5. A comparison of the three reconfigurable approaches is provided in Table 3-3.

3.3.3 Reconfigurable components toward a full reconfigurable RF front end

To realize a converged RF front-end structure, reconfigurable components for the RF front end design must be investigated and developed. Various examples of reconfigurable components will be discussed in this section. Since LNAs and up-and-down converters are typically designed on SI process and PAs are designed on GaAs process, they are discussed separately.

Table 3-3 A comparison between the three reconfigurable approaches

Approach	Advantages	Disadvantages
Switching between different signal chains	Simple designs, each standard has its own chain. Minimum power consumption.	Multiple modules are required. High cost. No simultaneous use of these services.
Common blocks reuse	Minimizes number of components. Saves real-estate area. Common blocks should be independent of modulation or standards.	Increased design complexity of the common blocks. Higher cost.
Full reconfigurable RF front-end design with reconfigurable components	Blocks change their functionality according to each standard specification. Reconfigured blocks fulfill all standards. Real-estate reduction. Better integration density.	Complicated designs. Difficult to realize. High power consumption.

3.3.3.1 Reconfigurable LNA designs

A reconfigurable LNA designed for a WLAN 2.4GHz, 5.2GHz, and 5.8GHz was reported in [14]. The LNA has one common output port and two different input ports. One port is for 2.4GHz and the other is for 5.2GHz to 5.8GHz, respectively, as shown in Figure 3.6.

Instead of multiple inputs and one common output, reference [15] reported reconfigurable LNAs with only one common input and one common output for multi-standard applications. According to the authors, this design can be realized by varying the shunt-to-shunt feedback capacitance. The LNAs are designed for WLAN 2.4GHz and 5.2GHz applications. Two approaches are used to vary the shunt-to-shunt feedback capacitance. One approach is to switch between two different bias currents, shown in Figure 3.7. The second approach is to use a combination of a switch (M1) and a capacitor, shown in Figure 3.8. The reconfigurable Silicon Germanium (SiGe) LNA achieved by switching the bias currents, shown in Figure 3.7, occupies a small area of only $355\,\mu m \times 155\,\mu m$, excluding measurement pads.

3.3.3.2 Reconfigurable VCO designs

Two reconfigurable VCO structures, with tunable inductors and capacitors (see Figure 3.9) and with switched inductors (see Figure 3.10), were reported in [16]. The circuits are designed and fabricated on both the CMOS and BiCMOS processes.

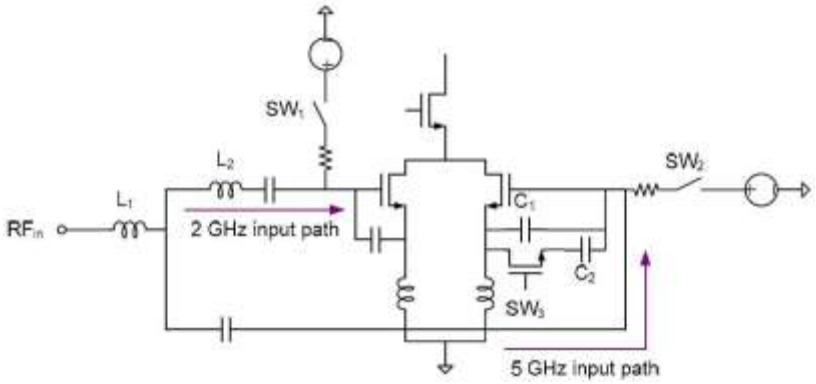

Figure 3.6 A reconfigurable LNA design with one output and two inputs [14]

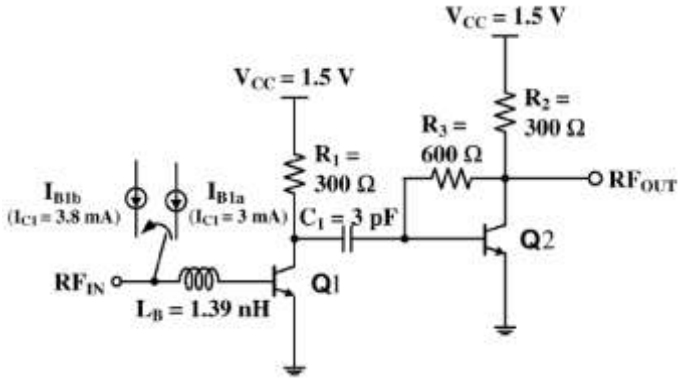

Figure 3.7 A reconfigurable LNA design with one common input and one output, based on bias current switching [15]

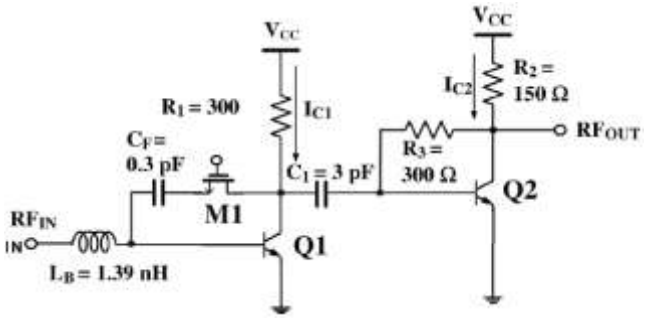

Figure 3.8 A reconfigurable LNA design with a common input and output, based on a series switch and a capacitance [15]

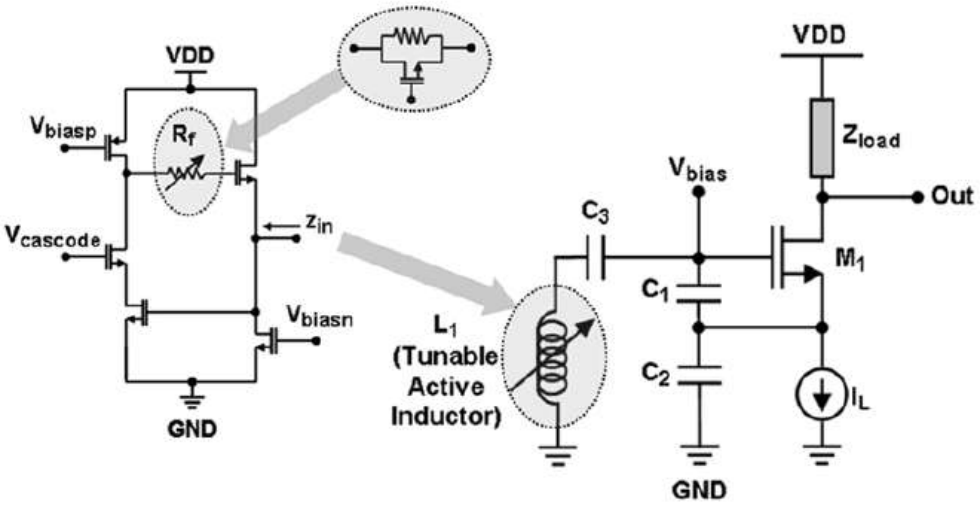

Figure 3.9 A reconfigurable VCO design with tunable inductors and capacitors [16]

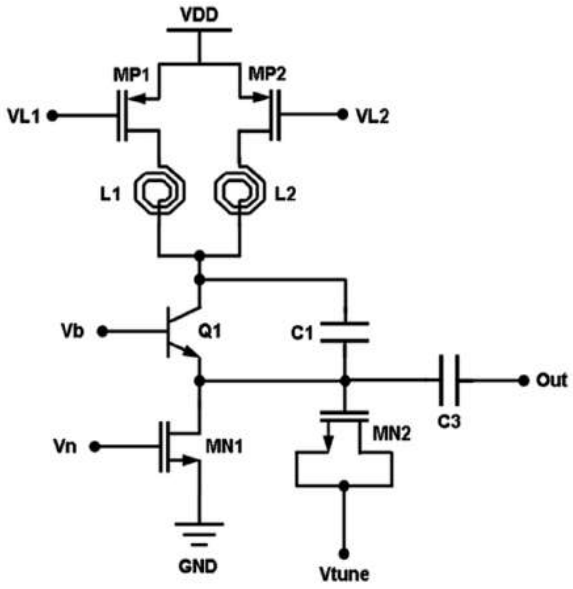

Figure 3.10 A reconfigurable VCO design with switching inductors [16]

Table 3-4 Comparison results of reconfigurable VCOs [16]

Type of VCO	Technology ($0.18\,\mu m$)	Tuning range (GHz)	Core power consumption (mW)	Active area (μm^2)	Output power (dBm)
Tunable inductor and capacitor	Si-CMOS	0.5-2.0	13.8	300×300	-29 to -20.8
	SiGe BiCMOS	1.6-5.1	2.7	170×220	-27 to -19
Switched capacitor	SiGe BiCMOS	2.1-2.7 5.0-6.1	7.5	600×625	-29 to -27.8

Reconfigurability is realized by utilizing tunable inductors and capacitors. The tunable inductors are active inductors actualized by structures similar to those depicted in Figure 3.10. The structures include a tunable active resistor realized by paralleling a passive poly-poly resistor with an NMOS Field-Effect Transistor (FET). A tunable MOS capacitor is achieved with 0.2-1.5pF values for 1-10GHz operations. The compared results are provided in [16] and organized in Table 3-4.

3.3.3.3 A reconfigurable mixer design

A reconfigurable mixer with a flexible input matching network was reported in [10] (see Figure 3.11). By using switches to control the capacitors and inductors values, the matching network is capable of operating at different frequencies.

3.3.4 Reconfigurable RF front end blocks developed at UT

The reconfigurable low noise amplifier (LNA) and the reconfigurable oscillator were previously researched by our group [17, 18] using MEMS. A prototype reconfigurable LNA and oscillator circuits were designed on a FR4 substrate for wireless applications. Micro-strip lines were used for the input and output matching network, rather than utilizing lumped elements, to minimize overall insertion losses. By tuning the length of the micro-strip lines, the circuits operated at a different frequency. A conceptual diagram of the reconfigurable LNA design is shown in Figure 3.12. A schematic diagram of the reconfigurable oscillator design is shown in Figure 3.13. Hard-wire designs were used to depict the feasibility of the reconfigurable LNA and the reconfigurable oscillator concepts, as shown in Figure 3.14 and Figure 3.15.

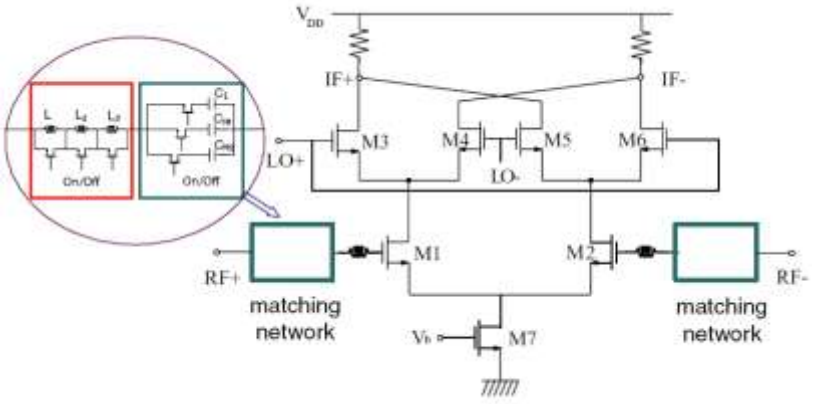

Figure 3.11 A reconfigurable mixer design with a switching passive network [10]

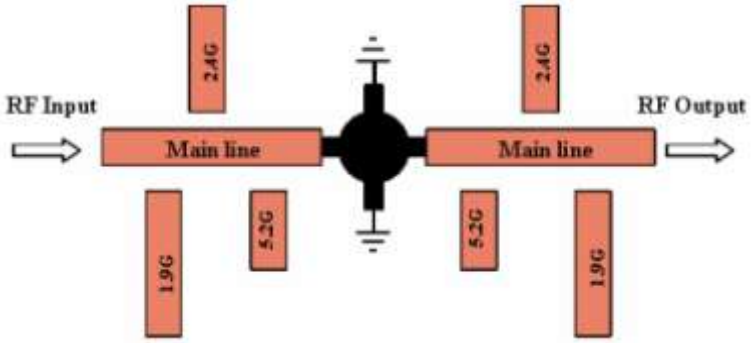

Figure 3.12 Reconfigurable LNA concept diagram with three various matching stubs to operate at 1.9 GHz, 2.4GHz and 5.2GHz [17, 18]

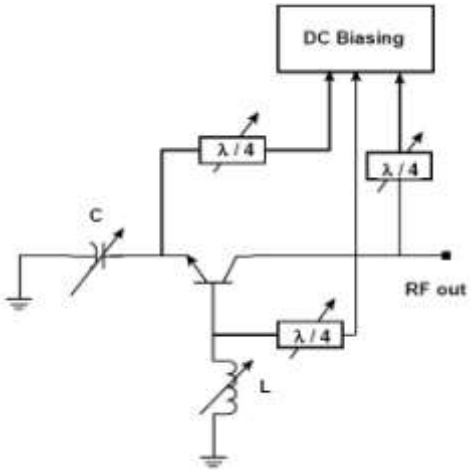

Figure 3.13 Reconfigurable oscillator schematic diagram [17, 18]

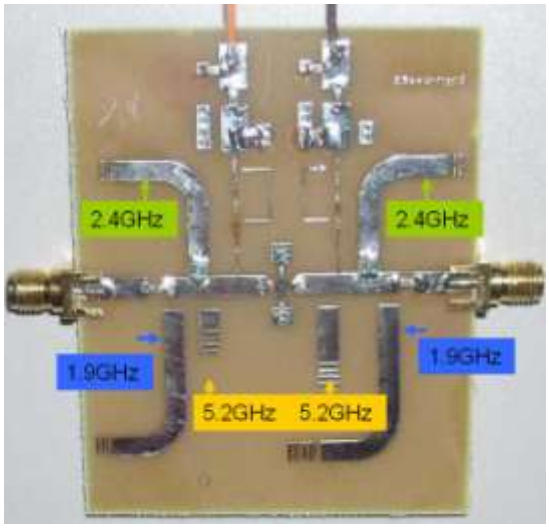

Figure 3.14 Hard-wire connected reconfigurable LNA configured at 2.4GHz which can also be reconfigured to operate at 1.9GHz and 5.2GHz [17, 18]

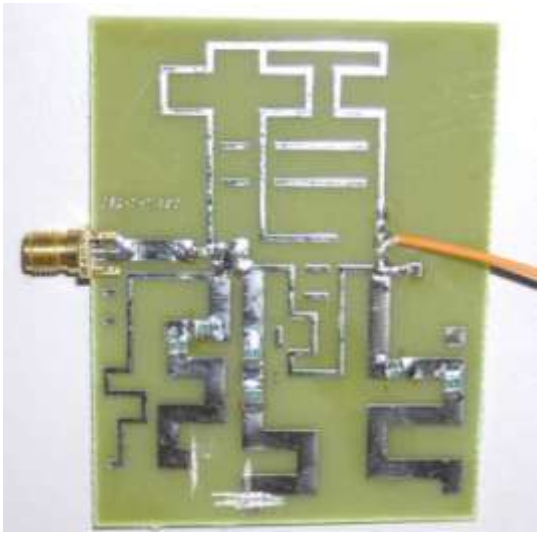

Figure 3.15 Hard wire connected reconfigurable oscillator configured at 850 MHz which can also be configured at 1.85GHz and 2.35 GHz [17, 18]

3.4 Conclusion

Varying standards have been developed for different communication services in the past few decades. The services will need to coexist in the 3G and beyond communication systems, creating multiple design challenges. Note that for the successful implementation of a multi-standard receiver, reconfigurable receiver architecture and reconfigurable component design techniques are essential. Even though several of the current systems in the market today support frequency bands operating with similar standards using basic re-configurability to address some of the above drawbacks, our goal is to extend this concept to combine multiple standards into a hybrid system. Reconfigurable structures can be based on component switching, functional block switching, or whole chain reconfigurability. The next generation's goal is to achieve full reconfigurability for the converged systems. The anticipated results are that reconfigurable structures provide better performance, lower development and manufacturing cost, lower power consumption, and an additional reduction in size and weight.

Chapter 4 RECONFIGURABLE POWER AMPLIFIER DESIGN FOR MULTI-SERVICE SYSTEM

4.1 Introduction

A Power Amplifier (PA) is one of the primary building blocks in designing mobile terminals. It is the component that significantly influences overall power consumption. In any multi-service system, the main parameters generally considered in its development are:

1) Operating frequency
2) Bandwidth
3) Efficiency and linearity
4) Real-estate size.

Among these parameters, PA efficiency is one of the primary considerations in mobile terminal design, as it directly affects the operating life-time of the battery.

Meanwhile, power amplifiers are required to address the diversity of wireless standards, and are designed for multi-band and/or multi-mode operation. However, a single PA is typically used for each service, which is an inefficient design. Even though a single PA can be utilized, in certain instances, for up to two services with close center frequencies and output power requirements, it is still inefficient, especially when additional services need to be augmented. Currently, for example, there are five individual, required PAs to operate seven services in a 3G cell phone [1], and the question will always be: what is the possibility of increasing services within the cell-size constraint?

The answer to the previous question is simple. Providing an individual PA for each service would increase the size of the real-estate to an unacceptable level. Note that such a design would be complicated and expensive when additional operating bands and/or services are required. Specifically, increasing the number of the switch-poles connected immediately after the PA would increase the overall insertion loss and worsen switch isolation. Typical performance degradation is shown in Table 4-1, which provides a comparison between the SPDT, SP4T, SP6T, and SP8T switches [19-22]. Note that increasing the switch's poles beyond four leads to a significant increase in its insertion loss and a noticeable and most likely unacceptable decrease in isolation. For instance, a typical 3G cell phone design currently needs a single pole, nine-throw switch, which causes a significant increase in insertion loss. This high loss translates into a

significant efficiency drop. In general, a 1dB additional insertion loss would account for an approximate 10% decrease in efficiency.

To reiterate, the conventional concept, in a multi-mode/multi-service, of employing a dedicated and optimized PA for each service is not acceptable. Its largest disadvantage is that operations in n-frequency bands require n-amplifier line-ups. This disadvantage results in an increase in the cost and size of the PA's poles, which increases significantly with the number of bands. Therefore, research activities to develop power amplifiers that can implement more than one service at a time have been performed in order to find a replacement for single service/band PA designs. Table 4-2 provides a brief description of common approaches currently implemented, such as the wide band and reconfigurable power approaches. The concepts discussed here utilize a single PA line-up in combination with a reconfigurable output matching network to encompass multiple frequency bands/modes. This novel approach should result in size and cost reduction when compared to the conventional approach, due to the re-use of circuits.

This chapter is organized as follows: challenges in the design of multi-band and multi-mode power amplifiers will be presented in section 4.2. Previous works on multi-band or multi-mode PA design will be reviewed in sections 4.3 and 4.4. In section 4.5, we will discuss our multi-chip reconfigurable PA module design. Its simulation results will be shown first, followed by measurement results and data analysis. Conclusions will be given in section 4.6.

Table 4-1 A comparison of SPnT GaAs switches [19-22]

	Frequency (GHz)	Insertion loss (dB)	Isolation (dB)	IP1dB (dBm)
SPDT (HMC284MS8G)	DC-3.5	0.5	45	25
SP4T (HMC241LP3)	DC-3.5	0.6	47	26
SP6T (HMC252QS24)	DC-3	0.8	41	24
SP8T (HMC253LC4)	DC-3.5	1.2	36	24

Table 4-2 A comparison of different PA design topologies

	Single Band	Wide-band PA	Reconfigurable PA
Design	Straight forward.	Complicated output matching network.	Very complicated layout and control.
Real estate	Large area.	More realistic.	Very compact.
Poles of the switch	Multiple	Multiple	Significant reduction in the number of poles.
Performance	Amplifiers have an excellent performance, but the switch causes significant insertion loss and a low isolation.	Amplifiers can be used for different bands that are close. Slight improvement in isolation and insertion loss performance.	Amplifier performance is degraded by the impact of the number of reconfigurable components or networks utilized, and the number of switches.
Cost	High	Medium	Low

4.2 Challenges in the design of multi-band and multi-mode Power Amplifiers

Several challenges arise when designing a PA for multi-band and multi-mode applications. To emphasize this point, we have included a summary of a 3G cell phone specifications in Table 4-3 [4] to indicate the diversity of the disparate requirements. It can be noted from this table that the design challenges of a multi-service PA model would include:

1) Multiple operating frequency bands.
2) Different services with varying bandwidth requirements.
3) Different services with varying output power requirements.
4) Wide frequency range coverage, from 800 MHz to approximately 6 GHz.
5) Different linearity requirements for the various services.
6) Different modes of operation for the same band/service, but with varying power level requirements.
7) Need to sustain high efficiency.

These diverse requirements can be met if we design separate amplifiers to cover each service, but again, this is not the preferred method. However, the designs can become complicated if we formulate alternative approaches. The challenge of adapting alternative approaches will be discussed in detail in this chapter.

Table 4-3 3G cell phone systems service requirements [4]

System	GSM	EDGE	WCDMA
Common Frequency Bands	US Cellular UL:824-849MHz DL:869-894MHz	US Cellular UL:824-849MHz DL:869-894MHz	US Cellular (Band V) UL:824-849MHz DL:869-894MHz
	EGSM UL:880-915 DL:925-960MHz	EGSM UL:880-915 DL:925-960MHz	
	DCS UL:1710-1785MHz DL:1805-1880 MHz	DCS UL:1710-1785MHz DL:1805-1880 MHz	
	PCS UL:1850-1910MHz DL:1930-1990MHz	PCS UL:1850-1910MHz DL:1930-1990MHz	PCS (Band ll) UL:1850-1910MHz DL:1930-1990MHz
			IMT2000 (Bandl) UL:1920-1980MHz DL:2110-2170 MHz
Output Power Specifications	33dBm (Low Band) 30dBm (High Band)	33dBm (Low Band) 30dBm (High Band)	24dBm (class 3)
Multiple Access	TDMA/FDMA	TDMA/FDMA	CDMA
Common Frequency Bands	US Cellular UL:824-849MHz DL:869-894MHz	US Cellular UL:824-849MHz DL:869-894MHz	US Cellular(Band V) UL:824-849MHz DL:869-894MHz

4.3 Alternative design options for multi-frequency PA operation

Recent research efforts, as previously mentioned, have been devoted to developing new design schemes, resulting in powerful multi-band topologies via the use of dual path topologies employing duplexers or reconfigurable networks. Duplexers are expensive and their design extension beyond two bands is difficult and expensive. Meanwhile, various proposed reconfigurable network approaches are promising and have been used to address these multi-band/multi-mode design challenges. Table 4-4 provides a comparison, among the three levels, for reconfiguring the PA architectures:

1) Switchable elements.
2) Switchable MNs.
3) Switchable Die.

In addition to reconfiguring the networks for multi-band operations, multi-mode reconfiguration is also required. Proposed methods to provide either multi-band or multi-mode, or even both, are aimed at reconfiguring both the active and passive components. This means reconfiguring the elements to operate at a certain bandwidth by adjusting the load line or biasing the PA to efficiently deliver a specific level of power. The die itself can also be reconfigured to accommodate operations at various output power levels. In this section, different concepts for output MN designs for multi-frequency operations, and their advantages and disadvantages, will be discussed. Alternative design options for multi-mode operations will be discussed in the next section.

Table 4-4 A comparison of the three common reconfigurable PA architectures

	Switchable elements	Band-Switchable MNs	Reconfigurable PA
Number of switches	Requires a large number of devices, leading to a higher level of complexity of the matching network.	Less number of switches. The insertion and isolation of these switches are detrimental to overall performance.	Active load line and DC control for efficiency optimization, but still requires switching of either the elements or MN networks, or both, for multi-band operation.

4.3.1 Frequency reconfigurable output matching network (MN) design

It is obvious that when designing a PA, the output matching network (MN) plays a significant role in determining the operating frequency. Novel design schemes have recently evolved to reconfigure their operations. For example, Figure 4.1 [23] depicts a generic matching network, based on element switching, where both the inductors and capacitors can be reconfigured using either shunt or series switches, respectively. Note that this approach, in addition to being expensive, is quite complicated and will suffer drastically from either significant insertion loss due to the large number of utilized switches connected in series, or from low isolation due to the large number of switches connected in shunt.

Alternatively, the input and output matching network operations can provide the transistor with an optimum impedance loading in each frequency band [24] utilizing a single stub matching scheme. The operating principle of the band-switchable MN for n-bands is illustrated in Figure 4.2. In the schematic of this reconfigurable PA, the input and output MNs can easily be reconfigured when employing these switches. When the amplifier operates at frequency f1, all switches are in an off state, separating all stubs from the MN. Since the characteristic impedance of the transmission lines (TL1, TL2, …TL(N-1)) is equal to the source and load impedance, Z0, the entire MN retains optimum matching at the f1 frequency. However, the MN is not optimized at the frequencies f2 and f3 since the impedance of the transistor varies according to the operating frequency. The impedance matching at other frequencies can be achieved by selecting one of the other stubs designed to be part of a single-stub matching network at that frequency. This method is efficient since it achieves both a high isolation (>30 dB), and an overall, relatively low insertion loss of the switches.

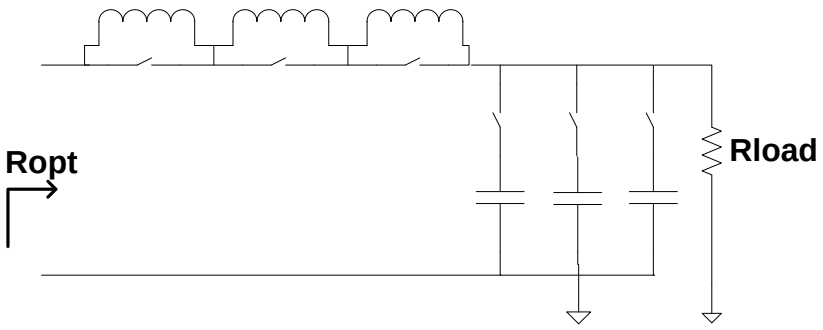

Figure 4.1 A reconfigurable output matching network structure [23]

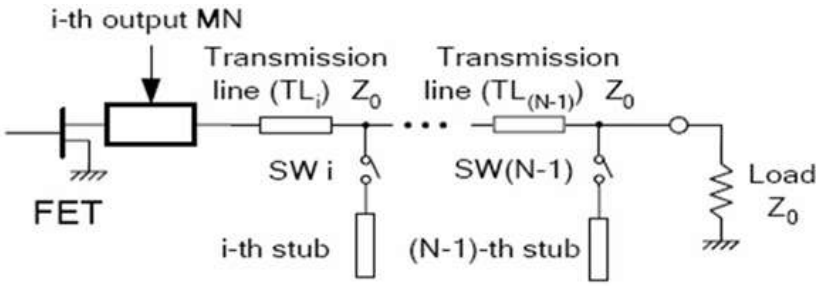

Figure 4.2 A reconfigurable output band-switchable matching network structure [24]

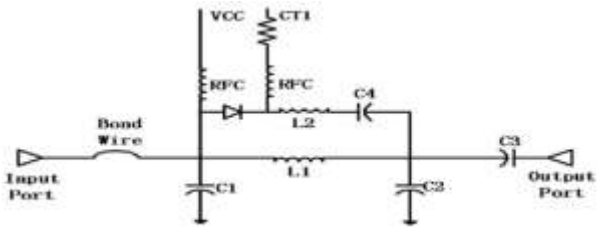

Figure 4.3 A reconfigurable output matching network structure with switchable inductors [25]

The concept of reconfigurability can be extended to offer optimization of efficiency for each frequency band by reconfiguring the elements of the output matching network; i.e. using switchable inductors [25], as shown in Figure 4.3, or capacitors [26], as shown in Figure 4.4, or both. In [25], for example, two inductors "L1 and L2" are connected in parallel and when the switch is off, we have only L1; but when the switch is on, we have L1 and L2 connected in parallel, affecting the tank circuit resonance frequencies. In [26], the output matching network topology is reconfigured by adjusting the utilized capacitors. Additionally, for high efficiency operation, it is possible to optimize both the fundamental and harmonic impedance levels in combination with a strong suppression of the higher harmonics at the output of the amplifier at different bands by switching components values. Moreover, the design shown in Figure 4.4 provides the possibility of optimizing the fundamental load impedance as a function of modulation type and power level for multi-mode operations.

4.3.2 Degrees of Freedom in Designing PA Matching Networks with a Reconfigurable PA

The basic function of the output MN, in a PA design, is to transform the optimized load of the device, dictated by the output power requirements, to the load (typically 50 Ω) at a specific operating central frequency within a specific bandwidth. For the single PA approach, for instance,

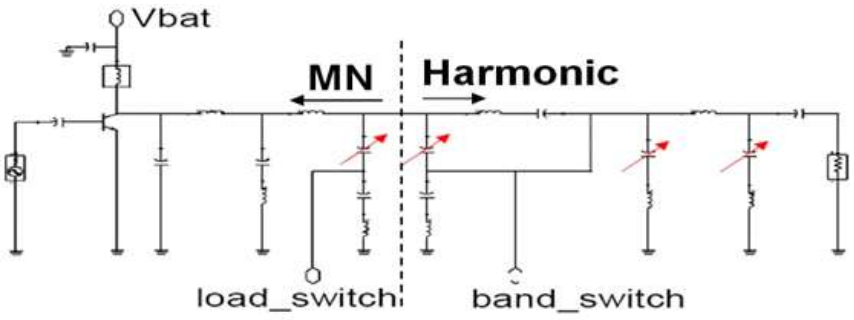

Figure 4.4 A reconfigurable output matching network structure with capacitors [26]

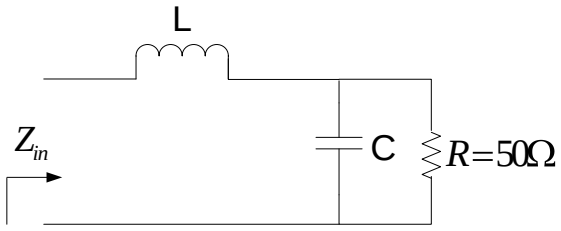

Figure 4.5 A simple low-pass MN

the output MN can be optimized for each standard. However, for the reconfigurable PA approach, the output MN needs to be adjusted to operate at different central frequencies to satisfy both the specific output power and bandwidth requirements.

Ideally, if the matching network is comprised of inductors and capacitors that are controllable, then the entire output MN could be optimized similar to that of a single PA approach—see the structure shown in Figure 4.1 [23]. Unfortunately, this approach has the same shortcomings as does the one utilizing separate, single amplifiers and it is generally advisable to increase the number of freedom degrees of the approach. This would require a flexibility in reconfiguring additional elements, the DC bias, the effective dynamic loading, or even the device topology.

Here we will consider what happens if we minimize the number of switchable elements utilized in reconfiguring the PA and the associated performance degradation. As an example, switching only one passive component, for bandwidth switching, could lead to a reduction of the available bandwidth and mismatching. To illustrate this problem, if the output MN is a low-pass MN, as shown in Figure 4.5, then we can switch the operating frequency by tuning either the inductor (L) or the capacitor (C) of the last section of the output MN, as given by

$$\omega = \frac{1}{\sqrt{LC}} \quad \text{Equation 1}$$

The MN needs to transform the device's complex impedance into a given, pure resistive load, which can be described by the following formula [27]

$$Z_{in} = j\omega L + R // \frac{1}{j\omega C} = \frac{R}{1+(\omega CR)^2} + j\left[\omega L - \frac{\omega CR^2}{1+\ \omega CR^{\ 2}}\right] . \quad \text{Equation 2}$$

From Equation 2, we can derive

$$R_{in} = \frac{R}{1+(\omega CR)^2} , \quad \text{Equation 3}$$

$$\omega L - \frac{\omega CR^2}{1+\ \omega CR^{\ 2}} = 0 . \quad \text{Equation 4}$$

If we want to reconfigure the circuit to operate at *f/2* by only tuning either the L or C, in Figure 4.5, then the L needs to be switched to 4L or the C needs to be switched to 4C. Let C', L', or R' represent the new values of C, L and R after switching, so that we have C'=4C, L'=L, R'=R $\omega' = \frac{1}{2}\omega$.

Then, we can derive Equation 5 and Equation 6 as follows

$$\frac{R_{in}^{'}}{R_{in}} = \frac{R}{1+\ 2\omega CR^{\ 2}}\ \frac{1+\ \omega CR^{\ 2}}{R} = \frac{\frac{R}{R_{in}}}{4\frac{R}{R_{in}} - 3} , \quad \text{Equation 5}$$

$$j\omega^{'}L^{'} - j\frac{\omega^{'}C^{'}R^{'2}}{1+\ \omega^{'}C^{'}R^{'\ 2}} = -j\frac{\frac{3}{8}\omega CR^2}{\left[1+\ \omega CR^{\ 2}\right]\left[\frac{1}{4}+\ \omega CR^{\ 2}\right]} \neq 0 . \quad \text{Equation 6}$$

Note that we need to select C' to cancel the imaginary part, as given by Equation 6. In addition, the real part in both states will vary and could degrade the return loss performance.

Similarly, if, C'=C, L'=4L, R'=R then

$$\omega' = \frac{1}{2}\omega \quad .$$

Equation 7 and Equation 8 are rewritten as

$$\frac{R'_{in}}{R_{in}} = \frac{4R}{4+\ \omega CR^{\ 2}}\ \frac{1+\ \omega CR^{\ 2}}{R} = \frac{4\dfrac{R}{R_{in}}}{\dfrac{R}{R_{in}}+3} \qquad \text{Equation 7}$$

,

$$j\omega' L' - j\frac{\omega' C' R'^{2}}{1+\ \omega' C' R'^{\ 2}} = j\frac{6\omega CR^{2}}{\left[1+\ \omega CR^{\ 2}\right]\left[4+\ \omega CR^{\ 2}\right]} \neq 0 \quad . \qquad \text{Equation 8}$$

From Equation 5—Equation 8 we find that:

1) This design topology tends to have a narrow bandwidth in multi-section matching network topologies.

For example, in Figure 4.6, when C3 = 2.86 pF, the MN operates at 1.8 GHz, but when C3=11.4 pF, the MN operates at 0.9 GHz, as shown in Figure 4.7 and Figure 4.8. Note that the bandwidth, when the MN operates at 0.9 GHz, is lower than the bandwidth of the MN at 1.8GHz

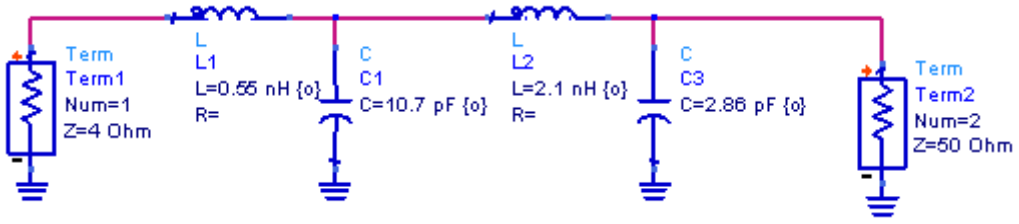

Figure 4.6 A two section low pass matching network

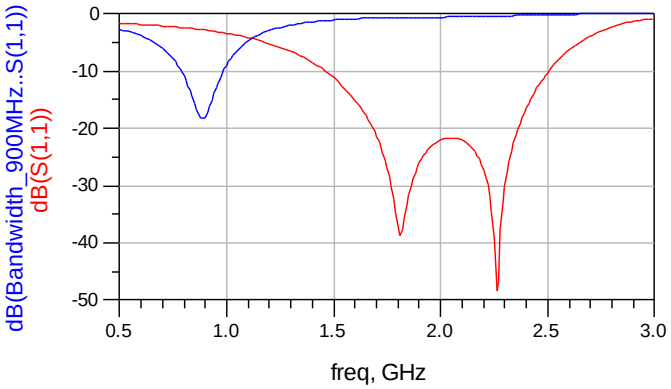

Figure 4.7 The return loss of a two section low-pass MN shown in Figure 4.6

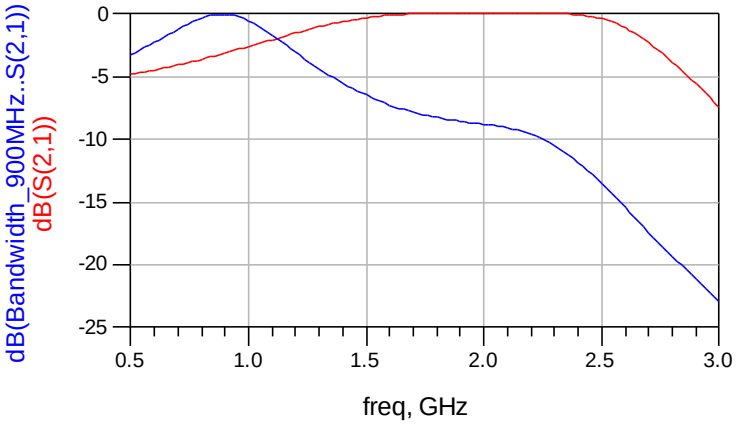

Figure 4.8 The insertion loss of a two section low-pass MN shown in Figure 4.6

Table 4-5 A comparison of single and multi-element tuning topology

Design topology	Advantages	Disadvantages
Single element tuning	Simple and low cost.	Limited flexibility, lower bandwidth, and poor mismatch problems.
Multi-element tuning	Multi-function flexibility with multi-band/multi-mode.	Complex, expensive, and relatively large real-estate

2) This design topology will cause both a mismatch and an efficiency drop by just tuning the capacitor or inductor values. At the same time, the structure does not have the flexibility to simultaneously address both switching the operating frequency and matching the load to the optimized impedance. A comparison between single element and multi-element tuning topologies is given in Table 4-5.

Therefore, a compromise between single element tuning (reconfiguring) and multi-element tuning for multi-band operations must be performed. In the following sections, we will discuss even further leveraging the switching the elements approach by reconfiguring the active device topology as well to cover more functionality.

4.4 Alternative design options for Multi-mode Operation

Since the different services in each group have varying output power requirements (as indicated in Table 4-3), their corresponding efficiencies will vary significantly. Typically, designers select the number of transistor cells based on the maximum output power requirements associated with one service, but this number would remain fixed for all other services. Consequently, the die will provide maximum efficiency for the service mode with maximum power output, but its efficiency will drop significantly when it operates at the other mode with a lower output power for a given multi-mode service. For example, designers use a large number of cells to achieve the 33dBm necessary to comply with GSM service. However, when switching to PCS service requiring only a 30 dBm, designers are forced to utilize (stuck with) the same number of cells, creating an unnecessarily large drain DC current, and thus suffering a significant drop in power efficiency.

Various approaches exist to circumvent the power efficiency drop whenever the output power is decreased for lower output power modes. These different methods are listed below.

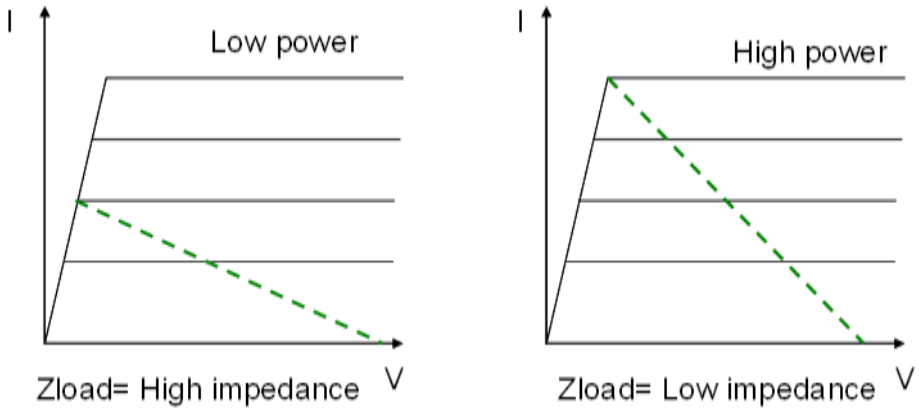

Figure 4.9 Illustration of the dynamic load line method [4]

1) Dynamic Load Line Method

The dynamic load line technique uses a higher load at the decreased output power level and a lower load at the maximum output power, as shown in Figure 4.9 [4]. For example, in [26], the authors described the ability of the dynamic load line technique to improve the operating efficiency, as a significant drop in DC quiescent and subsequently DC dissipation. A schematic of the dynamic load line matching network and its associated frequency response is shown in Figure 4.10. Based on Figure 4.11, note that a significant increase in the operating efficiency can be achieved if a high load line is employed at the reduced output power level.

2) Drain Voltage Control Method

Another method to optimize efficiency is to decrease the supply voltage, Vcc, thus reducing the maximum available linear power [4] (see Figure 4.12). This technique improves the efficiency at the low output power (backed-off) by dynamically (effectively) changing the quiescent point.

For example, in [28], the authors designed a dynamic gate bias circuit for biasing control. The proposed circuits, based on the authors' research, are composed of two NMOS transistors, a capacitor for coupling RF input signal, and four resistors for bias, as shown in Figure 4.13. This control can be used to maximize the power-added efficiency, based on operating in a class A amplifier mode. The comparison of the PAE, with and without bias control, versus the Pout results are provided in [28] and shown in Figure 4.14.

As an additional example, [29] used the voltage control for class C power amplifier to sustain an almost fixed efficiency over wide output power levels. Simulated results are shown in Figure 4.15, and note that the voltage gain is almost linearly proportional to Vdc. Therefore, a feedback mechanism is used to adjust the drain bias voltage as a function of the input power level. At low

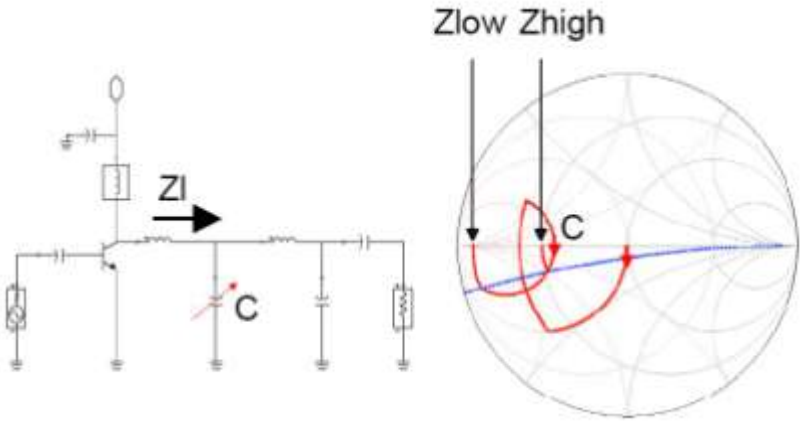

Figure 4.10 An example of a MN with dynamic load line [26]

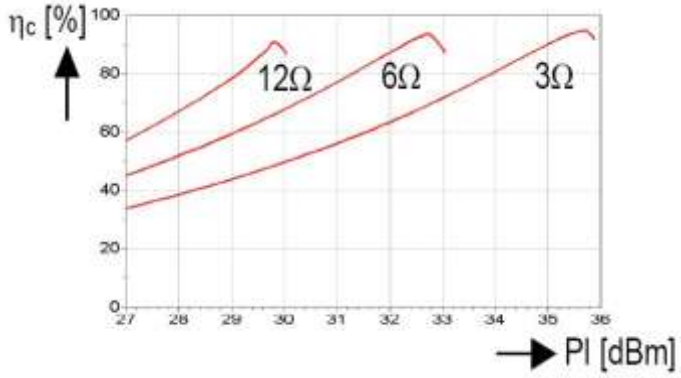

Figure 4.11 Output power vs. efficiency with different load lines [26]

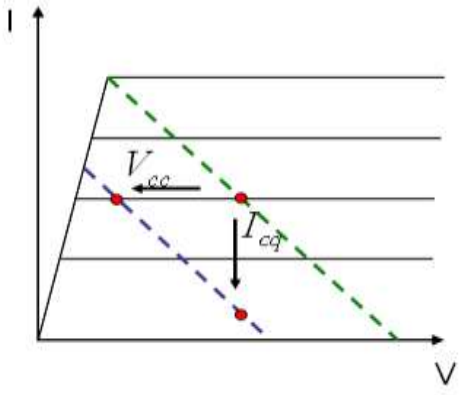

Figure 4.12 Illustration of the Bias control method [4]

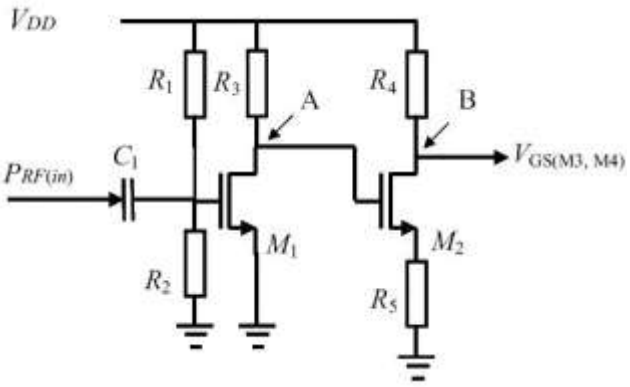

Figure 4.13 The proposed dynamic bias circuit [28]

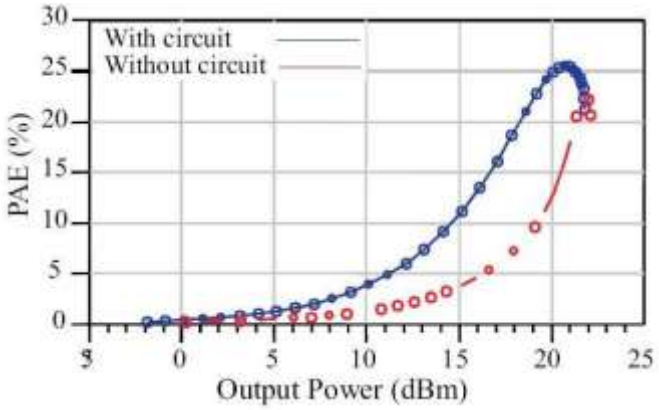

Figure 4.14 Output power vs. PAE [28]

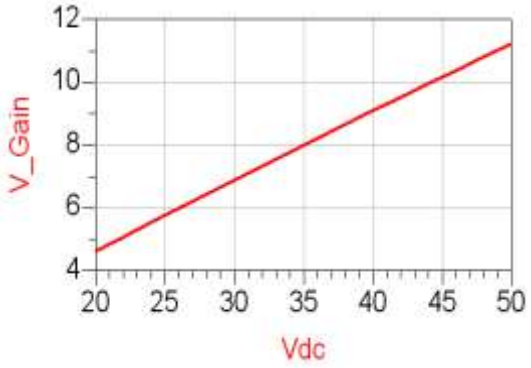

Figure 4.15 Drain voltage vs Voltage gain [29]

power levels, the control circuit applies low drain voltage and vice-versa. Subsequently, the output power, gain, and dc dissipation are adjusted based on the input power level, thus sustaining an almost fixed efficiency.

3) Integrated Power Control

On one hand, if the output stage device is not adequate, it will go into saturation at relatively low power levels and would create a gain compression and unacceptable signal distortion. Additionally, over-utilizing an active device can lead to exceeding the maximum allowed current levels, or beyond the manufacturer's maximum ratings, causing significant heating and performance degradation. On the other hand, if a device, larger than required, is used, it would result in a significant increase in DC power consumption and cause a lower operating efficiency. Consequently, it is preferable to employ the appropriate transistor size.

A simple method to choose the appropriate transistor size is to use two PAs in parallel, and employ switches to select the optimum power operation. For example, when we connect a medium and small output power amplifier in parallel, we can use the smaller device for low power levels and then switch to the other power amplifier for medium power, or even exploit one to drive the other for a high power operation. Each driving option can be controlled via a set of switches, as shown in Figure 4.16.

Recently, however, a trend exists to move to the concept for using one amplifier for almost all services. Therefore, instead of externally switching between different level amplifiers as indicated in Figure 4.16, it is appropriate to internally reconfigure the power amplifier cells. Such an approach will be discussed in the following section.

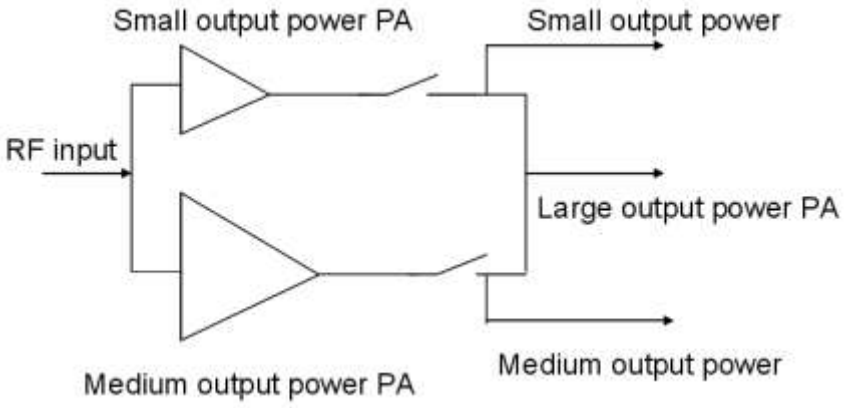

Figure 4.16 Illustration of the integrated power control method

4) Proposed Solution

Along the line of "global amplifier vision", efficiency enhancement can be addressed by controlling the number of turned-on transistor cells on the die itself. By combining this control with a reconfigurable output matching network, the reconfigurable PA can sustain high efficiency when operating at various power levels. For example, at the highest power level, all die cells will be turned on to achieve the maximum output power required, but a portion of these transistors can be turned off for a lower power service mode. This proposed technique adds another degree of freedom in the design of reconfigurable amplifiers. It avoids external switching and significantly saves real-estate. A comparison of the three common PA reconfiguration techniques is shown in Table 4-6.

4.5 A reconfigurable power amplifier design for multi-service applications

To demonstrate this novel reconfigurable PA design concept for both multi-band and multi-mode devices, a reconfigurable power amplifier for multi-service operations has been designed and implemented. The target operating frequency bands are 0.9GHz and 1.6GHz, with a target output power level of 33 dBm and 30 dBm, respectively.

Table 4-6 A comparison of the three reconfiguration techniques

reconfigurable techniques	Dynamic load control.	Supply voltage control, both VCC or VGG.	Number of transistor cells controlled
Output power	Discrete levels.	Wide tuning range for output power.	Discrete levels, also combinable with the other two approaches.
Flexibility	Require extra switches, high loss	Need extra DC control circuits	Requires developing MMIC design.
Efficiency	Limited improvement.	Noticeable improvement.	Significant improvement.
Control	Switching the RF matching network, by employing switches.	Using OPAMPs to control the supply voltage, a type of feedback could be required between the output power and control circuit.	Programmable DC control, based on mode of operation to select the number of cells.

The PA die is designed by capitalizing on a GaAs process, while the matching network, the die, and the switches are designed on a 4 layer-laminate substrate—i.e. a multi-chip module design. The design details will be presented in the following order:

1) Modeling the die.
2) Designing the output matching networks.
3) Implementing the design using a multi-chip module technology.

4.5.1 The reconfigurable PA die design

The reconfigurable die is designed on a GaAs HBT process as it offers:

1) Excellent linearity performance.
2) High power density.
3) Reduced size.
4) Ease of manufacturing.
5) Acceptable RF performance.

A detailed comparison of the various processes, including GaAs HBT, SiGe HBT, GaAs MESFET, and CMOS process, is listed in Appendix 1.

4.5.1.1 Transistor cells number Selection:

In building a high output power PA die, the transistor cells are typically connected in shunt. Each cell has a maximum current carrying capability. So, for n cells, the total maximum current is n times the maximum current carrying capability of each device, given by $I_{max/cell}$. This is a fabrication process and normally is identified by the foundry. The output power is typically related to the maximum current I_{max}. In our case here, the target maximum output power for the LB is 33dBm, which corresponds to a total maximum current, given by

$$I_{\max} = \frac{8 \times P_{out}}{V_{\max}} = \frac{8 \times 2}{7} = 2.28A. \qquad \text{Equation 9}$$

Meanwhile, for the HB with a 30 dBm (1W), the total peak current is

$$I_{\max} = \frac{8 \times P_{out}}{V_{\max}} = \frac{8 \times 1}{7} = 1.15A. \qquad \text{Equation 10}$$

In our implementation of this reconfigurable PA die, the used GaAs HBT process corresponds to an I_{max} of approximately 110mA/cell. Therefore, a total of twenty-four transistor

cells have been chosen for a 33dBm output power. For HB operations, we used only 18 cells, or six of the twenty-four transistor cells turned off. Then, we designed the chip out of 24 cells, with two bias control circuits, one for 18 cells and one for 6 cells.

4.5.1.2 DC bias control circuit for the reconfigurability

The die, as a whole, is divided into 4 sets. Each cell has 6 transistors connected in shunt. In our implementation, we connected three of the sets to form an 18 transistor unit. To realize the bias control, two DC bias circuits were implemented. One circuit was used to set up the quiescent point for the 18 transistor set, and the other bias control circuit was used for the remaining six transistors. Figure 4.17 shows a schematic of the die, where 6 cells are controlled by one bias supply and the other 18 cells are controlled by a second bias supply. The DC bias is provided using two current mirrors (I_1 for the 6 transistors and I_2 for the 18 transistors), as shown in Figure 4.17. The design of this type of current mirror is conventional and can be found in many textbooks like [1]. Brief design steps are described, however, in Appendix 2 for completeness. When the PA operates at LB, all transistors bases, from RF_IN_1 to RF_IN_4, are connected to one another and to the input RF signal. When the PA operates at HB, 18 transistor bases, from RF_IN_1 to RF_IN_3 only, are connected to one another and to the RF input. All collectors at the RF output are always connected together and connected to the output MN input.

4.5.2 The reconfigurable output MN design [30]

This section includes two parts. The first part is the operating principles of the proposed reconfigurable output MN, and the second part is the discussion of the realization of the proposed reconfigurable MN. To describe it, Table 4-3 has been reorganized based on the operating frequency of different services as Table 4-7.

4.5.2.1 Operation Principles of the Output Matching Network

The first step in the design of a reconfigurable MN is the design of a duplexer-like network. The duplexer divides the various services into two or more groups, based on their central operating frequencies. In our implementation, for example, we have divided the different services into two groups. Group 1 is for standards with operating frequencies at approximately 900MHz, and group 2 is for standards with operating frequencies near 1.6GHz. This step is followed by addressing the multi-mode operation by adjusting the equivalent loading of these sub-networks as necessary.

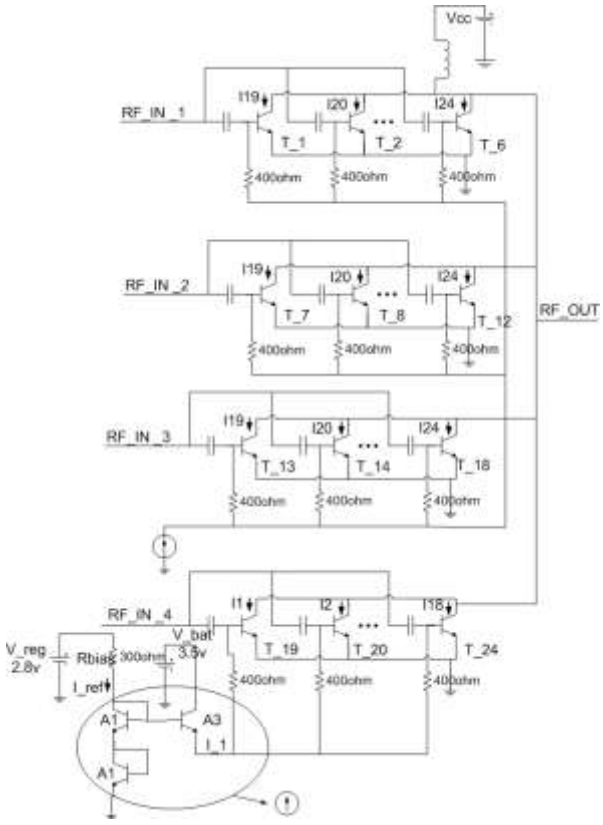

Figure 4.17 The schematic of the reconfigurable die

Table 4-7 Classifying the 3G cell phone services based on their operating frequencies

	Group 1	Group 2
Services	GSM US Cellular, GSM EGSM, EDGE US Cellular, EDGE EGSM, WCDMA US Cellular.	GSM DCS, GSM PCS, EGSM DCS, EGSM PCS, WCDMA PCS, WCDMA IMT2000.
Operating frequency	824MHz-915MHz.	1710MHz-1980MHz.
BW/ω	US Cellular: 3.0% EGSM: 3.9%	DCS: 4.3% PCS: 3.2% WCDMA IMT2000: 3.1%
Antenna power	GSM/EDGE: 33dBm WCDMA US Cellular: 24dBm	DCS/PCS: 30dBm (GSM/EDGE) PCS/IMT2000: 24dBm

Note: Group 1 operates at two different power levels: 33 dBm and 24 dBm, and Group 2 operates at two different power levels: 30 dBm and 24 dBm.

4.5.2.1.1 Step 1: Reconfigurable output MN switching between different sub-reconfigurable output MNs

The reconfigurable output MN design is similar to the standard duplexer design shown in Figure 4.18 (a). Typically, the standard duplexer design utilizes single-terminated filters with a low-pass filter design for the LB and a high-pass design for the HB. However, this standard design could be problematic in PA structures, as preferably a low-pass MN technique is used for a PA design in order to reject higher order harmonics; thus sustaining high linearity performance.

To avoid the complexities caused by employing a high-pass MN design, this conventional diplexer design has been modified to switch between two low-pass filters using a Single-Pole-Single-Throw (SPST) switch in the HB sub-reconfigurable MN, as shown in Figure 4.18 (b). When the reconfigurable output MN operates at the LB, the switch is open and provides adequate isolation to the LB sub-reconfigurable MN; when the reconfigurable PA operates at the HB, the switch is closed. Although in this state both the LB and HB sub-reconfigurable output MN are connected to the transistor collector, no significant loading exists from the low-pass matching network of the LB on the HB network. This presents sufficiently high impedance and its effect can be negated, i.e., the same operation principle as the duplexer.

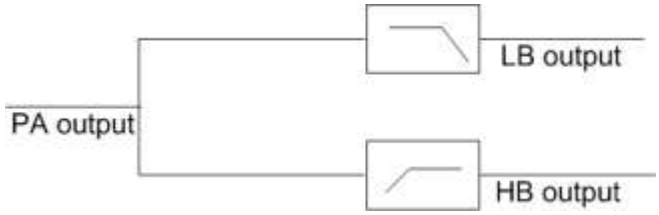

(a)

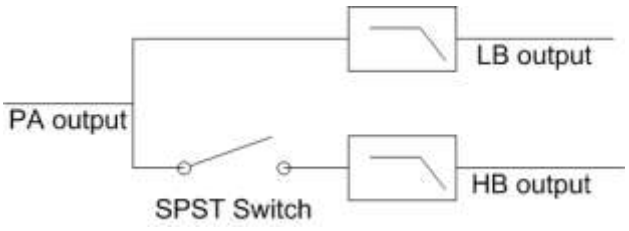

(b)

Figure 4.18 (a) Standard duplexer diagram; (b) Reconfigurable output MN operating between two sub-reconfigurable MN.

4.5.2.1.2 Step 2: Sub-reconfigurable matching network design

Upon the completion of step 1, each sub-reconfigurable matching network is a signal path for services with the same operating frequency, but with the same, or different, output power requirements. For example, the LB path should provide a signal path for GSM US Cellular, GSM EGSM, EDGE US Cellular, EDGE EGSM, and WCDMA US Cellular, even though they require different power levels.

Therefore, the sub-reconfigurable matching network has two functions. First, it should match the 50Ω to the optimum impedance of a specific service within the operating frequency range of that service. Second, it should be reconfigurable and have minimal loading on the other sub-reconfigurable network of the other specific service. In our implementation, we will assume the optimum impedance for GSM (LB) to be 2Ω and for WCDMA 4Ω (HB). Then, the LB sub-reconfigurable matching network should match the 50Ω to the 2Ω for that particular service and the HB should be able to match the 50Ω to the 4Ω for an acceptable efficiency performance for the other service as well; given that they do not load one another.

In our proposed reconfigurable output MN implementation (shown in Figure 4.19), the LB and HB sides have low-pass MN designed by utilizing lumped capacitors and printed spiral inductors. Meanwhile, a switch is used to select one of these services. Assuming that when the switch is off, we are utilizing the LB; if the switch is on, we are selecting the HB, given that the loading effects of the LB on the HB MN are minimal. As both the LB and HB are presumably designed to cover a wide range of services clustered at approximately 900 MHz or 1600MHz, fine tuning can still be implemented by switching on and off several of the shown parallel capacitors.

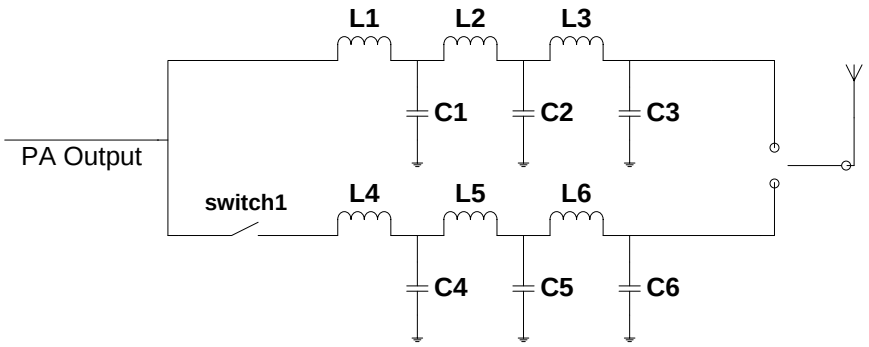

Figure 4.19 The demonstrated reconfigurable output matching network

4.5.2.2 The Reconfigurable Output MN Schematic Realization

The design of the output matching network for the power amplifiers is different from designing the network for small signal amplification. In the small signal case, optimum matching utilizes a conjugate match to produce maximum available gain. For a PA design, however, the output matching network is designed to:

1) Present an optimum load line to the device maximizing output voltage and current swing.
2) Transform the load to the desired system impedance, i.e. 50 ohms.
3) Present the proper impedance terminations to all higher order harmonics (specifically $2f_o$ and $3f_o$), in addition to the base band.

4.5.2.3 Optimum load impedance simulation using load pull

A simple calculation of the base-band impedance that should be seen by the collector of the HBT device is given by

$$P_{out} = \frac{(\frac{V_{\max}/2}{\sqrt{2}})^2}{R_L} \Rightarrow R_L = \frac{{V_{\max}}^2}{8P_{out}} \qquad \text{Equation 11}$$

where P_{out} is the targeted output power, $V_{\max}$ is the peak voltage, and R_L is the load line impedance.

A more accurate method to obtain the optimum R_L is the use of the load pull technique [31]. Hence, in our design, a load pull simulation was carried out utilizing ADS. The bench setup is shown in Figure 4.20. The simulation results, for both the LB and HB, are shown in Figure 4.21 and Figure 4.22, respectively. In this design, we chose our target optimum resistance for the LB to be 2 Ω and the optimum resistance for the HB to be 4Ω. These selected values can achieve approximately 45% PAE for the LB and 40% for the HB.

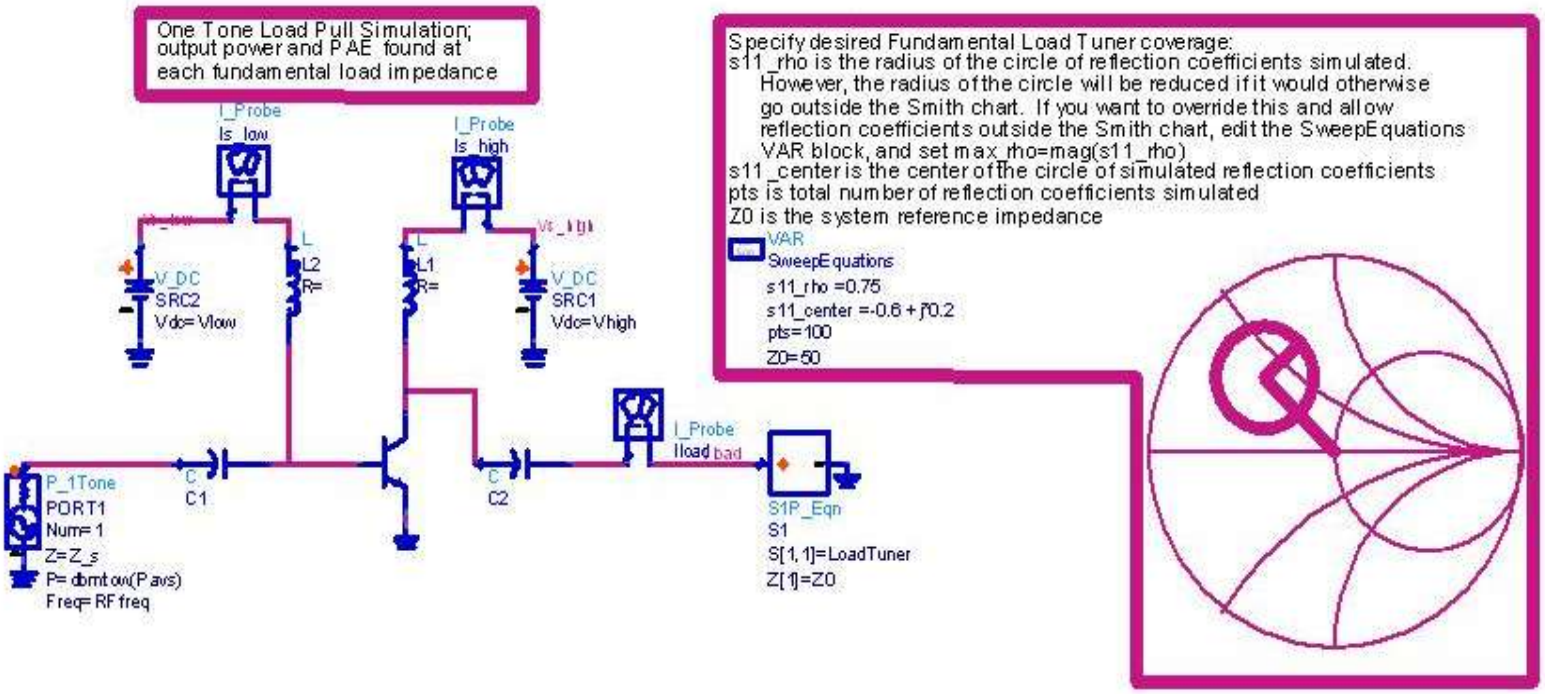
One Tone Load Pull Simulation;
output power and PAE found at
each fundamental load impedance
I_Probe
Is_low
I_Probe
Is_high
V_DC
SRC2
Vdc=Vlow
L
L2
R=
L
L1
R=
V_DC
SRC1
Vdc=Vhigh
I_Probe
Iload_bad
P_1Tone
PORT1
Num=1
Z=Z_s
P=dbmtow(Pavs)
Freq=RFfreq
C
C1
C
C2
S1P_Eqn
S1
S[1,1]=LoadTuner
Z[1]=Z0
Specify desired Fundamental Load Tuner coverage:
s11_rho is the radius of the circle of reflection coefficients simulated.
However, the radius of the circle will be reduced if it would otherwise
go outside the Smith chart. If you want to override this and allow
reflection coefficients outside the Smith chart, edit the SweepEquations
VAR block, and set max_rho=mag(s11_rho)
s11_center is the center of the circle of simulated reflection coefficients
pts is total number of reflection coefficients simulated
Z0 is the system reference impedance
VAR
SweepEquations
s11_rho =0.75
s11_center =-0.6 + j0.2
pts=100
Z0=50

Figure 4.20 Load pull simulation bench setup

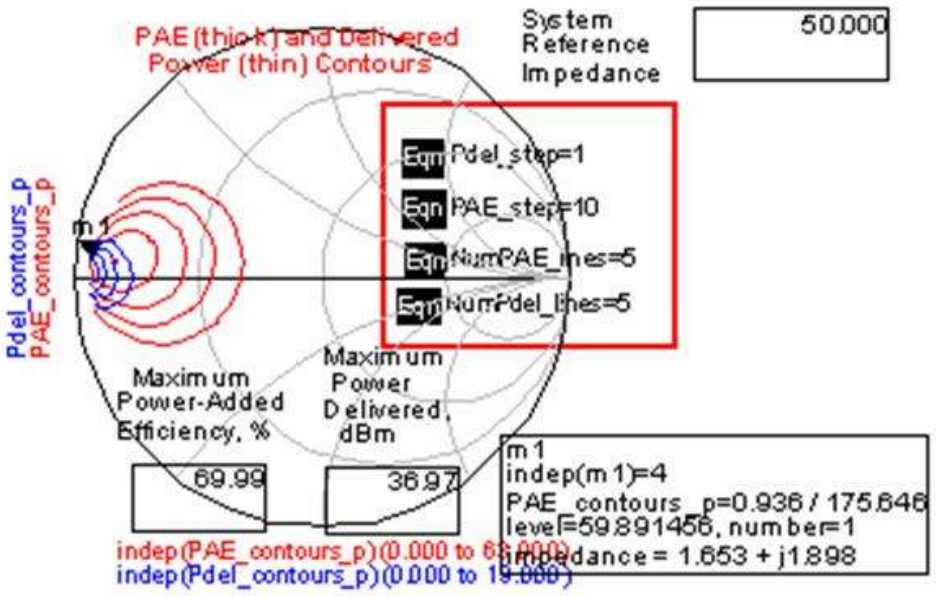

Figure 4.21 Load pull simulation result for LB

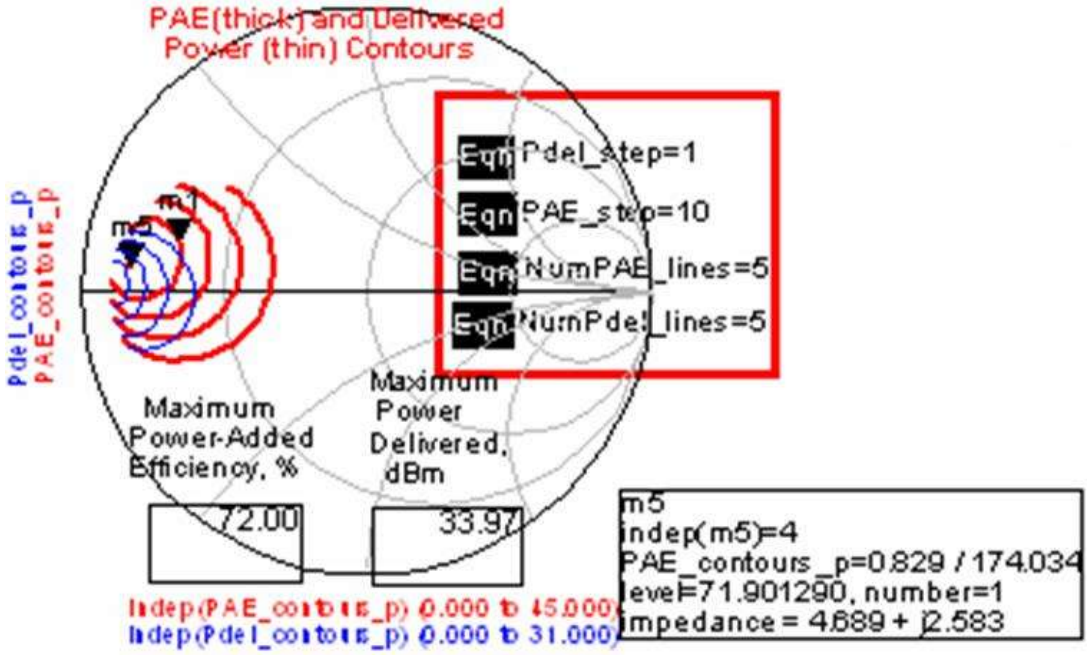

Figure 4.22 Load pull simulation result for HB

4.5.2.4 Matching network design with ADS

Typically, a low-pass MN can create both the impedance transformation in the band and the high harmonic rejection out of band.

In this design, for the LB, the matching network needs to transform 50 Ω to 2 Ω. The bench setup for the LB MN simulation is shown in Figure 4.23. Four optimization goals are used here. The first two goals are set to acquire a good matching. The third goal is set to realize the LP filter function and the fourth goal is set to realize a good insertion loss performance in the operating band. Simulation results are shown in Figure 4.24 and Figure 4.25. Similarly, the bench setup for the HB is shown in Figure 4.26. The simulation results for the HB performance are shown in Figure 4.27 and. Figure 4.28

4.5.3 Simulation results of the proposed reconfigurable PA

Extensive simulation of the PA was performed in ADS [32]. Both small signal and Harmonic-Balance simulations were performed. The bench setup is shown in Figure 4.29. When it operates at LB, the driver stage is represented by an equivalent load, given by (9-j25) Ω, and has been matched, using a conjugate match, to the reconfigurable die. When it operates at LB, the driver stage is represented by an equivalent load, given by (15-j35) Ω, and has been matched, using a conjugate match, to the reconfigurable die. The output matching network is branched into the HB and LB networks. The utilized switch is assumed OFF when operating at the LB and ON for the HB band.

Based on simulation results, the designed amplifier at the LB requires a 17.5 dBm input power to deliver a 33dBm output power, as shown in Figure 4.30. Meanwhile, it has a PAE of 45%, as shown in Figure 4.31. The amplifier's stability was also verified, based on the small signal analysis. It was determined that the amplifier is unconditionally stable within the operating frequency range, as shown in Figure 4.32. Figure 4.33 shows the maximum gain and S21. The predicted bandwidth is approximately 100MHz (820MHz to 920MHz), adequate for the GSM service.Similar simulations were performed at the HB operating frequency band. For an input power of 18 dBm, the output power could reach a 30 dBm, as shown in Figure 4.34. With a 30dBm output power, it has a PAE of 40 %, as shown in Figure 4.35. Figure 4.36 indicates that the PA is stable in the operating frequency band. Figure 4.37 shows the maximum gain and S21 at HB. Meanwhile, the bandwidth is approximately 200MHz (1500MHz to 1700MHz). In the simulation for both HB and LB, S-parameters of the MEMS switch for both Open and Close statues, provided by Radant [33], has been used.

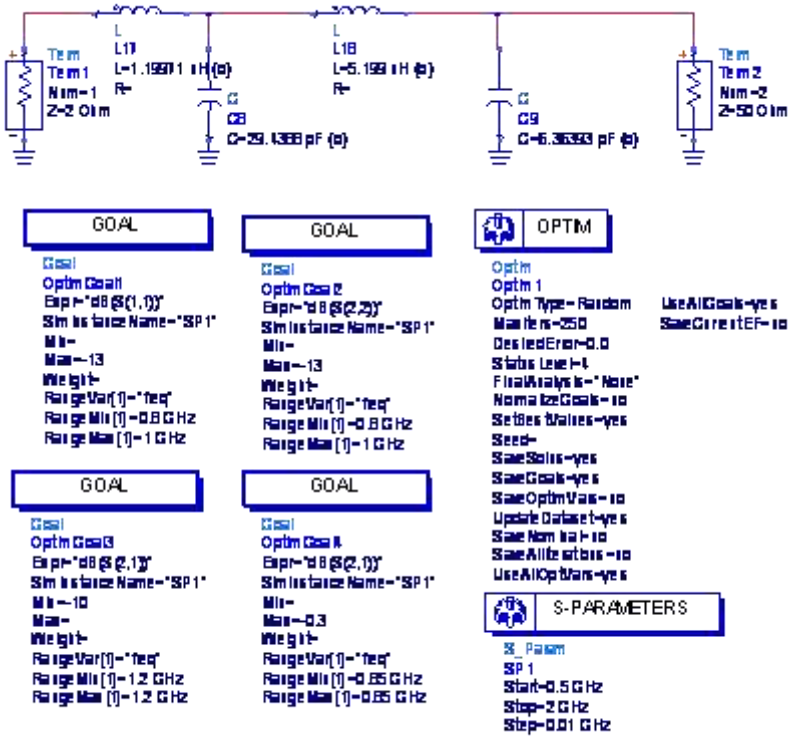

Figure 4.23 Simulation bench setup for LB output MN design

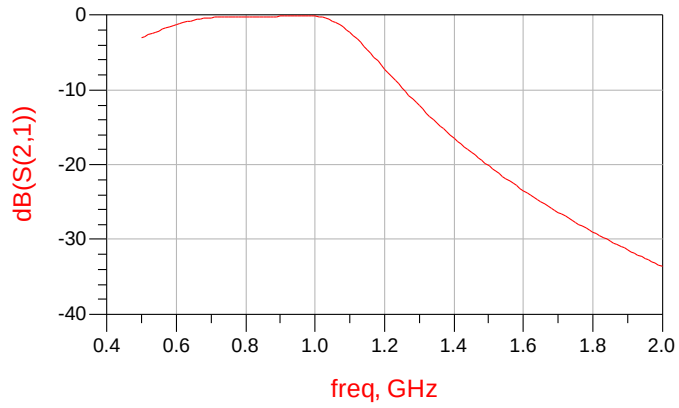

(a)

Figure 4.24 LB MN performance (a) insertion loss, (b) return loss

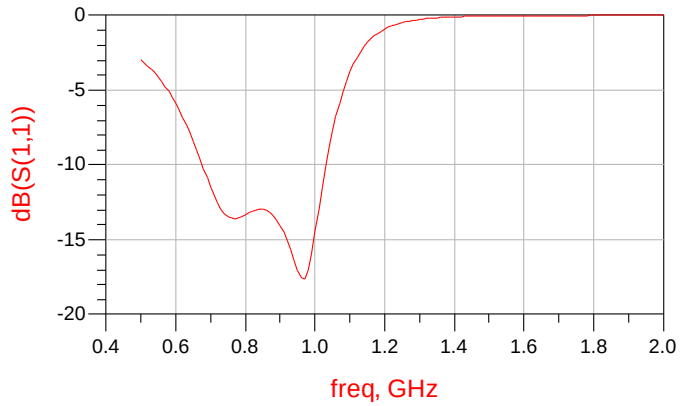

(b)

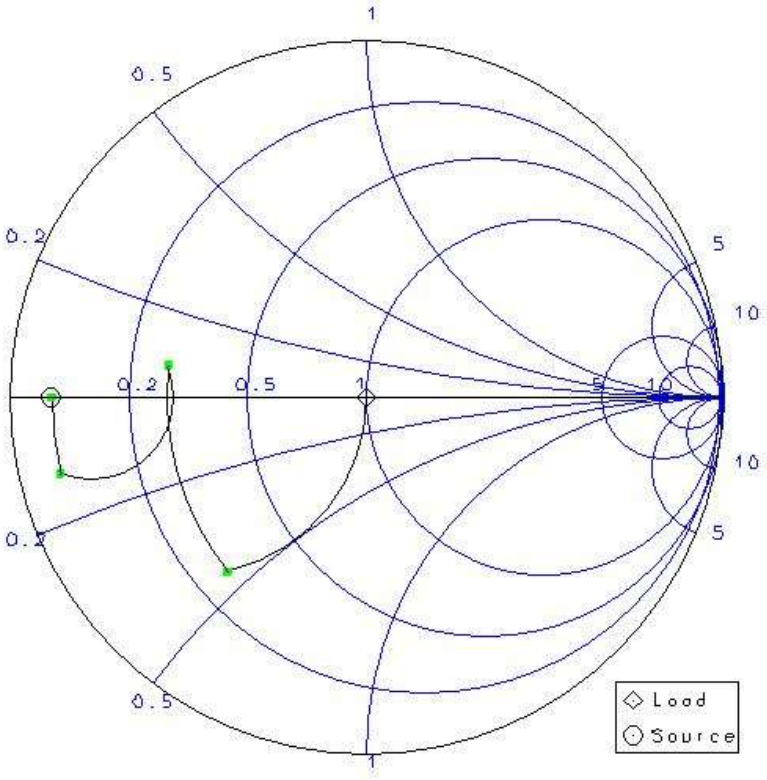

Figure 4.25 LB MN matching on Smith chart

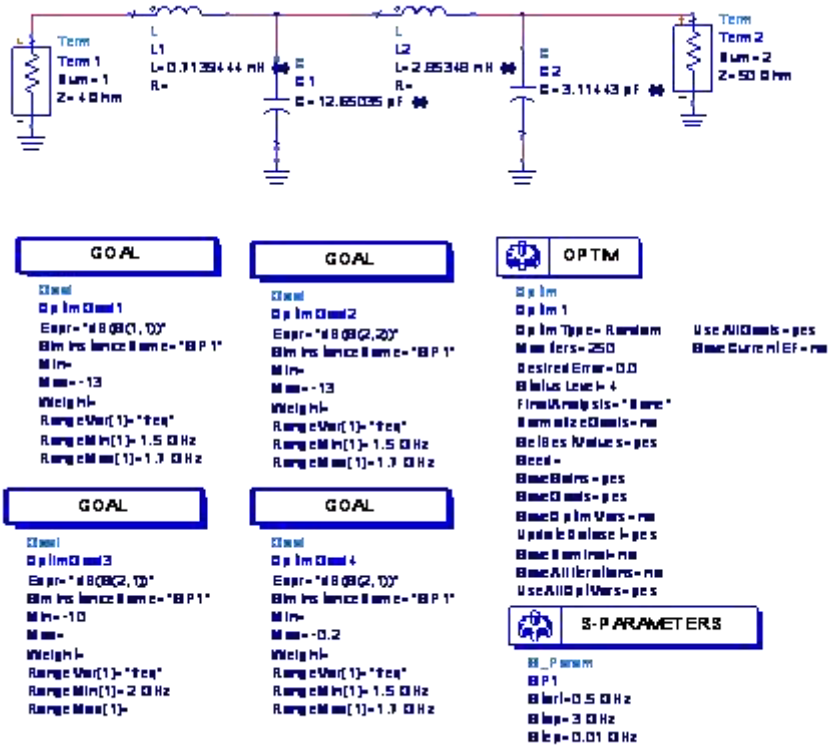

Figure 4.26 Simulation bench setup for HB output MN design

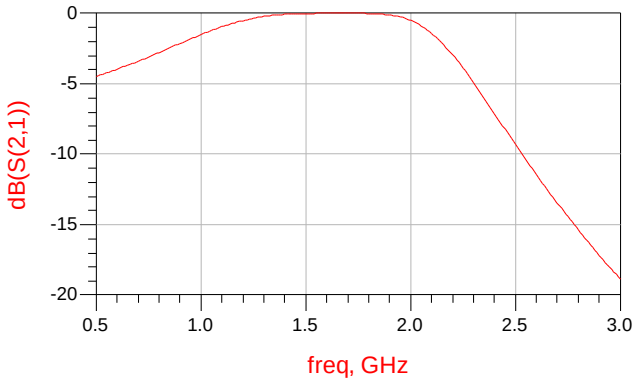

(a)

Figure 4.27 HB MN performance (a) insertion loss, (b) return loss

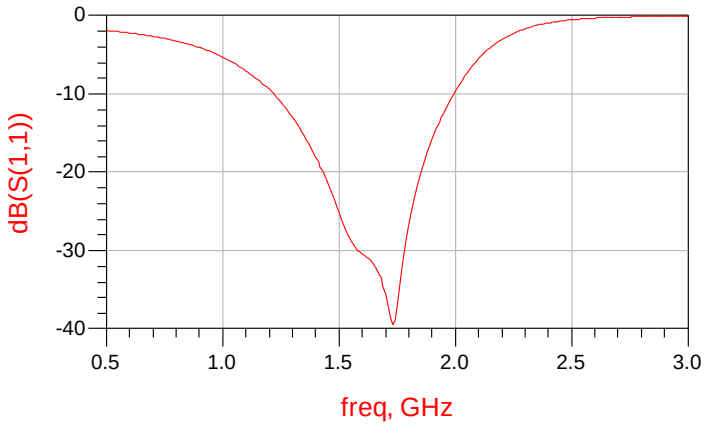

(b)

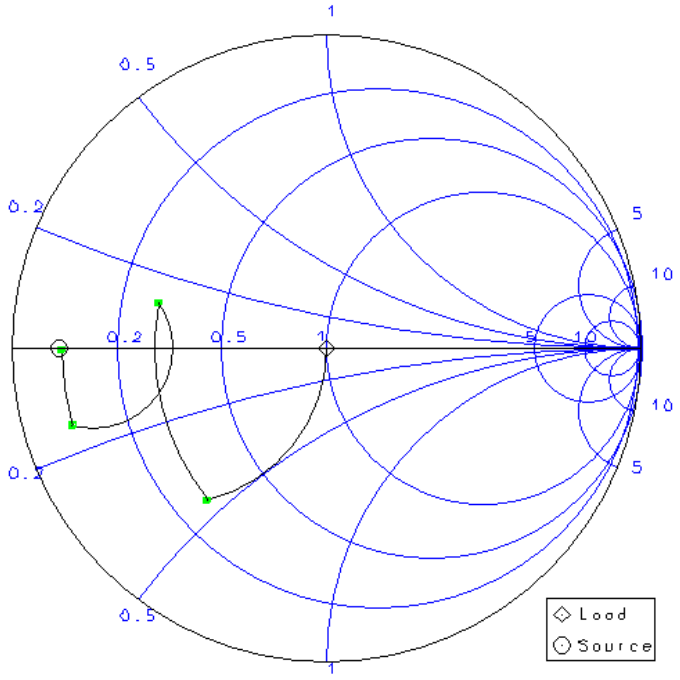

Figure 4.28 HB MN matching on Smith chart

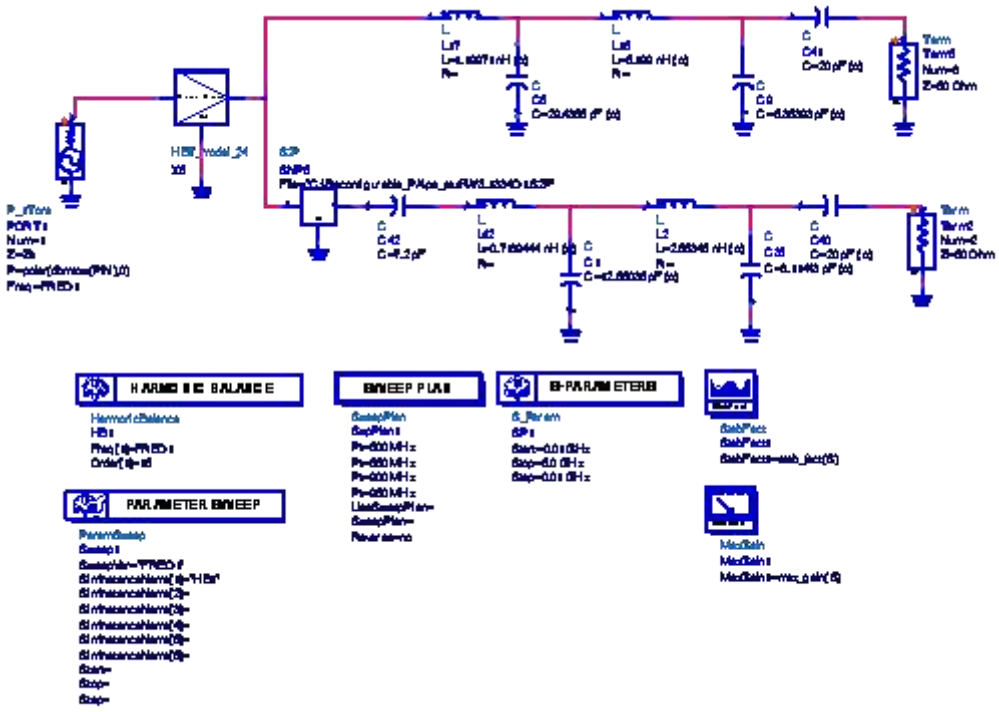

Figure 4.29 Bench setup for the Harmonic Balance and S-parameter simulation. (S-parameters of the MEMS switch provided by Radant has been used in the simulation [33])

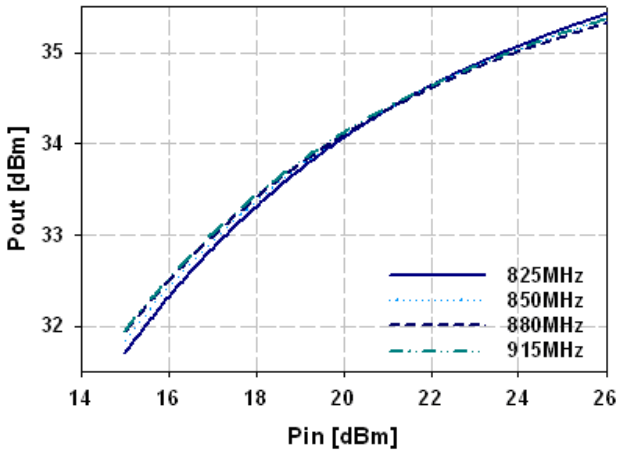

Figure 4.30 Pout vs. Pin, where a 17.5 dB input power is required to achieve a 33 dBm output power over the frequency range of interest

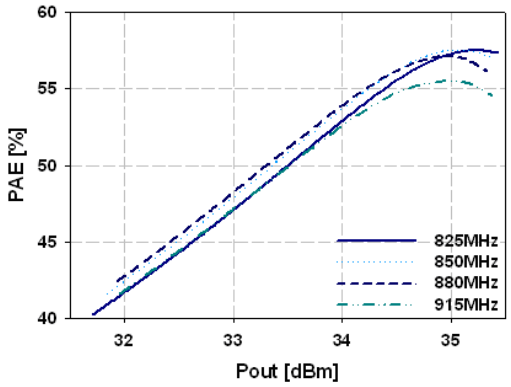

Figure 4.31 PAE vs. Pout at LB

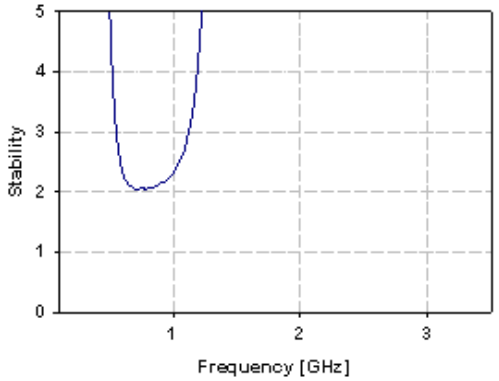

Figure 4.32 Stability (>1, the design is stable)

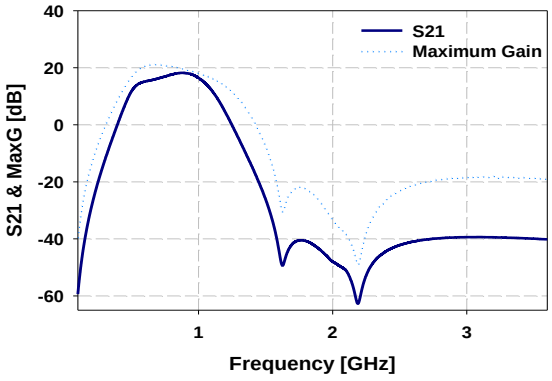

Figure 4.33 Maximum gain and S21

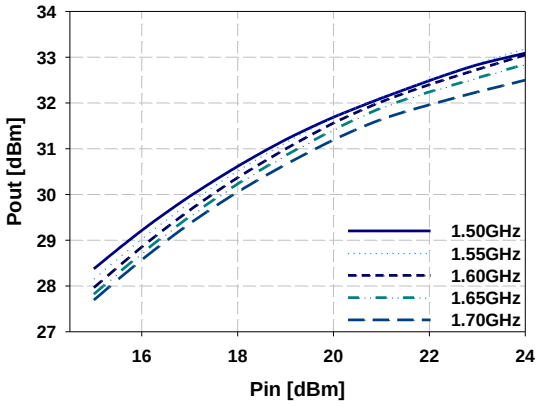

Figure 4.34 Pout vs. Pin, where an input power of 18-21 dBm is required to obtain 30 dBm output power over the 1.5 GHz to 1.7 GHz range

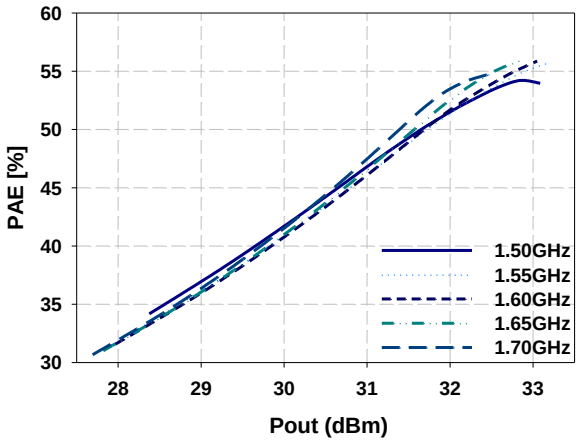

Figure 4.35 PAE vs. Pout

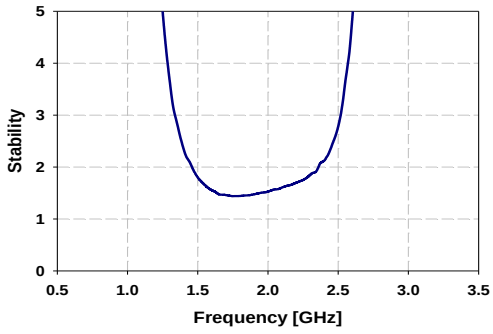

Figure 4.36 Stability (>1, the design is stable)

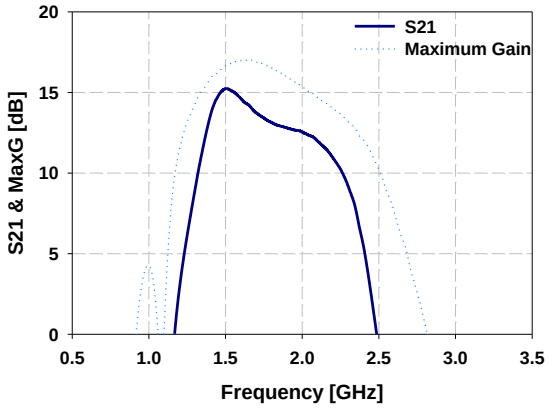

Figure 4.37 Maximum Gain and S21

Based on these simulation results, the reconfigurable PA design can sustain a high efficiency, multi-frequencies, and multi-mode operations with adequate bandwidths at each service (i.e. band or mode).

4.5.4 Reconfigurable PA module design Implementation:

The implemented reconfigurable amplifier is comprised of 4 blocks: the driver amplifier, the PA die, a switchable output MN and a MEMS switch. A schematic diagram of the integrated reconfigurable PA topology is shown in Figure 4.38. The driver amplifier unit is comprised of two amplifiers. The unit has two inputs and two outputs and its operation can be easily switched between these amplifiers to deliver either 24dBm at 900MHz or 22dBm at 1.6GHz. The output matching circuit consists of a multi-stage low pass MN for a wideband impedance matching.

The reconfigurable PA has two states. When the switch is OFF [33], path-1 is the selected signal path (shown in Figure 4.38). Simultaneously, the DC bias circuit turns ON all transistor cells to obtain the highest output power. It operates at 900MHz with a 33dBm output power, but when the Switch is ON, the reconfigurable PA operates at 1.6GHz with only 18 transistors turned on. Although in this state both path-1 and path-2 are connected to the transistor's collector, no significant loading from the low-pass LC matching network of path-1 at 1.6GHz exists, as it provides a sufficiently high rejection to the HB MN. Hence, the signal path in this case will effectively be path-2, as shown in Figure 4.38. For this path, only 75% of all transistor cells are turned on to deliver a 30dBm output power.

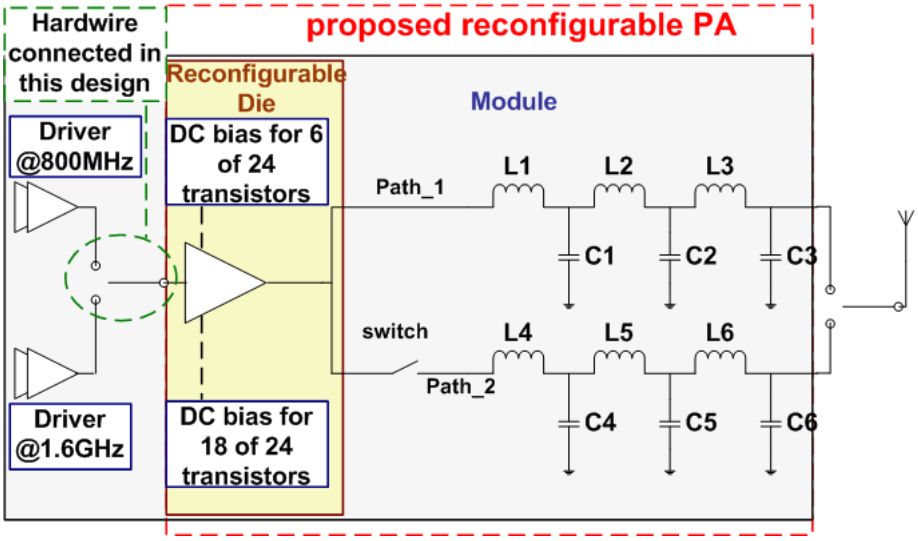

Figure 4.38 The schematic of the proposed reconfigurable PA module

4.5.5 Layout design and simulation

The layout step of the proposed amplifier is critical and the overall design should be re-evaluated prior to its final implementation. The reconfigurable PA die, as described earlier in this chapter, was designed using an HBT GaAs process. The output matching network was designed on a four-layer laminate substrate. The entire reconfigurable PA is a multi-chip module design.

4.5.5.1 Reconfigurable PA die layout

At low frequencies, the parasitic passive elements, such as the parasitic resistance inherent in the circuit, do not pose problems. At high frequencies, however, these parasitic components can dramatically impact the performance of the circuits. Therefore, we need to account for these parasitic in our design. Additionally, a simple layout design with minimal coupling between the elements can assist in realizing a stable circuit and good device performance.

4.5.5.1.1 Transistor layout [34, 35]

Basically, the presence of even minimal parasitic resistance will increase the DC power consumption, leading to a lower PA efficiency. To overcome this effect in our design, the transistor cells should be closely placed. The top layer metal was used to connect the collectors together and keep the signal path wide enough. In addition to the parasitic resistance, the thermal stability of the PA is another major issue for consideration in the final layout. From a thermal point of view, a disproportionate temperature distribution can create an uneven current density in each transistor cell and eventually destroy a portion of the transistors. In our design, the multi-cell

power devices are positioned side-by-side with equal spacing to avoid an uneven temperature distribution.

4.5.5.1.2 Current mirror layout [35]

Current mirrors are used to bias the HBT transistors. The current mirrors determine the PA performance via the quiescent current of the amplifier by multiplying the reference current. Note that the accuracy of this augmentation is important to the device's performance. From a layout point of view, however, this means the layout needs to provide a satisfactory symmetry. Symmetry also suppresses the effect of the common-mode noise and even-order nonlinearity. An asymmetric design will introduce input offsets. Additional detailed information about symmetry layout design can be found in [35].

The microphotograph of the designed reconfigurable die is shown in Figure 4.39, where two sets of bias control, 6 unit and 18 unit transistors, are indicated. The collectors (RF output collectors) are linked via a relatively wide metal line, as previously mentioned. The circuit has only one RF input and one RF output.

4.5.5.2 Reconfigurable module layout

A photo of the wire-bonded die attached to the module is shown in Figure 4.40. The driver amplifier of the die includes two medium power amplifiers, one for LB operations and the other for HB operations. In this prototype design, one of the amplifiers was connected at a time to the die via hardware. Thus, when the PA operates at LB, the LB driver amplifier is connected to all 24 transistors. When the PA operates at HB, the output of the HB driver amplifier is only connected to eighteen of the twenty-four transistors. This wire connection represents the interstage matching as well.

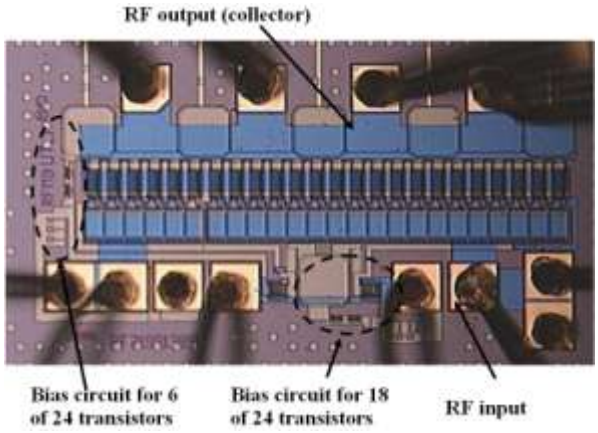

Figure 4.39 Microphotograph of the reconfigurable die

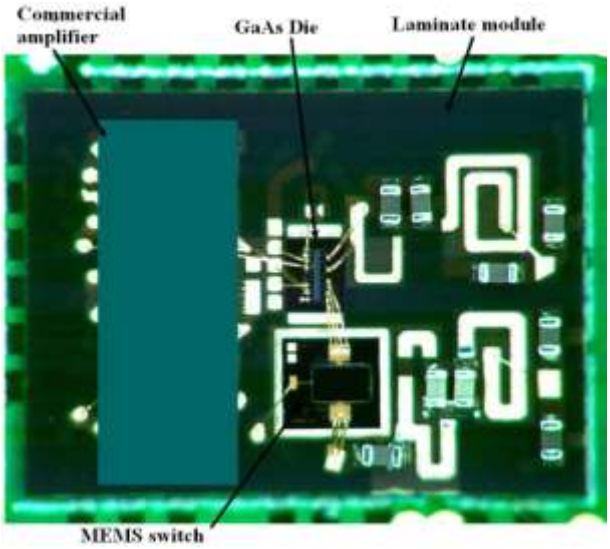

Figure 4.40 Microphotograph of the reconfigurable PA module on a laminate substrate

Both the LB and HB MNs are shown in Figure 4.40. In implementing the matching network, we use lumped element capacitors and printed spiral inductors (L1, L2, …LN). Inductors were connected to other components employing wire-bonding. Therefore, to account for this semi-lumped design, we performed a final design validation using a Momentum simulation to verify performance, after accounting for the various practical interconnected circuit implementations. The momentum simulation schematic and results are shown in Figure 4.41 and Figure 4.42.

The Momentum simulation includes the two states that account for the status of the switch. When the PA operates at LB, the switch is open, and when it operates at the HB, the switch is closed. The S-Parameters of the switch were used in the overall modeling of the MNs.

Based on the Momentum simulation, the MN accounts for an additional 0.6 dB insertion loss at LB, but this loss is significantly higher for the HB, due to the presence of the utilized MEMS switch. Using one MEMS switch has led to about 1.5 dB insertion loss in the HB. This creates a significant drop in the operating efficiency and will be discussed in the following sections.

4.5.6 Test bench setup and experimental results

Figure 4.43 depicts the bench setup used for measuring the PAE, $P_{out,}$ and drain efficiency. The signals applied to the board are the power supply and the input drive signal. The output was connected to the power meter via a 20dB attenuator, as a precaution for network analyzer measurements.

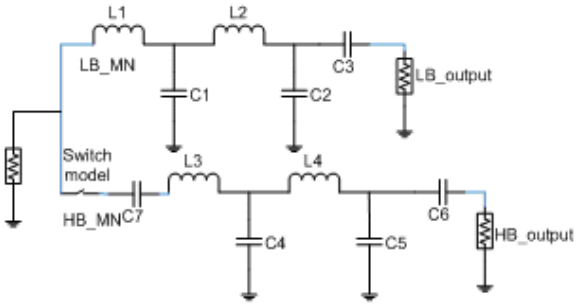

(a)

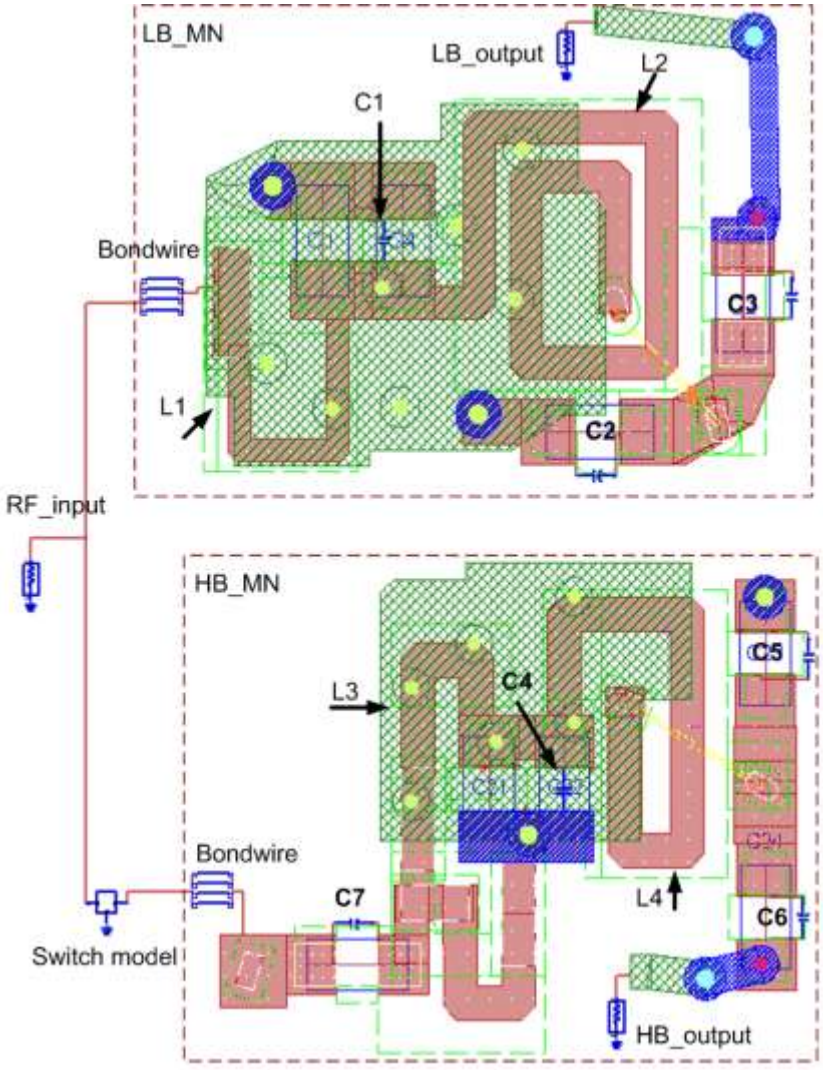

(b)

Figure 4.41 Momentum simulation setup (a) schematic; (b) layout

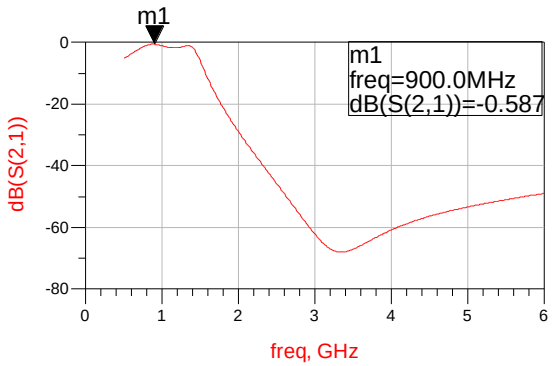

(a)

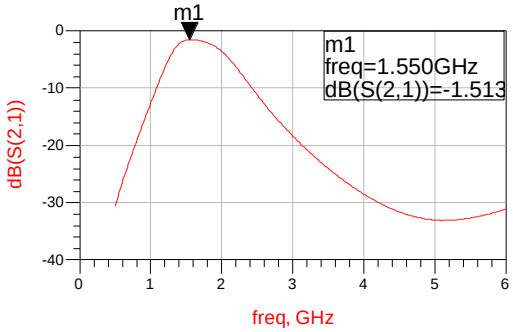

(b)

Figure 4.42 Momentum simulation result (a) LB; (b) HB

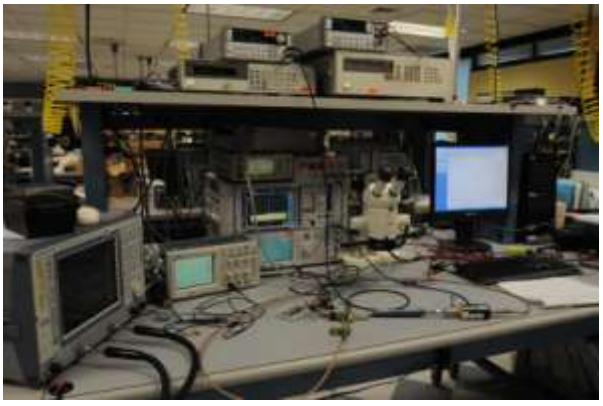

Figure 4.43 Measurement bench setup

The measured P_{out} and efficiency of the demonstrated reconfigurable PA is shown in Figure 4.44(a) and (b). The output power is approximately 33.8dBm at 0.9GHz with a 48% drain efficiency and 29.4dBm at 1.6 GHz with 55% drain efficiency. The PAE of the whole PA is shown in Figure 4.45(a) and Figure 4.45(b). It is over 43% and 26% efficiency for both the LB and HB, respectively.

By connecting the output of the PA to a network analyzer instead of to a power meter, the S-parameters of the whole PA are produced. The measured S21 parameters, when the reconfigurable PA operates at both the 900MHz and 1.6GHz, are shown in Figure 4.46.

4.5.7 Discussion of the measured results

In order to compare the impact of integrating the dual band amplifier using band-switchable matching networks on the overall performance, we have measured similar single band amplifiers designed on the same substrate to compare their performances. The measured insertion loss of the single band PA circuit was 0.726 dB at 900MHz, and 1.747 dB at 1.6GHz. When these results were compared to those of the reconfigurable amplifier, we concluded that only a slight increase of 0.1 dB in the case of the reconfigurable output MN at 900 MHz was noticed, but the loss at 1.6 GHz was substantial, a 0.96dB loss increase.

To analyze these results, we characterized the MEMS switch at both states, ON and OFF. The MEMS switch, when open at 900 MHz, provides a high isolation for the LB path. Note this is clearly demonstrated by the slight additional loss of 0.1 dB, when compared to the single band amplifier case. When operating at 1.6 GHz, the LB branch does not require the addition of a switch, as its effective loading on the HB branch was minimal. Note that only approximately 0.7 Ω. resistance at HB frequency and over a 35 dB isolation was measured between the two branches when the switch is ON at 1.6 GHz, as shown in Figure 4.47 (b). However, the MEMS switch, when in the ON state at 1.6 GHz, is in series with a 4 Ω path. Because the R_on resistance of the MEMS switch in this design is approximately 0.6 Ω..as shown in Figure 4.47 (c), a 0.72dB insertion loss is created, as shown in Figure 4.47 (d). When the PA operates at 1.6 GHz, the effective loading of the LB path, an additional 0.3dB insertion loss is created.

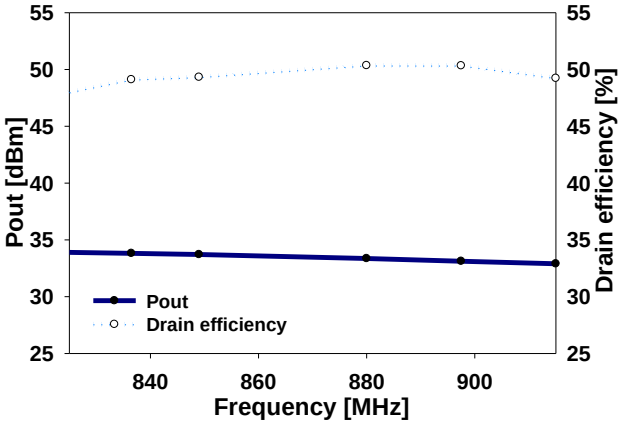

(a)

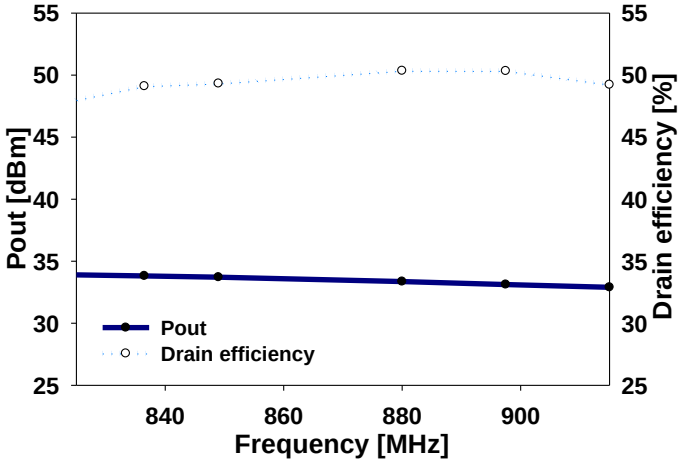

(b)

Figure 4.44 Reconfigurable PA output power and drain efficiency at (a) LB, (b) HB

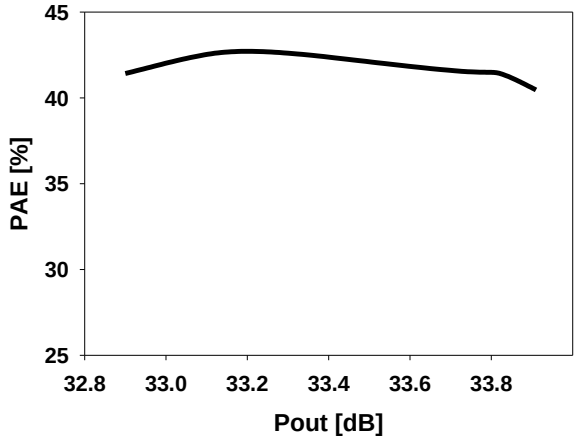

(a)

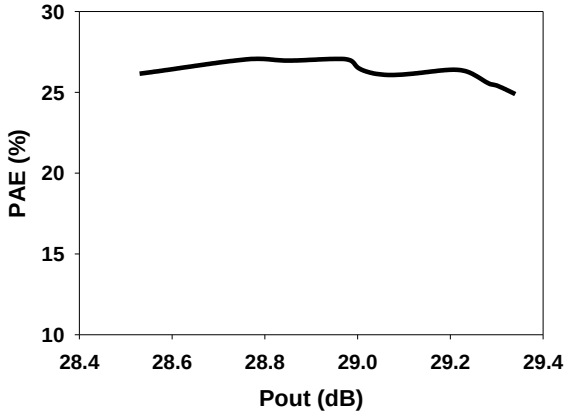

(b)

Figure 4.45 The reconfigurable PAE at (a) HB; (b) LB

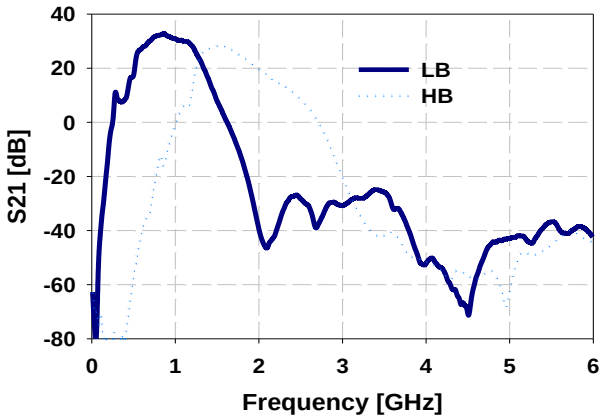

Figure 4.46 Large signal S-parameter measurement results

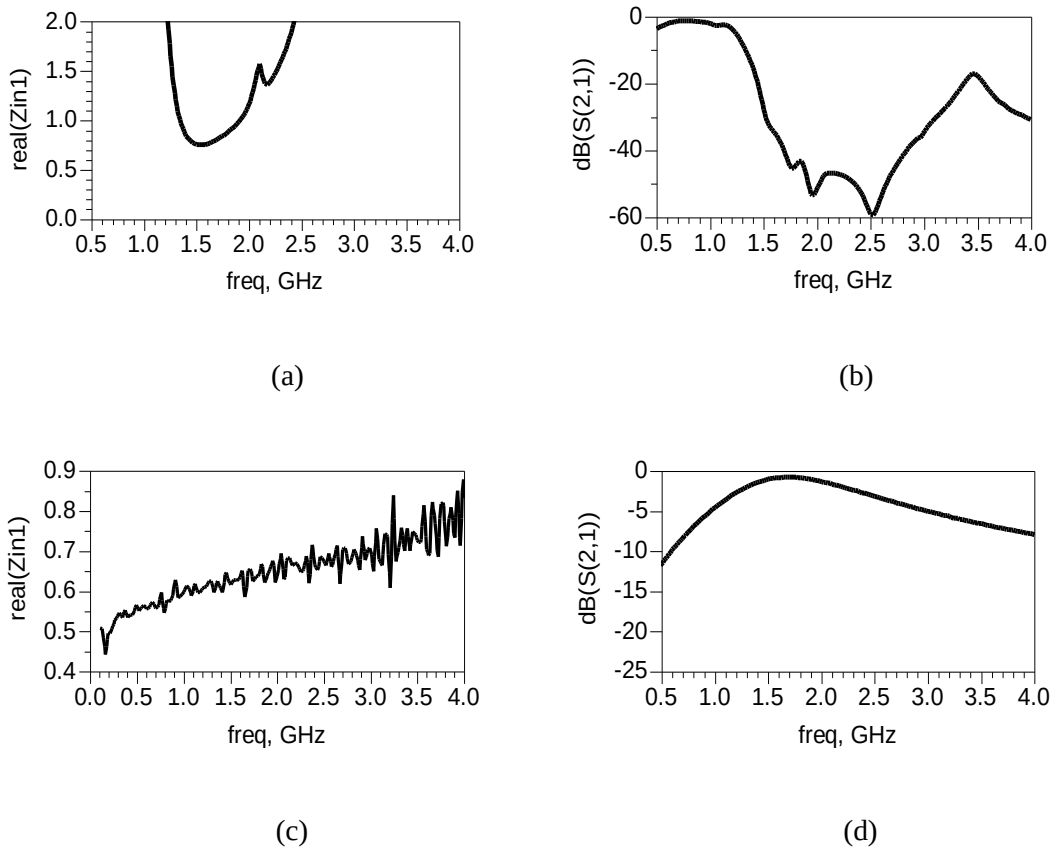

Figure 4.47 (a) Resistance of the LB path at the HB frequency, (b) Isolation of the LB path at the HB frequency, (c) Series resistance of the commercial MEMS switch, (d) Insertion loss

It is imperative to reduce the MEMS on-resistance. One way to demonstrate this is if we use more than one MEMS switch in parallel. The overall resistance could be significantly lowered. Adding three MEMS switches in parallel to our design, for example, would decrease the equivalent on-resistance from 0.7 Ω to approximately 0.2 Ω. Note that based on the simulation, shown in Figure 4.48, the additional insertion loss will decrease from 1.3dB to 0.7dB, which corresponds to a 6% PAE increase. At the same time, when operating at LB, all three switches are open. The circuits are expected to maintain at least a 30dB isolation, based on our simulation.

Table 4-8 summarizes our measured results and compares it to common approaches representing state-of-the art devices. As can be seen, this work demonstrated multi-frequency and multi-mode services application with good output power and a potential for adequate PAE performance.

4.6 Conclusion

The quick development of wireless communication system proves that multiple standards need to be supported by the wireless devices. The circuit board size limitation, isolation performance turning down, and single-pole-multi-through switch design challenges make the reconfigurable PA a viable choice for the traditional single PA design.

We have demonstrated a novel reconfigurable PA structure for multi-service applications. The reconfigurable PA structure can significantly decrease the real-estate, cost, and complexity of the PA design. For two services, the die and module sizes can be decreased by 50% and 20% of

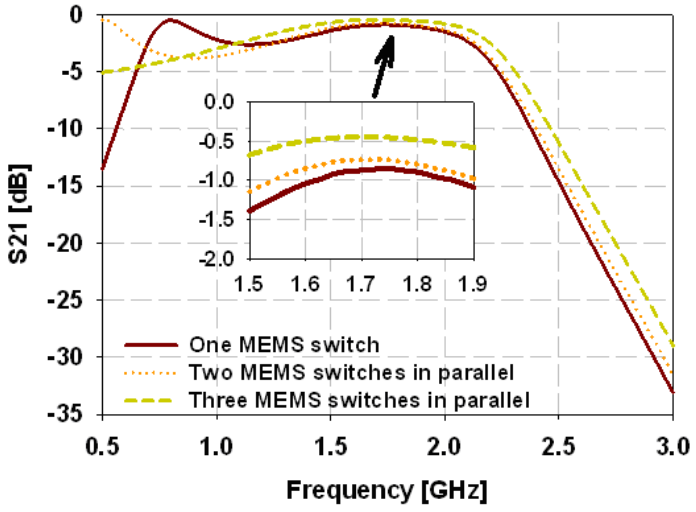

Figure 4.48 The insertion loss decreasing with less R_on

Table 4-8 Design target description

	Multi-frequency (MHz)	Multi-mode (dBm)	Performance and Implementation			
			Class	Pout	PAE	Realization
[36]	Yes	Yes	N/A	N/A	N/A	N/A
[23]	Yes	Yes	N/A	N/A	N/A	N/A
[24]	Yes 900 (LB), 1500(MB) & 2000 (HB)	No	Class B	29.8dBm (LB) 29.5dBm(MB) & 29.3dBm(HB)	60% (LB) 61%(MB) & 62%(HB)	Die (GaAs commercial), Module (Au-clad substrate with microstrip line)
[26]	Yes 850-950 (LB) & 1710-1950 (HB)	No	Class A	31dBm(LB) 31dBm(HB)	40% (LB) 40% (HB)	Die (InGaP/GaAs), Module (FR4 with SMD)
[25]	Yes 900 (LB) & 1800 (HB)	No	Class F	31dBm(LB) 30dBm(HB	40% (LB) 34% (HB)	Die (BiCMOS) Module (laminate)
This work	Yes 824-915 (LB) & 1500-1700 (HB)	Yes	Class A	33.8dBm(LB) 29.4dBm(HB)	43% (LB) 27% (HB)	Die (GaAs) Module (laminate)

Note: [36] and [23] are patents, with no measurement or simulation results.

SMD is a surface-mount device.

the single PA design size, respectively. For additional services, a greater size reduction can be achieved, compared to a traditional single PA design. This can effectively help to solve the emerging size limitation and isolation degradation problems. Further, by decreasing the number of output ports, the structure's complexity, with the single pole multi-throw switch structure connected immediately after the power amplifier, would be significantly reduced and hence, the overall insertion loss at the antenna port would be reduced as well. The additional insertion loss of the dual band amplifier, when compared to the single band PA approach, is influenced by the duplexer structure of the reconfigurable MN and the type of switch utilized for reconfiguring the MN. The measured efficiency in the developed power amplifier prototype is relatively low and can be improved by a custom-designed MEMS switch operating at a lower impedance level, for example, in a 4 ohm environment rather than in a 50 ohm system. The overall loss can be reduced further in multiple ways; such as utilizing a lower loss substrate and higher Q components.

Chapter 5 RECONFIGURABLE ANTENNA DESIGN FOR MULTI-SERVICE APPLICATIONS

5.1 Introduction

Previously, we discussed the multi-service requirements and various options necessary to solve the associated challenges in designing a RF front-end. It was concluded that few options exist to design antennas for multi-service communication systems. These options include using one of the following methods: individual, wide-band, multi-band, or reconfigurable antennas.

The first option, the single design approach (Figure 5.1(a)), is generally the least preferred method. The single design approach leads to a discrete RF front-end design instead of 4G goal of achieving a converged design. The second option is the utilization of wide-band antennas—an appealing alternative (Figure 5.1 (b)) where only one antenna is required for a multi-service system.

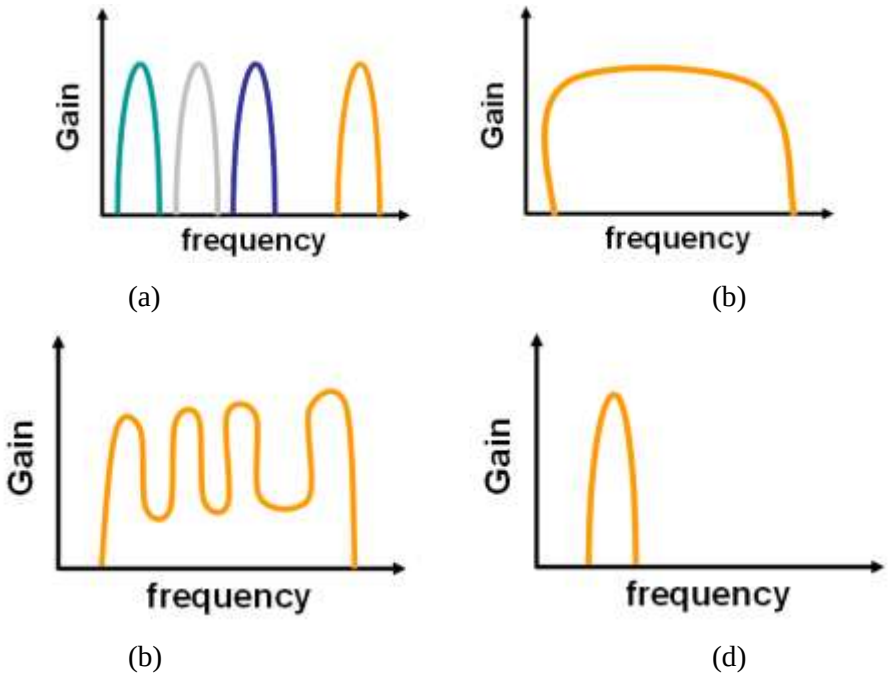

Figure 5.1 Different topology alternatives for multi-services wireless application (a) Use of separate receivers, one for each service, b) Wide band receiver where high Q filters are required, c) Multi-band design where performance is optimized at selected bands, and d) reconfigurable structure to receive one service at a time.

However, such a system would require a bank of highly selective filters which are used to reduce the effect of the relatively high input noise due to the wide noise bandwidth. The third option is multi-band antennas. Compared to wide-band antennas, the multi-band antennas could offer considerable rejection of out-of-band noise, thus reducing the required filter specifications and their associated cost (Figure 5.1(c)). Reconfigurable antennas (Figure 5.1(d)), which are reconfigured in accordance with their operating system requirements, have been investigated recently because of their flexibility to support multiple standards and their good out-of-band noise rejection performance. Therefore, reconfigurable antennas have great potential in realizing the next generation converged RF front-end.

In section 5.2 of this chapter, we will compare the differences among the different antenna design topologies and switching techniques. Based on our experience in developing various reconfigurable antenna structures, we will discuss in detail the various design challenges involved in developing these reconfigurable antennas in section 5.3. For illustration, two reconfigurable antenna structures, the reconfigurable patch and the reconfigurable monopole antennas, have been investigated for handset and laptop applications in a multi-service system. A detailed analysis of these reconfigurable antennas, including the processes which have led to the two antenna designs, will be presented in section 5.4-5.7. The conclusions will be given in section 5.9.

5.2 Various antenna topologies for a multi-service communication system

For the transmitter, the antenna is the final component before the modulated signal is transmitted into the air. The antenna is always connected to the signal path, in the transmitter, through a single-pole-multi-through antenna switch. With an increase in the number of signal paths required in a multi-service transmitter, the number of poles needed for the antenna switch increases as well. As previously mentioned in Chapter 2, unfortunately, with an increase in the number of poles of the switch, the insertion loss will also increase and the isolation will be decrease significantly. Meanwhile, for the receiver, the antenna is the first component before the selected signal traverses the system. In addition to the selected signal, a large quantity of noise is also received at the same time. To reduce the noise, multiple filters are added to the system. The majority of these filters are SAW or BAW filters, which are lossy and expensive. For example, the typical insertion loss of a SAW filter is between 2-3dB. A BAW filters insertion loss is considerably higher than that of the SAW filters.

Initially, the use of a single pole multi-throw antenna switch and filters in the system was not a cause for concern as it was supporting a relatively small number of standards. However, this is a

Table 5-1 A comparison among the common antenna topologies for multi-service communication systems

	Advantages	Disadvantages
Wide-band antennas	Relatively simple design.	Relatively large size; poor out-of-band noise rejection performance, requires a bank of high selective filters which increase the cost
Multi-band antennas	Medium design complexity; acceptable out-of-band noise rejection performance.	Poor out-of-operating-band noise rejection performance that requires a bank of high selective filters in the multi-service system which increase the cost and real estates.
Reconfigurable antennas	Acceptable out-of-operating-band noise rejection performance, less filters needed; flexible design.	Complexity design; need switches, which will cause DC consumption and insertion loss issues.

serious issue when additional poles for the antenna switch and filters are needed and becoming the primary consideration when choosing an antenna topology for the system. **Table 5-1** shows a comparison among the different antenna options for such an implementation: wide-band antennas [37-42], multi-band antennas [43-45], and reconfigurable antennas [46-52]. As can be concluded from the table, a reconfigurable antenna is a viable design candidate for a fast developing multi-service communication system.

5.3 Background on reconfigurable antenna design

A frequency reconfigurable antenna, which will be referred to as a reconfigurable antenna in the following portion of this dissertation, is an antenna that can dynamically change the operating frequency by adjusting either the antenna structure or the antenna effective aperture, or even both. Because the reconfigurable antenna dynamically changes the operating frequency among all supporting services, this topology can produce an acceptable out-of-operating-band noise rejection performance. As this is an important advantage in a multi-service system, the reconfigurable antenna design has recently become a hot research topic.

The reconfigurable antennas are typically based on a wide-band or multi-band antenna design and then we introduce a means for its reconfigurability. Many antenna structures, such as

the loop, patch, slot, monopole, and dipole antennas, are all suitable candidates for the reconfigurable antenna design.

The reconfigurable antenna design concept is not new and it has been utilized by multiple researchers. For example, a reconfigurable ground-slotted patch antenna using PIN diode switching, as shown in Figure 5.2, was reported in [49]. According to the authors, by controlling the PIN diode conduction, the antenna can switch between 1.85GHz and 2.35GHz with a 10dB return loss for approximately 60MHz bandwidth at 1.85GHz and 100MHz bandwidth at 2.35GHz.

In [52], the authors reported various rectangular antenna structures using MEMS switches. Slot antennas with six MEMS switches, shown in Figure 5.3, and a microstrip patch antenna with five MEMS switches, shown in Figure 5.4, were discussed. By controlling the MEMS switches, the antenna operating frequencies can be tuned.

However, reconfigurable antennas, when compared to the well developed wide-band and multi-band antennas, contain multiple issues that still need to be addressed prior to being commercially used. These issues include the need for a full solution for the various requirements of the multi-service systems and the design issues associated with the number, cost, and location of the reconfiguring switches.

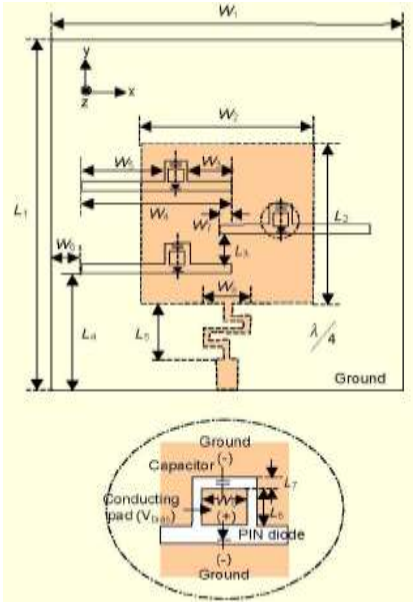

Figure 5.2 A reconfigurable ground-slotted patch antenna using PIN diode switches [49]

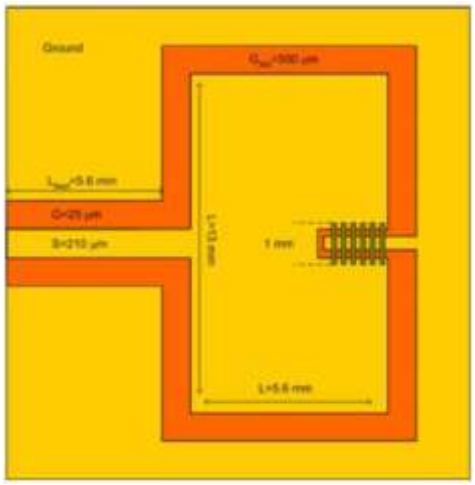

Figure 5.3 A reconfigurable slot antenna with MEMS switches [52]

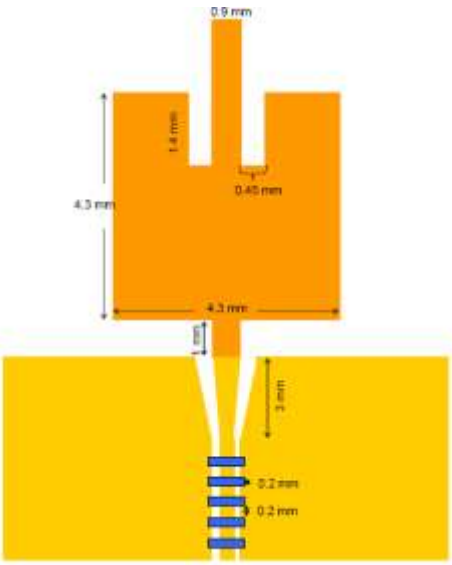

Figure 5.4 A reconfigurable patch antenna with MEMS switches [52]

5.3.1 A full solution for the various requirements of the multi-service systems

Based on the application requirements of a multi-service system, the reconfigurable antennas can be classified as a single service reconfigurable antenna, a mixed-service reconfigurable antenna, and a multi-band reconfigurable antenna.

1) For some multi-service systems, such as a 2.5G GSM cell phone system, only one service operates at a time, which means that the reconfigurable antenna can be designed only to resonate at one frequency at a time and still be reconfigurable among the other services. The advantage of this topology is that the antenna maintains the best noise rejection performance, minimizing the requirements for filters in the receiver chain. However, this topology requires a large number of switches in the antenna structure, which will increase the overall DC consumption, insertion loss, and further complicate the antenna design.
2) On the other hand, in a laptop system, it may require a WLAN 2.4GHz to operate continuously, and any other service can be tuned out. In this type of application, the antenna can be designed as a mixed-service reconfigurable antenna, which has a fixed structure for fixed services and a tuneable structure for the reconfigurable services.
3) A hybrid approach, which provides the reconfiguration capabilities to multi-band antenna structures, can be an acceptable compromise between the noise rejection performance, DC consumption, insertion loss, and complexity of the antenna design.

5.3.2 Switch design issues

One of the primary challenges of a reconfigurable antenna design is to integrate the switches into the antenna structure. Additional items that illustrate the difficulty of this challenge include:

1) Three-port commercial switches (MESFET switches and MEMS switches) are primarily designed for a 50Ω system. This is typical for RF circuit design, but not typical for an antenna structure.
2) The models of three-port commercial switches (MESFET switches and MEMS switches) provided by the manufacturers are the S-parameter models tested on a good ground test board. The antenna, however, typically can not provide such an environment for the switch.
3) The DC control lines can affect the antenna's resonance characteristics due to the coupling effects among the antenna, control line, and the parasitic radiations introduced by improperly isolated DC lines.

5.4 A reconfigurable patch antenna for a single service application

One example of a reconfigurable antenna design is a reconfigurable patch antenna design. Generally, the patch antenna is an attractive candidate for wireless devices because of its low profile, light weight, and ease of integration with RF circuits. Traditional patch antenna sizes are impractically large for wireless devices, especially for services in the 800-900 MHz range. However, significant patch size reduction can be achieved by utilizing the symmetry of the structure and can render smaller areas by approximately 75% of the area of the traditional patch antenna design.

Here, we developed a reconfigurable PIFA type patch antenna designed for a wide frequency range by using a nesting, or segmentation, approach. Both a PIFA concept and half U slot techniques have been used to achieve size deduction in the antenna. The reduced patch-size can still provide multi-band operations with noticeably similar bandwidth and radiation patterns to that of full size patches [53]. To demonstrate the development of this reconfigurable patch antenna, the design of the printed patch antennas with a PIFA structure is introduced first. Next, U slots are integrated into the patch antenna for multiple resonances. Subsequently, reconfigurability is introduced into this multi-band patch antenna structure to provide the multi-band operation.

5.4.1 Printed patch antenna with PIFA structure [54-56]

For a traditional patch antenna design, the patch dimensions of length L, width W, and thickness t, that is fed from a coaxial line at the center of the left edge (as shown in Figure 5.5), can be calculated. This is based on equations Equation 12 to Equation 14 [55]

$$L < \frac{\lambda_0}{2\sqrt{\varepsilon_r}} \quad , \qquad \text{Equation 12}$$

$$W < \lambda = \lambda_0 / \sqrt{\varepsilon_r} \quad \text{, and} \qquad \text{Equation 13}$$

$$t \square \lambda_0 / 100 \quad . \qquad \text{Equation 14}$$

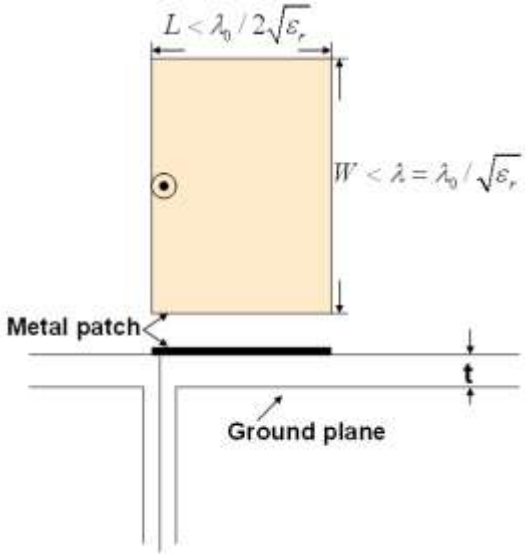

Figure 5.5 Top and side view of the conventional patch antenna fed by coaxial line at left [55]

To decrease this traditional patch antenna size; i.e.~λ/2xλ/2, the PIFA concept can be employed. The antenna structure, which is a patch structure in this example, is printed on a substrate. Meanwhile, the ground plane, which basically is a large piece of metal, is printed on another substrate. These two metal parts are separated by a distance, H, which is mostly air-filled, as shown in Figure 5.6.

The patch structure is then shorted to ground to decrease the size of the patch by a factor of 2 [57]. The resonant frequency for such structure, as shown in Figure 5.6, can be calculated based on equations Equation 15 to Equation 17[57]

$$L1 + L2 = \lambda / 4, \qquad \text{Equation 15}$$

when $W / L1 = 1$, then $L1 + H = \lambda / 4$ and Equation 16

when $W = 0$, then $L1 + L2 + H = \lambda / 4$. Equation 17

where *L1* and *L2* are the patch side dimensions, *W* is the shorting pin (plate) width, and *H* is physical spacing between the patch and its ground plane.

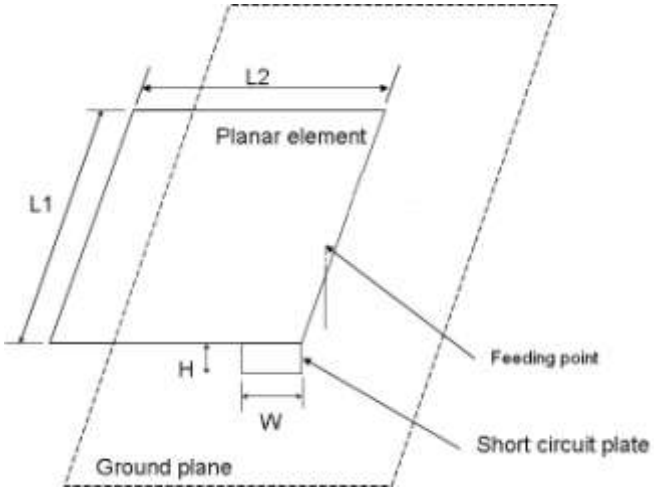

Figure 5.6 Planar Inverted F Antenna [57]

The presence of the ground plane of the PIFA antenna is an advantage for cell phones because of their relatively low SAR (Specific Absorption Rate).

5.4.2 Multi-Band operation

In 1997, Huynh and Lee introduced a U-slot patch antenna [58] for multi-band operations. Recently, size reduction techniques, such as using a shorting wall or shoring pin, used in the design of the PIFA patch antenna, have been successfully applied to the U-slot patch antenna designs [59]. The lower resonant frequency of the U-slot patch antenna can be roughly calculated from Equation 15 to Equation 17. Meanwhile, the upper resonant frequency, controlled by the width and length of the slot, is given by

$$f_L = \frac{c}{4(L+W)\sqrt{\varepsilon_r}} . \qquad \text{Equation 18}$$

Note: L and W are the length and width of the patch.

To realize a multi-band patch antenna, three slots are integrated into the patch structure. This patch antenna with three slots will resonate at four frequency bands. Segmented patch sizes were

selected, based on Equation 15 to Equation 18, to operate at distinct and multi-resonant frequencies in order to cover some or all of the GSM, GPS, PCS, and WLAN services.

To further reduce the patch antenna size, another size reduction technique which would decrease its size by half based on its symmetry, has been used to achieve an additional 50% size reduction, as shown in Figure 5.7. Introducing a half U-slot in the PIFA structure, based on reference [53], did not appreciably degrade the performance characteristics of these modified structures when compared with their original sizes. Bandwidths of 20% and 25% were achieved for half U-slot patch antennas with a shorting pin and half E-shaped patch antenna, respectively. Radiation patterns and radiation efficiencies of the half structure antennas were similar to that of their full-size geometries [53].

Even and odd symmetries have been utilized. Where even symmetry reduces the structure's size by approximately 50%, odd symmetry achieves an additional 25% size reduction of the original full-size patch structure. The developed multi-band antenna is comprised of multiple nested patches in order to attain the necessary compactness. However, a bank of highly selective filters, to follow the antenna, is still required to reduce the overall input noise from any unused bands.

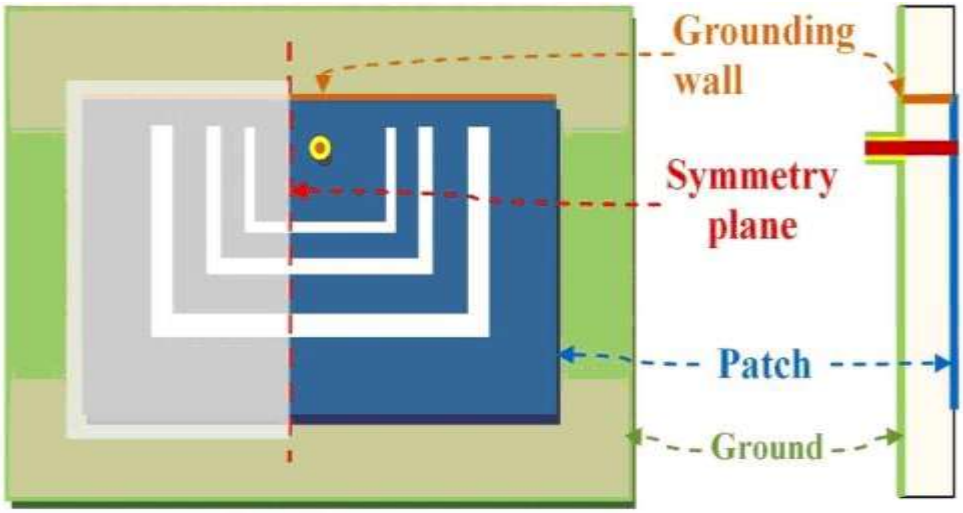

Figure 5.7 The reduced size nested-patch multi-band antenna

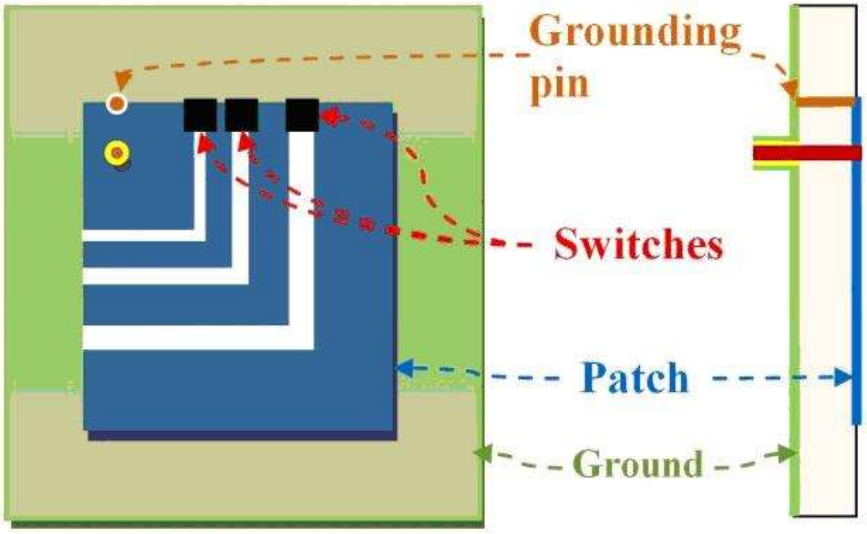

Figure 5.8 The reduced size nested-patch reconfigurable antenna

5.4.3 Reconfigurable operation

The multi-band structure, shown in Figure 5.7 [46, 56], has been redesigned for reconfigurability by employing four switches to control the interconnectivity of the patch's different segments. The redesigned multi-band structure is illustrated in Figure 5.8 [46, 56]. To realize this, the shoring wall has been replaced by a shorting pin, as shown in Figure 5.8. The overall size, as indicated earlier, is 25.2mm x 29.7mm x 8.2mm, and it is approximately 25% of the original full-size patch antenna. This developed design has been implemented on a 1.6mm thick FR4 substrate.

Nested patches were printed on the top layer. MEMS switches were utilized to minimize DC power consumption. DC control lines were printed on the bottom layer and the MEMS control voltage for the utilized Radant switch is 90V. The ground plan is printed on another 1.6mm FR4 substrate and the space between the antenna and ground plane is 4.5mm. Foam was used to sustain the spacing between the patch and the ground plane.

Figure 5.9 shows the schematic of the reconfigurable patch antenna. Figure 5.10 shows the fabricated circuit and Figure 5.11 shows the acceptable measured return loss. Figure 5.12 to Figure 5.15 show the reconfigurable antenna measured radiation patterns at various frequency bands. The antenna position for measurements is the same as in

Figure **5.9**.

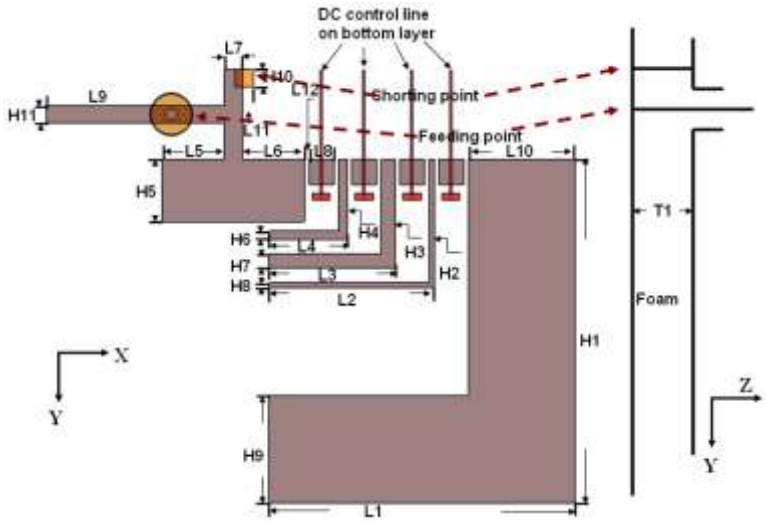

Units (in mm)

L1	20.2	L2	12.3	L3	9.3	L4	6.9
L5	3.5	L6	3.5	L7	1	L8	1.45
L9	10	L10	6	L11	1	L12	0.25
H1	19.2	H2	7.2	H3	6.1	H4	4.5
H5	3.5	H6	0.5	H7	0.8	H8	0.3
H9	6	H10	1	H11	1	T1	4.5

Figure 5.9 The reconfigurable patch antenna schematic

Figure 5.10 Photograph of the fabricated reconfigurable patch antenna

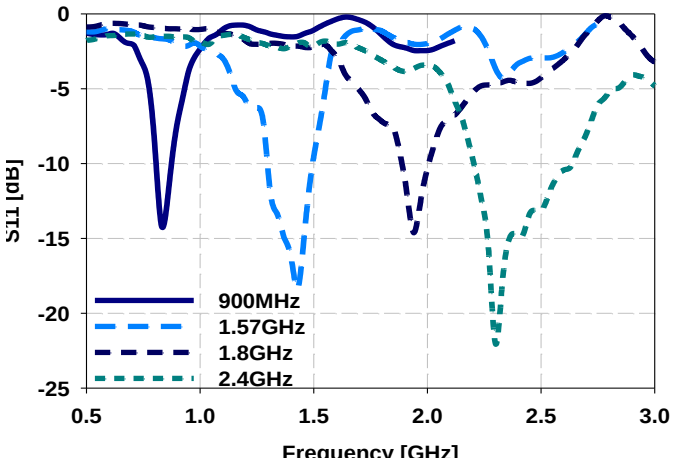

Figure 5.11 Measurement return loss of the reconfigurable patch antenna

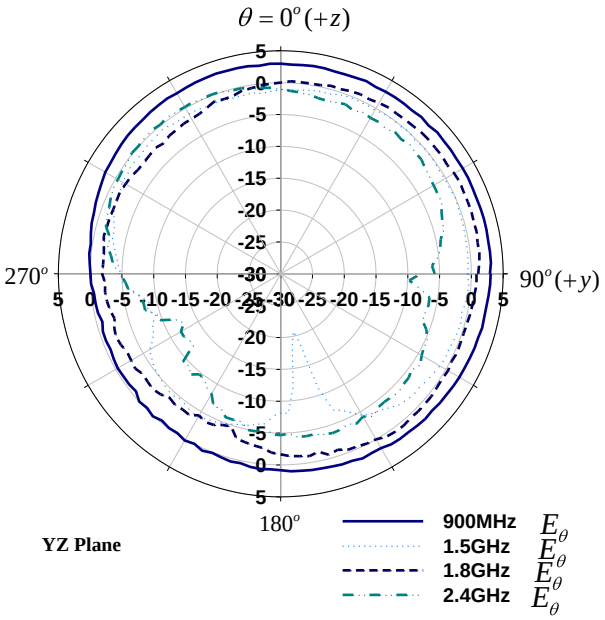

Figure 5.12 Measurement radiation patterns (direction is the same as in Fig. 1.5)—YZ plane E_θ

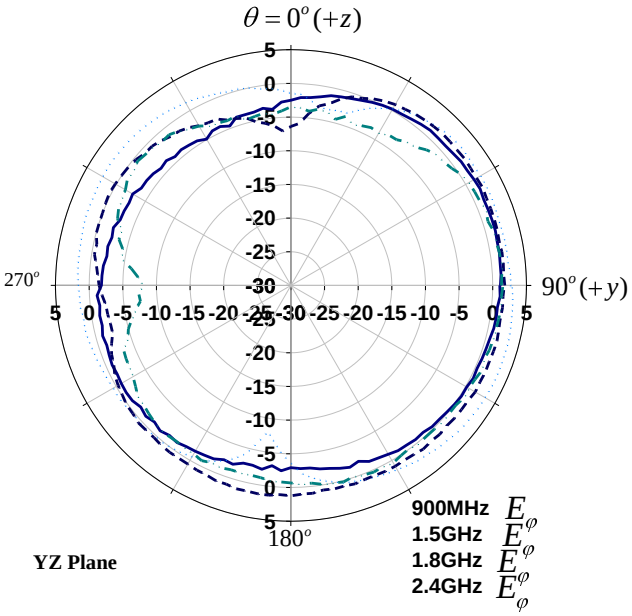

Figure 5.13 Measurement radiation patterns (direction is the same as in Fig. 1.5)—

YZ plane E_{φ}

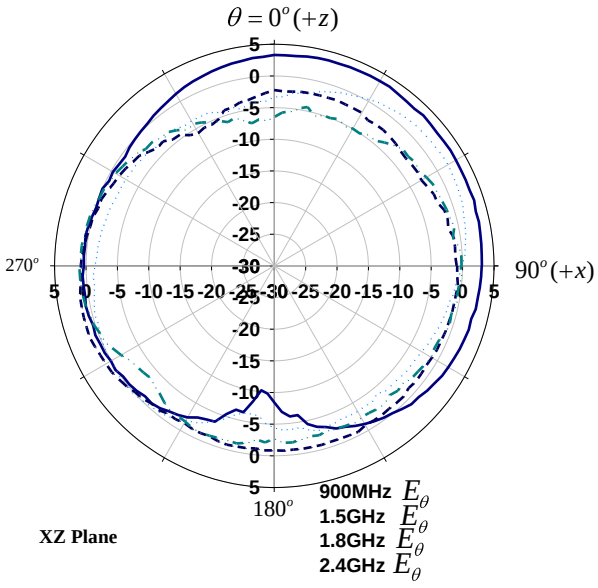

Figure 5.14 Measurement radiation patterns (direction is the same as in Fig. 1.5)–

XZ plane E_{θ}

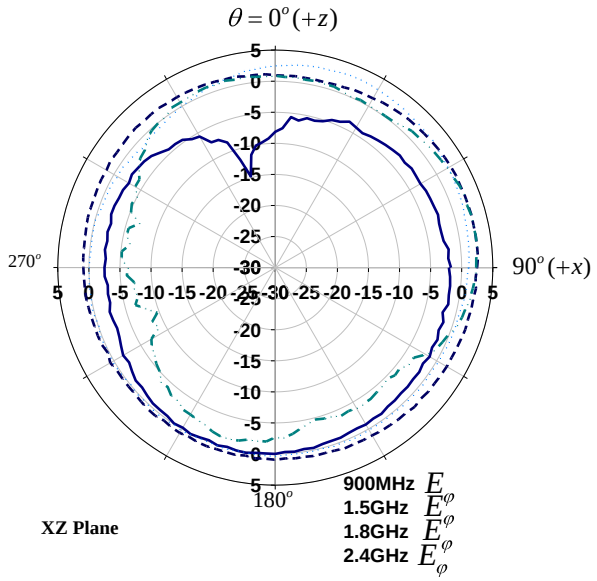

Figure 5.15 Measurement radiation patterns (direction is the same as in Fig. 1.5) – XZ plane E_φ

5.5 Reconfigurable antenna design for mixed services application [46, 56]

The developed multi-segmented reconfigurable antenna can be easily optimized to cover one band at a time with minimal input noise. Although these structures can have higher order resonances; i.e. spurious modes, the resonances can be eliminated simply by using filters that are relatively wideband. They are also easily implemented because the spurious resonances are displaced at a distance from the operating range.

This developed reconfigurable structure is only adequate for switchable bands, such as the GSM, DCS, and PCS which will not be used simultaneously. However, a number of services, such as WLAN, may be ON at all times. Therefore, it is necessary to split the input-feed into two branches: one for the fixed services and the other for switchable services.

To realize this, a printed monopole has been incorporated into the patch antenna structure for the fixed services. Typically, a monopole antenna's length is $\lambda/4$. In this design, because the monopole antenna not only shares the same feeding point with the patch antenna but also the shoring pin, by shorting the monopole to the ground, the length of the monopole has been effectively decreased to half of its original length.

The developed structure, and its hard-wire connected reconfigurable antenna's performance at the fixed service (the 2.4 GHz service here), is shown in Figure 5.16 through Figure 5.18.

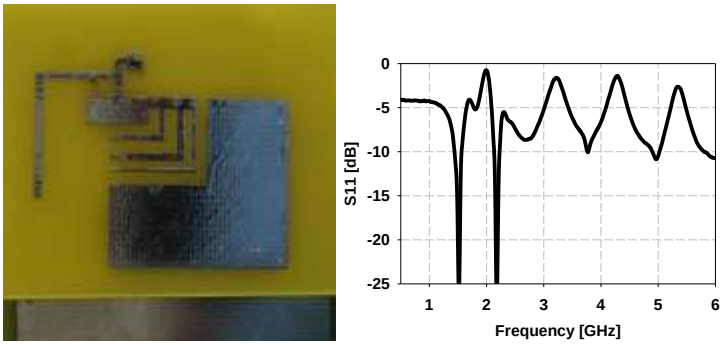

Figure 5.16 Hard wire connected reconfigurable antenna structure and measured return loss of the reconfigurable patch @ 1.57GHz and fixed Monopole @ 2.4GHz

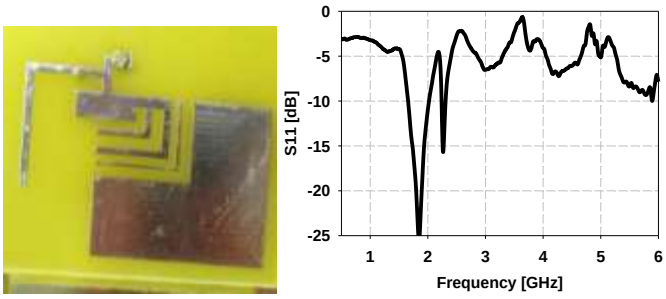

Figure 5.17 Hard-wire connected reconfigurable antenna structure and measured return loss of the reconfigurable patch @ 1.9GHz and fixed Monopole @ 2.4GHz

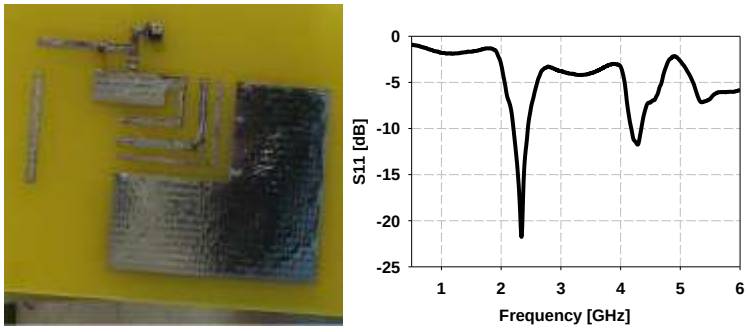

Figure 5.18 Hard-wire connected reconfigurable antenna structure and measured return loss of the reconfigurable patch @ 2.4 GHz and the fixed Monopole is disconnected (turned off)

5.6 Conclusions on the reconfigurable patch antenna for the single and mixed services applications

The developed patch antennas, with a 75% size reduction, are advantageous for handheld wireless devices. They are compatible with multi-layer PCB (Printed Circuit Board) technology and could offer inherent back radiation shielding. They are suitable for both multi-band and reconfigurable operations. The developed reconfigurable patch antenna does not require stringent subsequent filtering stages and has demonstrated improved S/N and anti-jamming features. It can also be adapted for one service at a time to address either switchable services or mixed services by using branched structures.

However, the developed reconfigurable antenna is relatively limited if more than one service is needed concurrently. The need for multiple switches could drastically increase its cost and unnecessarily increase complexity. Meanwhile, multi-band antennas are low cost, relatively simple to manufacture, and currently popular, but they suffer from relatively poor noise bandwidth and weak anti-jamming performance. Therefore, as an optimum solution, we can combine both strategies and develop a reconfigurable multi-band approach to achieve a compromise among complexity, cost, and performance. This approach will be investigated in the second illustrative example.

5.7 The reconfigurable multi-band antenna design for multi-service application [60]

Reconfigurable antennas are tailored to reject the noise over all bands that are not in use, which leads to a significant noise rejection performance enhancement. However, the multitude of switches required to operate a reconfigurable antenna could increase power consumption and drastically increase fabrication cost.

To realize the advantages of reconfigurable antennas while limiting their power consumption and fabrication costs to an acceptable level, a reconfigurable multi-band antenna was designed for wireless applications. The design is based on a hybrid concept in which various service groups are established and a means for switching among the service sets is provided. This concept is a satisfactory comprise between better noise rejection and less number of switches. However, several rules should be considered for frequency bands groupings:

1. The competing standards which are used for the same service in different countries can be classified into one group.
2. The standards which operate at the same time should be classified into one group.

3. The standards that are close in the frequency domain and do not need to operate at the same time should be classified into different groups.

In this design, each service set is comprised of three frequency bands and the reconfigurable antenna switches between two multi-band designs, one for each set. With these two sets, we can cover up to six services while utilizing only three switches.

5.7.1 The demonstration of the reconfigurable monopole antenna Structure and Implementation

In this section, the design process, which led to a reconfigurable monopole antenna, will be introduced. Its slim compact design of 96 mm x 9 mm x 3 mm is within laptop size constraints, but the size of the antenna can be reduced even further by meandering its branched-lines. The measured preliminary performance of the reconfigurable monopole antenna for both the hard-wire connected and switches-connected reconfigurable antenna will be provided to demonstrate feasibility. However, the final design refinement should be performed for a given packaging environment as it will have pronounced effects.

Here, we use a two-branched monopole structure. Each branch is a multi-branched monopole which itself provides a multi-band operation, but all branches share the same feeding point. Three switches are used to provide reconfigurability.

First, two branches are printed on a 0.05mm Kapton substrate, as shown in Figure 5.19. Because the final form is a 3-D structure, we will name the branch on the top half of the picture as the back part and the other branch at the bottom of the picture the front part. Then, the antenna is folded from the central section and separated by a piece of foam with a thickness of 3 mm. The

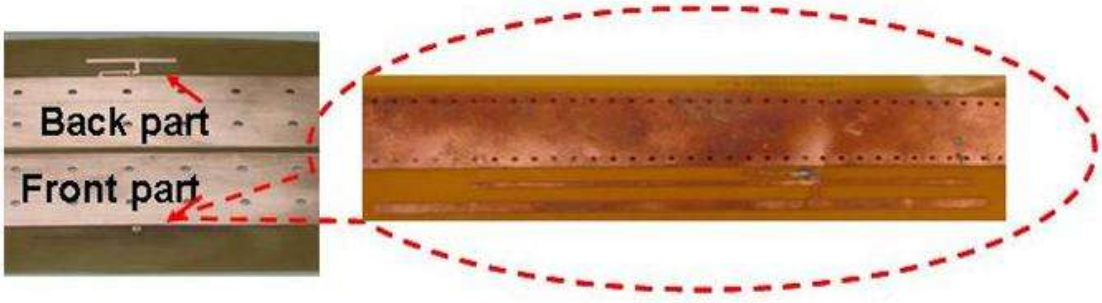

Figure 5.19 Proposed two parts of the reconfigurable Multi-band Antenna printed on Kapton substrate

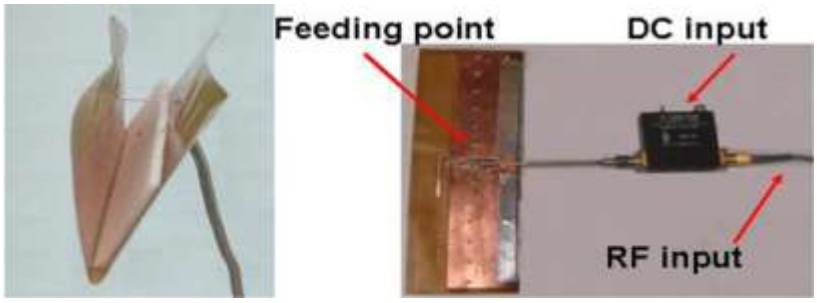

(a) (b)

Figure 5.20 (a) folded from center, foam was used to fix two sides, (b) RF and DC signals input though Bias Tee. (No extra DC control line).

front part is glued to the top surface of the foam and the back part is glued to its bottom, as shown in Figure 5.20(a). The two sides are connected via the inner conductor of the feeding cable which is connected to a Bias-T at the front part. Both the RF and DC signals (See Figure 5.20(b)) are then simultaneously fed through a cable, with no extra DC control lines required. The entire antenna is subsequently mounted above the top edge of a large ground plane in order to emulate a laptop. In this design, switches have been intentionally placed close to the ground and are assembled to either turn ON the front side or the back side of the antenna.

First, the performance of the separate front and back parts of the antenna will be discussed, and then the performance after assembling (i.e. integrating) the two parts will be described in detail (See Figure 5.21). As expected, however, the ultimate performance of the separated parts could be significantly different upon integration. This initial design, therefore, must be optimized in the final stage of the design.

5.7.1.1 Back Part Performance [61]

A schematic of the back part of the antenna is shown in Figure 5.21(a). It is comprised of one T-shaped branched-monopole for multi-band operations. The monopole has two horizontal arms denoted by 6-7 and 6-8, each of which is a different length. The two arms are fed by a coaxial line at point 5, while the short-circuited stub, L8, is used as part of the monopole antenna structure for matching. The lengths of the long arm, 6-8, and the short arm, 6-7, are adjusted to provide resonances at 2.4GHz and 5.2GHz, respectively, as shown in Figure 5.21(b).

Upon turning OFF the diode, i.e., switch 3, the monopole is no longer matched at 2.4 or 5.2 GHz, as depicted in Figure 5.21(c). However, upon integration, the back part of the monopole will be subsequently connected to another short circuit on the front part. It will have a different

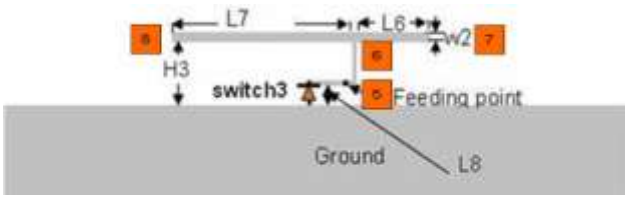

Unit: mm

L6	7	L7	24	L8	0.5	W2	1.5
H3	3.5						

(a)

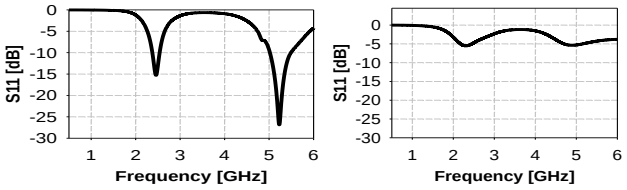

(b)

(c)

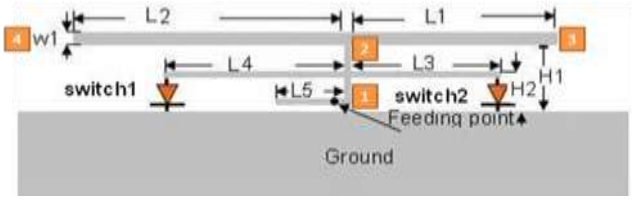

Unit: mm

L1	28	L2	67	L3	26	L4	52
L5	11	W1	2	H1	6.5	H2	3.5

(d)

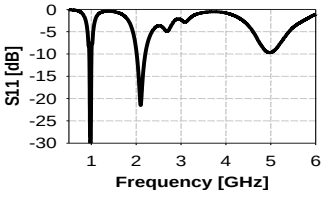

(e)

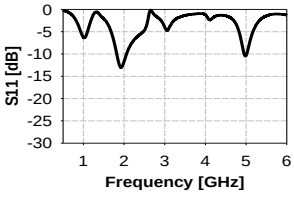

(f)

Figure 5.21 (a) Schematic of the back part, (b) The back part return loss with shorted strip, (c) The back part return loss without shorted strip, (d) Schematic of the front part, (e) The front part return loss with shorted strip, (f) The front part return loss without shorted strip.

set of resonant frequencies that are significantly lower than the frequencies when switch 3 is ON, given that the length of this short circuit stub on the top is relatively longer—as will be described in 5.7.2.1.

5.7.1.2 Front Part Performance [62]

Design ideas similar to those of the back part have been implemented for developing the front part as well. A branched structure is utilized here, but its arms, 2-3 and 2-4, are significantly longer than the back part arms, 6-7 and 6-8, in order to operate at relatively lower frequencies. However, as it is not practical here to utilize the λ/4 sections, we have loaded the monopoles with shunt-stubs (L3&L4) to effectively reduce their required overall lengths, L5 and L6. These stubs can be terminated in either open or short circuit terminations for reconfigurability. This monopole structure has been designed to operate at both 1 GHz and 2.1 GHz (see Figure 5.21(e)). However, these resonances are slightly higher than the resonances required at 900 MHz and 1.9 GHz after integration, in anticipation of an effective resonance-shift due to the anticipated significant proximity coupling effects upon assembling the two parts.

On the other hand, when the two front switches are OFF, the two resonances are now at 2 GHz and 5 GHz (as seen in Figure 5.21(f)). Note that when the front and back parts are connected, these resonances will be slightly different due to their new interconnectivity to another short circuit, which is now on the bottom part. Fine tunings are needed in the final stage.

5.7.2 Integrated Hard-Wire Connected Antenna Performance:

5.7.2.1 State1:

In this state, the front part switches are ON and the back part switches are OFF. The front part resonates at 900MHz and 1.9 GHz, while the effective loading of the back part has caused a resonance of approximately 4.8 GHz (as seen in Figure 5.22). This resonance could be due to the new loading of the previous resonance of the back part at 5.2 GHz.

5.7.2.2 State2:

By reversing the polarity of the DC bias, the back part switch should be ON and the two switches on the front part are OFF. This configuration creates four distinct resonances. The two resonances associated with the back part should be at 2.4 and 5.2 GHz. In addition, there are two additional resonances operating at 0.8GHz and 1.7 GHz, as shown in Figure 5.23. The 0.8GHz and 1.7 GHz resonances are due to the frequency shift of the 1GHz and 2.1 GHz seen before for the unassembled front part, but the 5.2 GHz resonance has significantly shifted to 4.8 GHz.

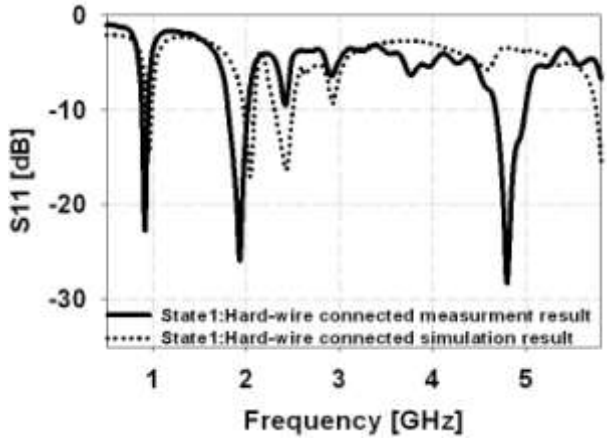

Figure 5.22 Hard wire connected reconfigurable antenna simulation result and measurement result at state1

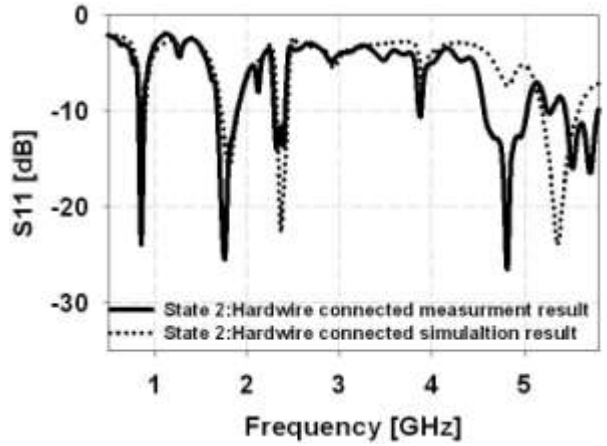

Figure 5.23 Hard wire connected reconfigurable antenna simulation result and measurement result at state 2

As can be seen, the resonating frequencies shift because of the coupling effects between the two parts. Fine tunings are needed when switches are integrated into the antenna.

5.7.3 Integrated Switches Connected Antenna Performance:

This reconfigurable antenna was first assembled using hard-wire connections for feasibility, and then an antenna with PIN diodes was implemented. Simulation results with ideal PIN diode model were in agreement with the measured results of the reconfigurable antenna prototype (see Figure 5.24 and Figure 5.25). The parasitic capacitance of the PIN diode switches needs to be accounted for to model these reconfigurable structures, especially above 3 GHz. PIN diodes have been modeled here as a small capacitance in the OFF state and a resistor in the ON state. Based on the PIN diode datasheet [63], we utilized a 0.15pF capacitor for the OFF state of the switch and a 2.5 Ohm resistor for the ON state. Now, the antenna is in state 1, as seen in Figure 5.24, and has resonances at 900 MHz, 1.9 GHz, and 5.25 GHz. Meanwhile, at State 2, it has resonances at 800 MHz, approximately at 1.7 GHz and 2.4 GHz.

Radiation patterns of the developed antenna have been measured. The measurement position of the antenna is as position 1, shown in Figure 5.26. Examples of the measured radiation patterns are shown in Figure 5.27 through Figure 5.30. It was found that a hard-wire connected antenna's gain at the various states, covering the different services, was in the 2 to 4dBi range. Meanwhile, when measuring the reconfigurable structures with the real switches, less than a 0.9 dB drop in gain has been noticed at the different frequency bands, when providing approximately a 100mA DC bias current for each switch in the ON-state.

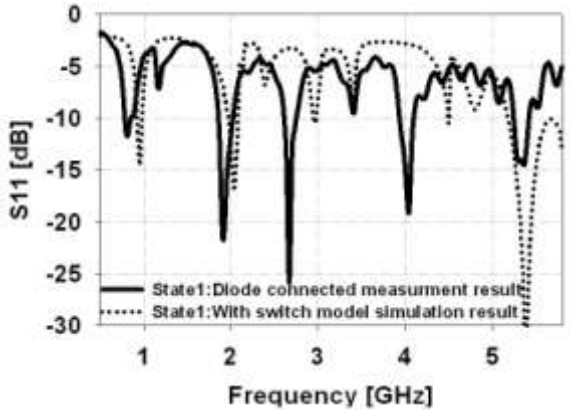

Figure 5.24 Reconfigurable antenna simulation result and measurement result at state1

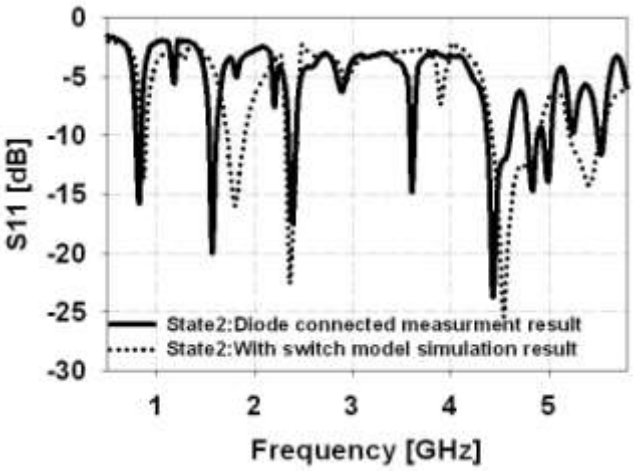

Figure 5.25 Reconfigurable antenna simulation result and measurement result at state 2

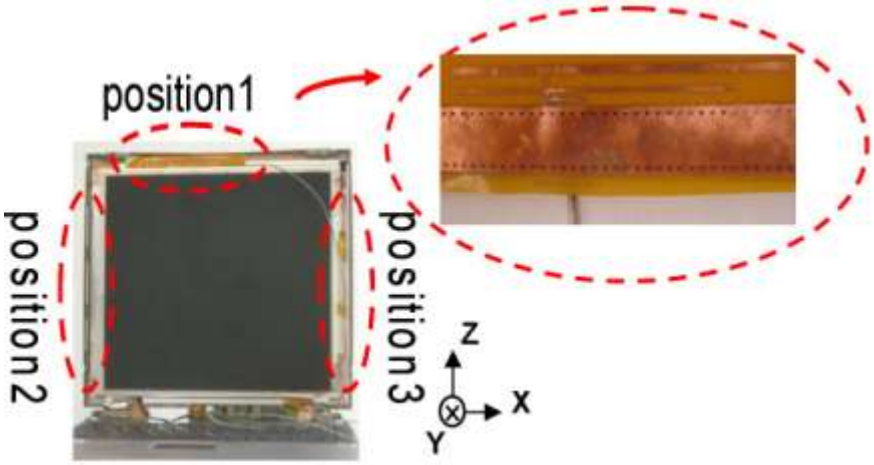

Figure 5.26 Possible antenna positions in laptop (measurement radiation pattern results were measured as position 1)

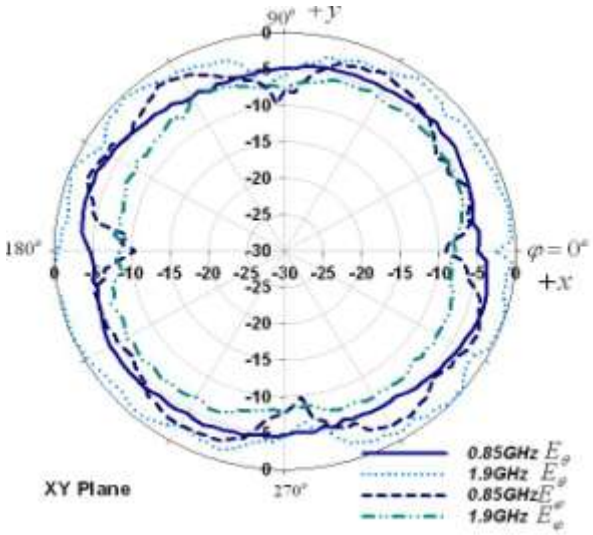

Figure 5.27 State1 XY plane

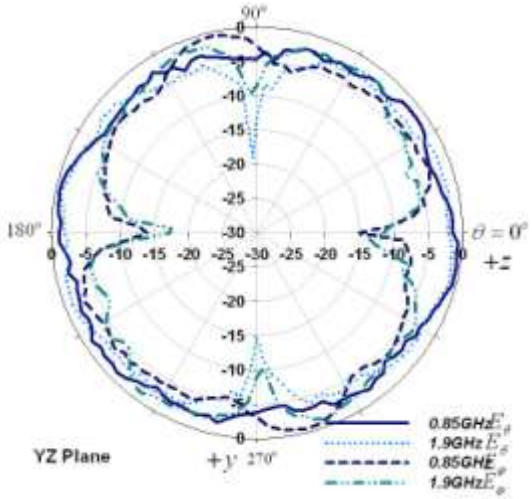

Figure 5.28 State1 YZ plane

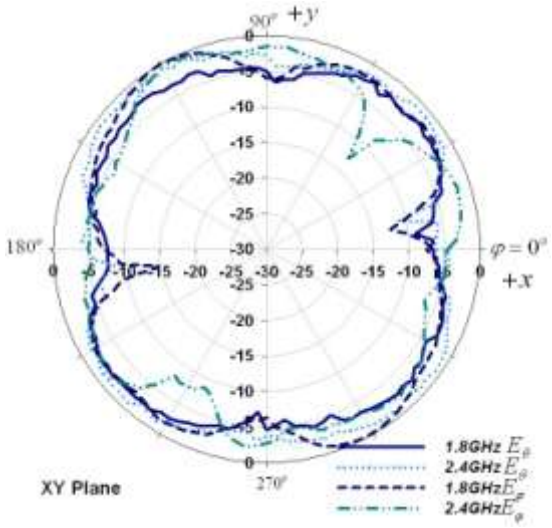

Figure 5.29 State2 XY plane

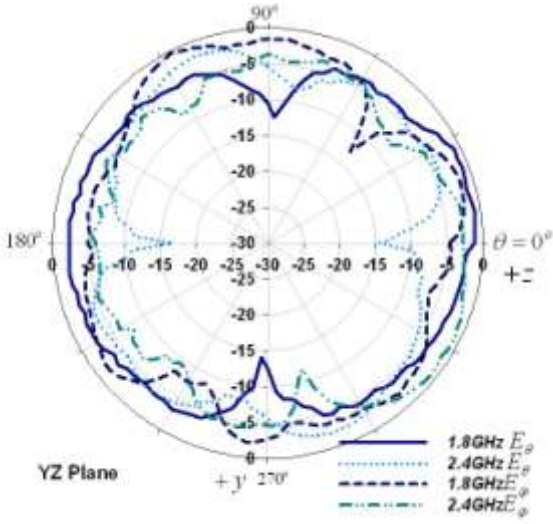

Figure 5.30 State2 YZ plane

5.7.4 Conclusion on the reconfigurable multi-band monopole antenna for multi-service applications

A novel low profile antenna has been developed that is suitable for laptop applications. The developed antenna was designed to operate at six bands, including 800MHz, 900MHz, 1.7GHz, 1.9GHz, 2.4GHz, and 5.2GHz. The developed antenna is already compact, but a further size reduction can be readily achieved upon meandering the monopole arms. A simplified switch implementation has been developed where PIN diodes are directly connected to the RF ground plane. This type of connection avoids the complexity of placing switches with their DC biasing networks and DC grounds close to the radiating elements, which is a common problem in reconfigurable antenna structures. Due to the coupling between the two layers and the interconnectivity between the two layers in both states, it is difficult to design the front and back parts separately. It was essential to go back and forth in the design to obtain the required performance. Measured results are close to our simulated results, even though modeling of this type of structure is more challenging at higher frequencies, i.e. greater than 3 GHz. The effects of using the PIN diodes were minimal on the radiation patterns, but caused a noticeable gain drop.

5.8 Integration of the switches

As already mentioned in section 5.3, one of the primary challenges of the reconfigurable antenna design is to integrate the switches into the antenna structure. Multiple techniques have been used in the reconfigurable patch antenna and monopole antenna designs in section 5.4-5.7 to surmount these challenges:

1) Three-port commercial switches (MESFET switches, MEMS switches) are typically designed for a $50\,\Omega$ system. The way to solve this issue is to choose the proper antenna structures and positions for the switches. For example, in the reconfigurable multi-band monopole antenna, we intentionally created the shorting path parallel and close to the ground, which simplified the switches integration problem.
2) The models of the three-port commercial switches (MESFET switches, MEMS switches), provided by the manufacturers, are S-parameter models tested on a good ground test board. The antenna, however, can not typically provide this type of an environment for the switch. To solve this problem, MEMS switches can be modeled with a 3-D full wave EM simulation tool. A MEMS switch model has been successfully introduced in [64], where the internal switch structure is simplified as a combination of microstrip line, silicon substrate, and bond wires. Ansoft HFSS EM simulation tool was

used [64, 65], and the simulated results of the antenna structure with this model are close to the measured results. For a MESFET switch, lumped elements can be used to synthesize the S-parameters provided by the manufactures. The developed model can simply be integrated into the EM simulation tool as lumped element boundary conditions [6]. Two-port commercial switches (PIN diode switches) can be modeled as a small resistance when the switch is closed and a small capacitor when the switch is open. This lumped model can be simulated as lumped element boundary in the EM simulation tools as well.

3) The DC control lines can affect the antenna's resonance characteristics because of the coupling effect between the antenna and the control line, and the parasitic radiations introduced by the improperly isolated DC lines. One way to decrease the coupling effect is to place the DC control lines vertical to the antenna structure, and also attempt to place the DC control lines and the antenna structure on different layers of the PC board, as described in the reconfigurable patch antenna (Figure 5.8). The other way is to properly employ the antenna structure to decrease the need for extra DC control lines, as we did in the reconfigurable monopole antenna design. Switches are intentionally placed at positions close to the ground. The line antenna (monopole) structure itself can act as a DC line for the antenna. A RF choke was used to input the DC and RF signals. This design totally avoids the DC control line effects on the antenna structure as no extra DC control lines are required in this design.

5.9 Conclusions

Multi-band antennas are currently popular because they are simpler structures and have a better out-of-band noise rejection performance compared to wide band antenna design. However, with the development of modern communication systems, additional services are being added into the system. To maintain a good isolation performance for a system with multi-band antennas, a large number of high Q filters are added. These filters are lossy, bulky, and expensive.

Reconfigurable antennas, as discussed in previous sections, have a much better noise rejection performance in a multi-service system as compared with multi-band antennas; which can decrease the system’s needs for the filters and lead to a good integration and low cost system. However, the requirements for switches, to realize the reconfigurability, increase the design complexity, insertion loss, and DC consumption, making the reconfigurable multi-band antenna a viable choice.

This approach has already attracted manufacturer's attention. Intel Corporation has already developed reconfigurable antenna technology implementation based on our recommendations for an ultra-thin mobile laptop [5]. This is an example that demonstrates reconfigurable antenna integration with multi-radio platform and maximizes the platform advantages. We believe that as many services do not operate at the same time, a reconfigurable /multi-band configuration should be a valuable alternative.

Chapter 6 CONCLUSIONS AND FUTURE WORK

6.1 Dissertation summery

The core of the work presented in this dissertation is the established methodology applicable for the realization of the reconfigurability of the antennas and PA designs for wireless equipments, in particular for the multi-service platform applications for cell phones and laptops.

The reconfigurable antenna can partially realize the filter function in the system, decreasing the requirement for filters in the system. Considering that these filters are lossy, bulky, and expensive, the reconfigurable antenna can help in decreasing the loss, size and cost of the system.

Traditionally, a RF front-end, especially PAs, adopts discrete circuit approach. With the wireless services increasing, many additional circuits have to be integrated into the wireless equipment, which causes the equipment to be bulky and expensive. Moreover, to switch among the different systems, a single-pole-multi-throw switch is needed. However, with the increases in the number of poles, the switch insertion loss will increase dramatically and the isolation will decrease. To maintain a high isolation performance of the system, this means additional filters are needed in the system and further losses will be incurred.

Reconfigurable circuits are a viable way to design an "All-in-One" system. In this work, the reconfigurable antennas and reconfigurable power amplifiers are investigated, designed, and implemented. Key research contributions from this work are summarized here.

The reconfigurable antenna design contributions:

1) Investigated the reconfigurability of the antenna structures for wireless equipments. Defined the class of low profile antennas, especially printed antenna structures with multi-band function, as suitable for reconfigurability. Additionally, the antennas can easily provide a DC control voltage for the switch. Simple methods were identified to minimize feed lines effects on radiation patterns.
2) Validated the noise performance improvement of the reconfigurable antenna structure compared with multi-band antennas. The experiment clearly depicts that the reconfigurable antennas have an acceptable jamming resistance when compared to other alternatives, such as the multi-band antenna structures. Proposed and successfully implemented three different types of reconfigurable antennas: the single service reconfigurable antenna, the mixed services reconfigurable antenna, and the multi-band

reconfigurable.

3) Designed a patch antenna for single and mixed services reconfigurable antennas, targeting cell phone applications. The developed novel patch antenna structure occupies only 25% of the traditional patch antenna size and has successfully demonstrated the potential use of MEMS switches as an integral part of the reconfigurable antenna structures.
4) Designed a very compact planar reconfigurable monopole antenna for multi-band reconfigurable antenna operations, targeting laptop applications. The monopole antenna fits the laptop size requirements for the antennas. The structure itself can provide DC signal paths for the switches' DC control lines. No additional DC control lines are necessary. PIN diodes are integrated into the reconfigurable antenna structures. Such a design was the basic building block for similar antennas adopted by Intel Corporation for slim laptop designs of reconfigurable antennas.

The reconfigurable PA design:

5) Identified the limitations of current wireless power amplifier designs for handheld equipment applications, including the PA design for multi-frequency and multi-mode applications.
6) Proposed and successfully implemented a reconfigurable PA structure for multi-mode multi-band operations.
7) Obtained adequate results for the Low band. High band efficiency results were relatively low. Based on the simulation results, a strategy to improve this performance has also been identified.

6.2 Proposed future work

If this work were to be continued, the following items would be included in the research.

The reconfigurable antenna design:

1) Other switching techniques, such as RFIC switches, should be investigated for the reconfigurable antenna design, including the possibility of exploring the integration of MEMS switches.
2) Developing additional antenna structures which can provide DC signal path for the DC control of the switch should be investigated.

The reconfigurable PA design:

3) Custom-designing the MEMS switch for low impedance design applications. The standard commercial MEMS switches are designed for only a $50\,\Omega$ impedance path, which causes a relatively high insertion loss for low impedance design applications.
4) Design a wide band driver amplifier for the reconfigurable output stages.
5) Investigate PHEMT switching applications for the reconfigurable PA designs.

REFERENCES

1. Berndt, H., *Towards 4G technologies services with initiative*. 2008, Hoboken, NJ: John Wiley & Sons, Ltd.
2. Etoh, M., *Next generation mobile systems 3G and beyond*. 2005, Hoboken: John Wiley & Sons, Ltd.
3. Walsh, K. and J. Johnson. *3G/4G Multimode Cellular Front End Challenges*. Available from: <http://www.mwjournal.com/article.asp?HH_ID=AR_7120>.
4. Teeter, D.A. and E.T. Spears, *RF and Microwave circuits, measurements and modeling*. 2nd ed. 2007, Boca Raton, FL: CRC Press Taylor & Francis Group.
5. Karabuto, A. *Intel Developer Forum 2007*. 2007; Available from: http://ixbtlabs.com/articles2/editorial/idf07pekin-day0a.html.
6. Yang, S., *Antennas and arrays for mobile platforms-Direct broadcast satellite and wireless communication*, in *Electrical Engineering Department*. 2008, University of Tennessee: Knoxville.
7. Boeck, G., et al., *RF front-end technology for reconfigurable mobile systems*, in *SBMO/IEEE MTT-S international microwave and optoelectronics*. 2003: Brazil. p. 863-868.
8. Gupta, R.K., *low power wireless networked system design*. 2003.
9. Eul, H. *Complexity Challenges towards 4th Generation Communication Solutions*.
10. Kim, J.H., Y.K. Jang, and H.J. Yoo, *Design of reconfigurable RF front-end for multi-standard receiver using switchable passive networks.* Analog integrated circuits and Signal Processing, 2007. **50**(2): p. 81-88.
11. Crols, J. and M. Steyaert, *CMOS wireless transceiver design*. 1997, Norwell, MA Kluwer academic publishers.
12. Cipriani, S., et al., *Fully integrated zero IF transceiver for GPRS/GSM/DCS/PCS application*, in *Solid-State Circuits Conference (ESSCIRC 2002) Proceedings of the 28th* 2002: Florence, Italy.
13. Agnelli, F., et al., *Wireless multi-standard terminals: system analysis and design of a reconfigurable RF front-end*, in *IEEE circuits and systems magazine*. 2006. p. 38-59.
14. Hong, E.-P., D.-J. Kim, and H.-J. Yoo, *A reconfigurable CMOS low noise amplifier for wireless LAN applications*, in *ITC-CSCC*. 2008: Japan.
15. Yang, Y.-C., et al., *Reconfigurable SiGe low noise amplifiers with variable miller capacitance.* IEEE transactions on circuit and systems, 2006. **53**(12): p. 2567-2577.
16. Mukhopadhyay, R., et al., *Reconfigurable RFICs in Si-Based Technologies for a Compact Intelligent RF Front-End.* IEEE Transactions on Microwave Theory and Techniques 2005. **53**(1): p. 81-93.
17. Han, Y., et al., *Toward multi-service wireless universal receiver*, in *URSI national radio science*. 2005: Boulder, Colorado.
18. Han, Y., *Towards a universal multi-standard RF receiver*, in *Electrical engineering* 2006, University of Tennessee: Knoxville.
19. *HMC284MS8G data sheet*. Available from: http://www.datasheetcatalog.org/datasheet/hittite/HMC284MS8G.pdf.
20. *HMC241LP3 data sheet*. Available from: http://www.hittite.com/content/documents/data_sheet/hmc241lp3.pdf.
21. *HMC252QS24 data sheet*. Available from: http://www.hittite.com/content/documents/data_sheet/hmc252qs24.pdf.
22. *HMC253LC4 data sheet*. Available from: http://www.hittite.com/content/documents/data_sheet/hmc253lc4.pdf.
23. Barlett, J.L., et al., *Integrated tunable high efficiency power amplifier*, U.s. patent, Editor. 2001.

24. Fukuda, A., et al., *A 900/1500/2000-MHz triple-band reconfigurable power amplifier employing RF-MEMS switches*, in *IEEE MTT-S internal microwave symposium*. 2005: Long beach, CA, USA. p. 12-17.
25. Graauw, A.J.M.d., et al., *MEMS based reconfigurable multi-band BiCMOS power amplifier*, in *IEEE Bipolar/BiCMOS circuits and technology*. 2006: Maastricht, the Netherlands.
26. Zhang, H., H. Gao, and G. Li, *Broad-band power amplifier with a novel tunable output matching network.* IEEE Transactions Microwave Theory and Technique, 2005. **53**(11): p. 3606-3614.
27. Radmanesh, M.M., *Radio frequency and microwave electronics*. 2001, Delhi: Addison Wesley Longman (Singapore) Pte. Ltd., Indian Branch.
28. Ye, F., et al., *Dynamic bias circuits for efficiency improvement of RF power amplifier*. Tamkang journal of science and engineering, 2004. **7**(3): p. 183-188.
29. Lin, S., *Passive and active components development for broadband applications*, in *Electrical Engineering department*. 2009, University of Tennessee: Knoxville.
30. Zhang, C. and A.E. Fathy, *A novel reconfigurable power amplifier structure for multi-band and multi-mode portable wireless applications using a reconfigurable die and a switchable output matching network*, in *2009 International microwave symposium*. 2009: Boston, USA.
31. Cripps, S.C., *RF power amplifiers for wireless communications*. 2 ed. 2006, Boston: Artech Hourse.
32. Technologies, A. *Advanced design system*. Available from: http://www.home.agilent.com/agilent/product.jspx?nid=-34346.0.00&cc=US&lc=eng.
33. *Radant MEMS RMSW 100 Data sheet*. Available from: http://www.radantmems.com/radantmems/products.html.
34. Narayanswami, R.S., *RF CMOS class C power amplifiers for Wireless communications*, in *Electrical Enginneering* 2001, University of California, Berkeley: Berkeley.
35. Razavi, B., *Design of analog CMOS integrated circuits*. 2001, Singapore: McGRAW-HILL internation edition.
36. Boesch, D. and K.P. Conroy, *Impedance matching circuit for power amplifier*, U.S. patent, Editor. 1999.
37. Zhang, Z., J.C. Langer, and K. Li, ***Nine-Band Cell Phone Stubby Antenna***, in *IEEE Antennas and Propagation Society International Symposium 2006*. 2006: Albrquerque, new mexcio p. 2645-2648.
38. de Leon, L.P., J.-O. Mattsson, and C. Kinezos, *Ultra Wide Band Antenna for a Multimode Cellular Phone*, in *IEEE Antennas and Propagation Society International Symposium, 2007* 2007: Honolulu, Hawaii. p. 4141-4143.
39. Kim, M., et al., *A Design of Wide Band Small Chip Antenna Using The Branch Structure for Mobile Phone*, in *Asia-Pacific Microwave Conference* 2006: yokohama, Japan. p. 1604-1610.
40. Wong, K.-L., L.-C. Chou, and H.-T. Chen, *Ultra-wideband metal-plate monopole antenna for laptop application.* Microwave and optical technology letters, 2004. **43**(5): p. 384-386.
41. Pazin, L., N. Telzhensky, and Y. Leviatan, *wideband flat-plate inverted-F laptop antenna for Wi-Fi/WiMAX operation.* IET Microwaves, Antennas & Propagation, 2008. **2**(6): p. 568-573.
42. Jeon, S.G., D.H. Seo, and J.H. Choi, *Design of an internal widebadn antenna for DTV laptop application*, in *Progress In Electromagnetics Research Symposium*. 2007: Prague, Czech Republic.

43. Wong, K.-L., *Planar antennas for wireless communications*. 2003, New Jersey: John Wiley & Sons, Inc.
44. Liu, Z.D., P.S. Hall, and D. Wake, *Dual-frequency planar inverted F antenna.* IEEE Trans. Antenna Propagation, 1997. **45**: p. 1451-1458.
45. **Qi, D., B. Li,** and **H. Liu,** *compact triple-band planar inverted-F antenna for mobile handsets.* Microwave and optical technology letters, 2004. **41**(6): p. 483-486.
46. Zhang, C., et al., *A Reconfigurable Multi-Band Patch Antenna for Wireless Applications Using MEMS Switches.* Microwave and optical technology letters (to be published).
47. xiao, S., B.Z. Wang, and X.S. Yang, *A Novel Frequency- Reconfigurable Patch Antenna.* Microwave and optical technology letters, 2003. **36**(4): p. 295-297.
48. A.H.M.Alam, N.B.M. Sahar, and N.B. Zamani, *Design of MEMS Based Triple Band Reconfigurable Antenna*, in *Information & Communications Technology (ICICT)*. 2006: cairo.
49. Byun, S.B., et al., *Reconfigurable Ground-Slotted Patch Antenna using PIN diode switching.* ETRL Journal, 2007. **29**(6).
50. Shynu, S.V., et al.; Available from: http://www.ursi.org/Proceedings/ProcGA05/pdf/B04P.10(0571).pdf.
51. Lee, J.A., et al., *Reconfigurable Antenna for Wideband Code Division Multiple Access and Korean Satellite Digital Multimedia Broadcasting Controlled by Pin-Diodes.* Microwave and optical technology letters, 2007. **49**(6): p. 1334-1337.
52. Topalli, K., E. Erdil, and O.A. Civi. ***Reconfigurable antenna structures using MEMS technology***. Available from: http://www.ursi.org/Proceedings/ProcGA05/pdf/B04P.20(0210).pdf.
53. Ricky Chair, et al., *Miniature wideband half U-Slot and Half E-Shaped patch antennas.* IEEE Transactions on Antennas and Propagations, 2005. **53**(8): p. 2645-2652.
54. Balanis, C.A., *Antenna theory analysis and design*. 2 ed. 1997, New York: John Wiley & Sons, Inc.
55. Kraus, J.D. and R.J. Marhefka, *Antennas for all applications*. 3 ed. 2004, New Delhi: Tata McGraw-Hill publishing company limited.
56. Yang, S., et al., *Frequency-reconfigurable antennas for multiradio wireless platforms.* IEEE Microwave Magazine, 2009. **10**(1): p. 66-83.
57. Rosu, I. *PIFA-Planar Inverted F Antenna*. Available from: http://www.qsl.net/va3iul/Antenna/PIFA/PIFA_Planar_Inverted_F_Antenna.pdf.
58. Huynh, T. and K.F. Lee, *Single layer single patch wideband microstrip antenna.* Electron Letter, 1995. **31**(16): p. 1310-1312.
59. Dalia M. Nashaat, Hala A. Elsadek, and H. Ghali, *Single feed compact quad-band PIFA antenna for wireless communication applications.* IEEE Transactions on Antennas and Propagations, 2005. **53**(8): p. 2631-2635.
60. Zhang, C., et al., *A low profile branched monopole laptop reconfigurable multi-band antenna for wireless applications.* IEEE antennas and wireless propagation letters to be published.
61. C. M. Su, W. S. Chen, and K.L. Wong, *Metal-plate shorted T-shaped monopole for internal laptop antenna for 2.4/5 GHz WLAN operation*, in *IEEE APS international symposium and USNC/URSI national radio science meeting*. 2004: Monterey, CA.
62. A. Rennings, et al., *A dual-layer printed antenna system for DCS/PCS/UMTS*, in *European microwave conference*. 2004: Amsterdam, The Netherlands. p. 1294-1252.
63. *MPP4201-4204, MPL4700 Monolithic microwave surface mount micro-pak PIN diodes*. Available from: http://www.datasheetcatalog.org/datasheet/microsemi/MSC1361.pdf.

64. Daly, M.P. and J.T. bERNHARD, *RF MEMS switch model for reconfigurable antenna design*, in *IEEE antennas and propagation society international symposium*. 2008: San Diego, CA. p. 1-4.
65. *HFSS*. Available from: http://www.ansoft.com/.
66. Hicks, R.F.; Available from: http://www.seas.ucla.edu/prosurf/images/hbt.jpg.
67. Ali, F. and A. Gupta, *HEMTs and HBTs: Devices, Fabrication, and Circuits*. 1991, Boston, USA: Artech House.
68. *MMIC semiconductor tradeoffs*. Available from: http://www.microwaves101.com/encyclopedia/MMICsemi.cfm.
69. Garlapati, A., et al., *A model for multi-finger HBTs including current gain collapse effect.* Solid State Electronics, 2003. **47**(11): p. 1983-1987.
70. Hajji, R. and F.M. Ghannouchi, *Small-signal distributed model for GaAs HBT's and S-parameter prediction at Millimeter-Wave Frequencies.* IEEE Transactions on Electron Devices, 1997. **44**(5): p. 723-732.
71. Noh, Y.S., T.W. Lee, and C.S. Park, *linearized high efficiency HBT power amplifier module for L-band application.* IEEE Microwave and Guided Wave letters, 1994. **4**(3): p. 65-67.

APPENDICES

Appendix A

GaAs HBT process overview

GaAs HBT (heterojunction bipolar transistor) devices have excellent linearity performance and high power density, which leads to a reduced die size. An example of HBT device grown on GaAs substrate is shown in Figure 1 [66].

The ease in manufacturing along with a good RF performance has made the GaAs HBT a popular choice for wireless handset equipments power amplifiers. Table 1 shows a comparison between GaAs HBT devices and some other major RF/Microwave device processes [67, 68].

The transistor cell small signal model

Because of unevenly distributed heat, use of a big device always leads to a lower efficiency. Therefore, a few small size HBT transistors (cells) are connected in parallel to obtain a given required power level.

The small signal lumped parameter RF model of a transistor cell can be described in Figure 2 [69, 70]. The values of the lumped components can be derived based on the large signal S-parameters of the transistor cells, which is provided by foundry. For example, Table 2 lists the values of the lumped element components of a transistor cell which was used in this work

The bench test setup, which is used to extract the lumped element HBT model using the large signal S-parameters, is shown in Figure 3. The Measure_TB in Figure 3 uses the model shown in Figure 4. The Modeled_TB in Figure 3 uses the model shown in Figure 5. Results have been compared in Figure 6. As can be seen, a good agreement has been achieved.

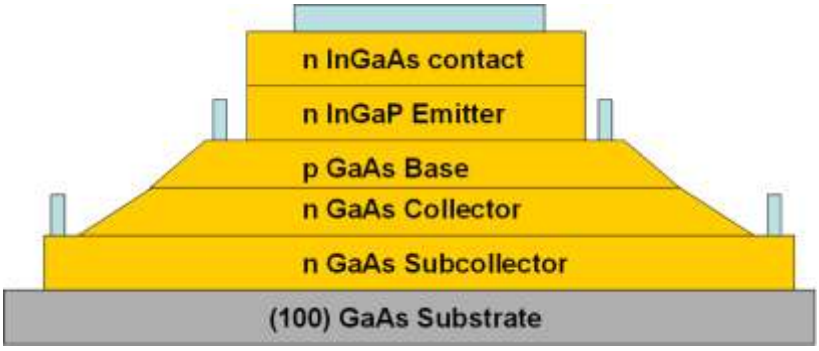

Figure 1 A HBT device grown on GaAs substrate [66]

Table 1 A comparison of different processes [67, 68]

	Advantages	Disadvantages
GaAs HBT	Use a single power supply; used for higher speed compared to MESFET; fabricated using all optical process, which means low cost; high current density; good linearity	Thermal management; reverse isolation is not as high as with PHEMT amplifiers
SiGe HBT	Low cost, easily integrated with digital circuits	Low breakdown voltage; SI substrate is lossy; high setup charges due to expensive mask set. Poorer noise and power performance compared to GaAs device
GaAs MESFET	Classical fabrication technique, low cost, high break down voltage	Typically use both positive and negative voltages; have poorer noise and power performance compared to GaAs HBTs; complicated techniques for higher frequency application
CMOS	Low cost, high integration	SI substrate is lossy, poorer RF performance; low break down voltage, which means poorer power performance

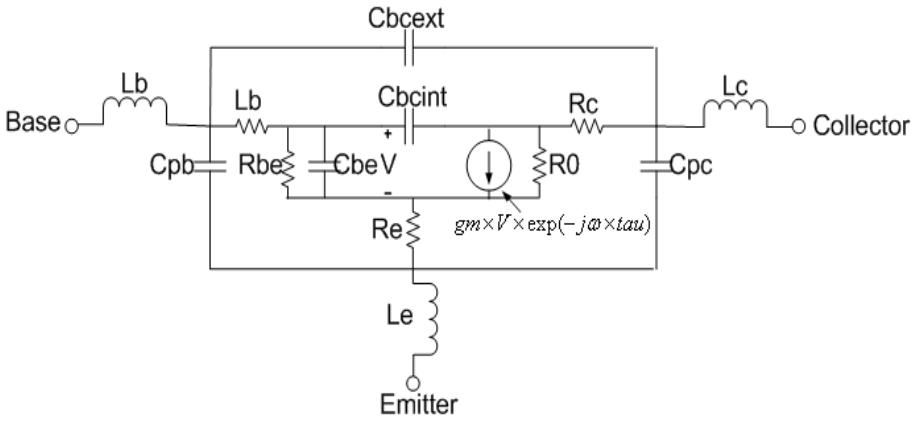

Figure 2 Electrical equivalent circuit of the HBT lumped model [69, 70]

Table 2 The parameters values for the lumped element equivalent circuit of the HBT model

Parameter	Value	Parameter	Value	Parameter	Value
Lb	0.0197 nH	Lc	0.4089 nH	Le	0.0549 nH
Cpb	4.974 pF	Cpc	0.0526 pF	Rb	2.202 Ohm
Rc	29.984 Ohm	Re	1.535 Ohm	R0	3 MOhm
Rbe	30.287 Ohm	Cbe	1.026 pF	Cbcint	0.116 pF
Cbcext	0.01 pF	gm	64.23 S	tau	1.788 pS

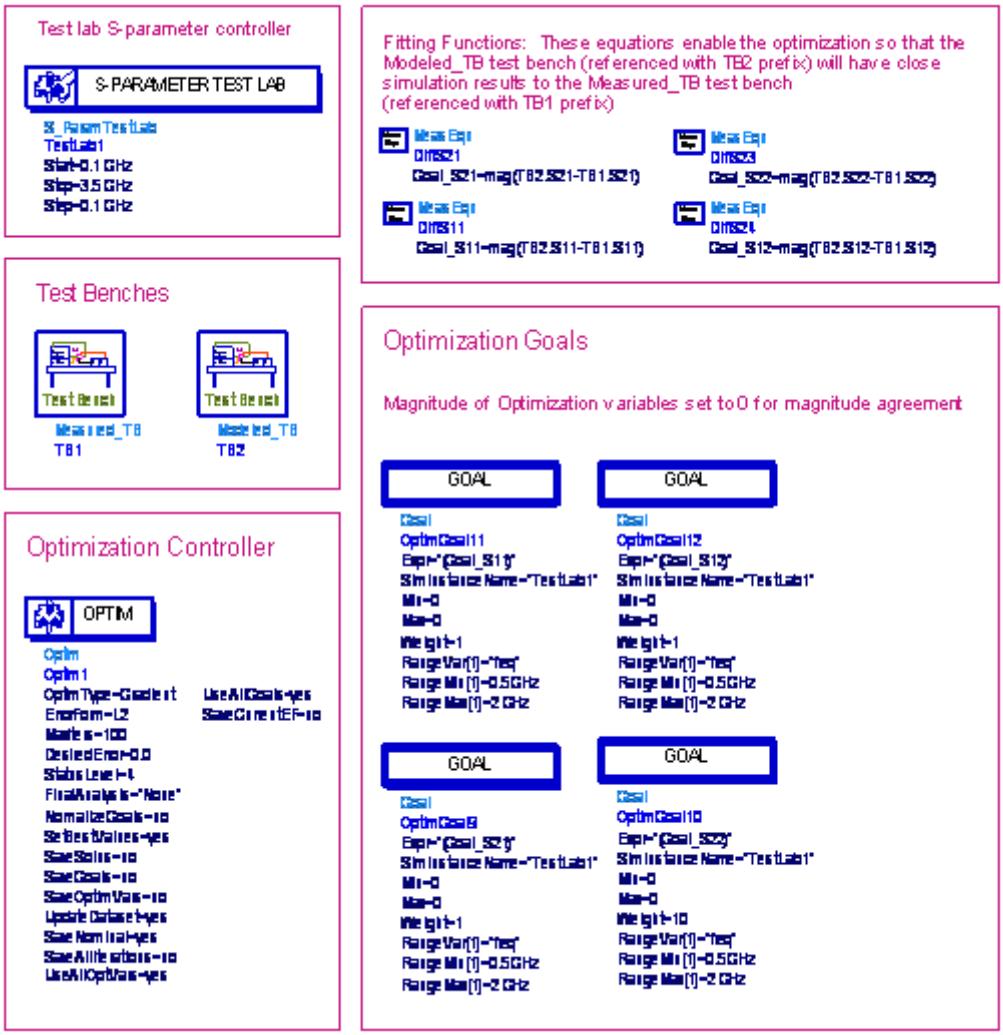

Figure 3 Lumped element components value extraction bench top level setup

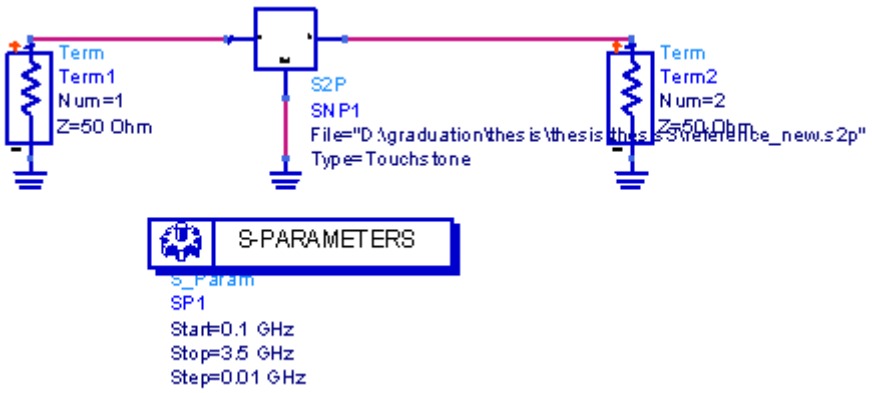

Figure 1 Measured_TB bench setup

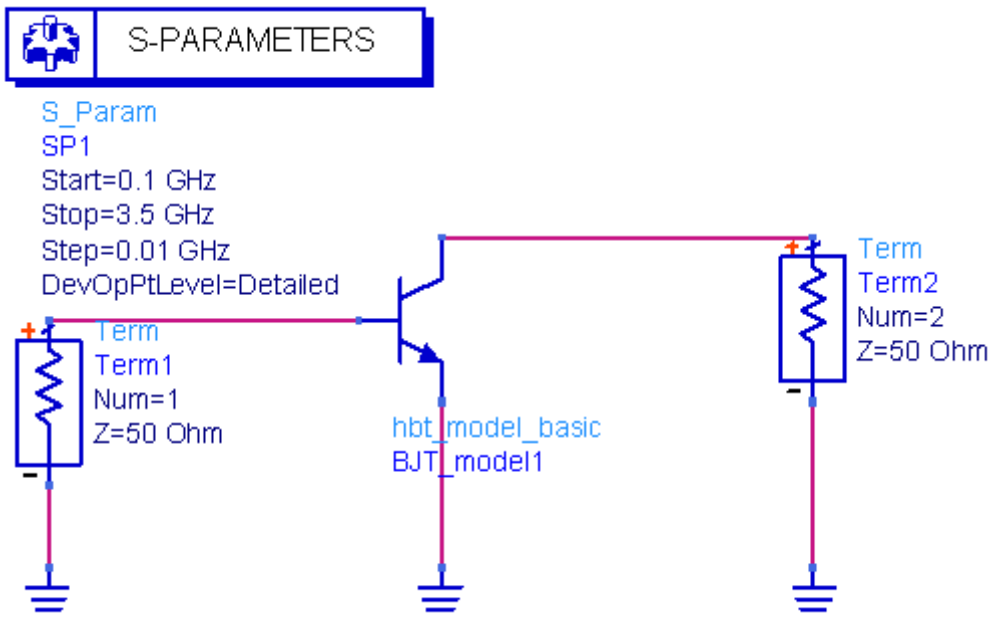

Figure 5 Modeled_TB bench setup

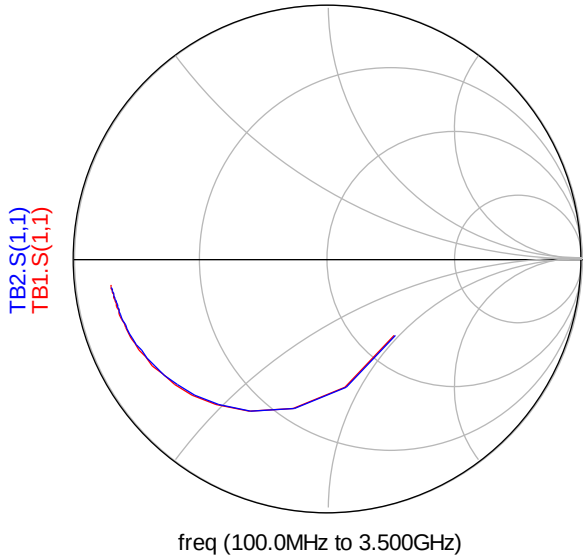

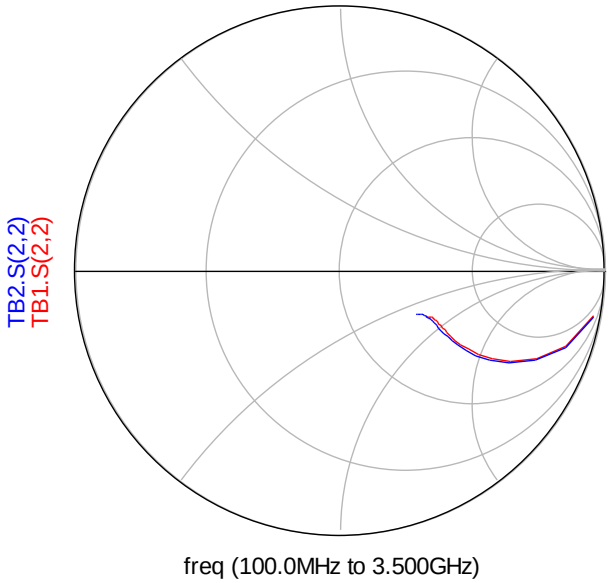
TB2.S(2,2)
TB1.S(2,2)
freq (100.0MHz to 3.500GHz)

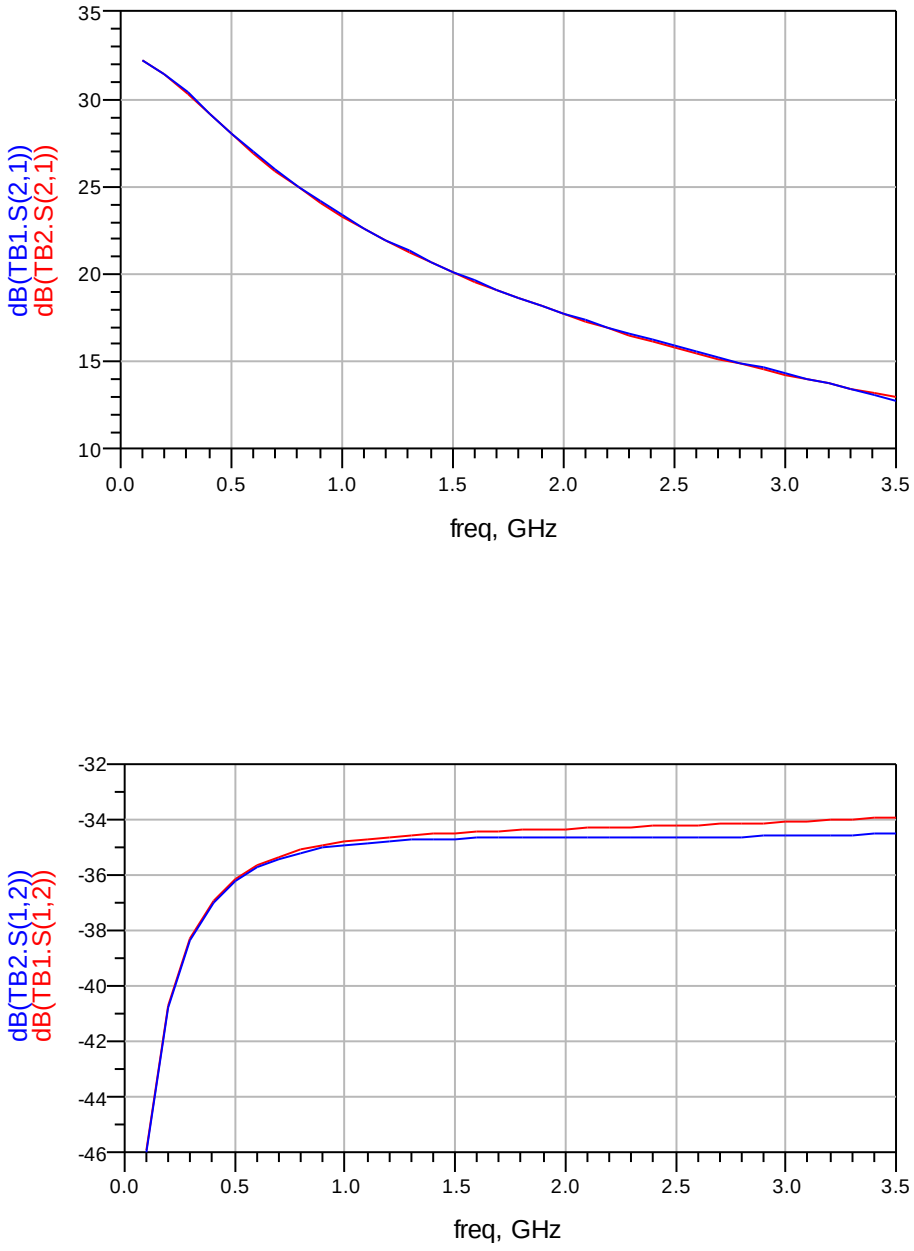

Figure 6 S-parameter comparison between large signal S-parameter of the transistor cell and the lumped model of the transistor cell

Appendix B

Current mirror design

Current mirror is typically used in a PA bias network design. A simple analysis of the current mirror performance will be shown here, and in depth discussion of current mirrors can be found in many introductory analog circuit design textbooks [35].

Figure 1 shows a schematic of the DC circuit for a simple current mirror. If we suppose $\beta = \infty$,

$$I_{cc} = \frac{A_2}{A_1} I_{reg} \qquad \text{Equation 1}$$

$$I_{reg} = \frac{V_{reg} - V_{th}}{R_{bias}}$$	Equation 2

Where A_1 is the area of the reference device and A_2 is the area of the power transistor to be biased, V_{be} is the thermal voltage, V_{reg} and I_{reg} are voltage and current in the reference path.

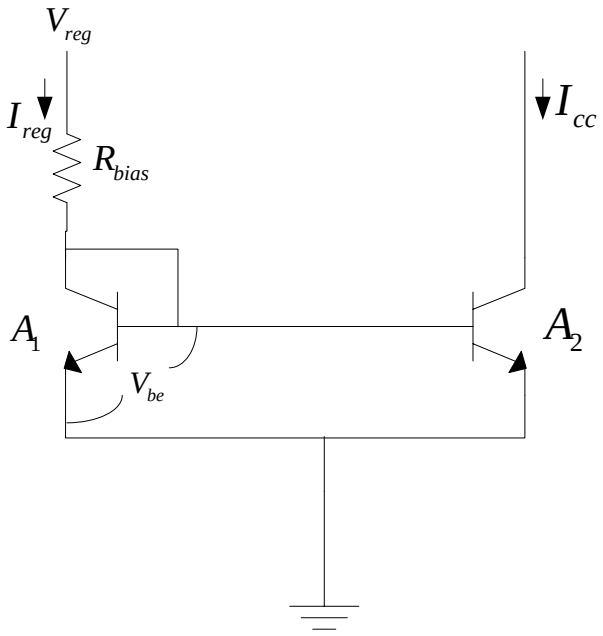

Figure 1 An example of a basic current mirror

Although this basic current mirror can be found in the wireless device designs, cascade current mirror, as shown in Figure 2, are more widely used [4, 71]. The additional of the emitter follower requires an extra V_{be} drop.

$$I_{reg} = \frac{V_{reg} - 2V_{be}}{R_{bias}} \qquad \text{Equation 3}$$

And

$$I_{cc} = \frac{A_2}{A_1} I_{reg} \qquad \text{Equation 4}$$

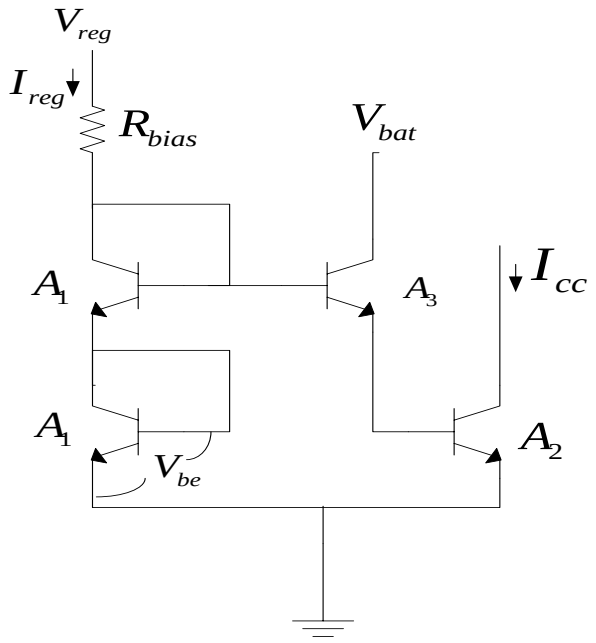

Figure 2 An example of current mirror with an addition emitter follower

VITA

Chunna Zhang started her Ph. D studies in University of Tennessee, Knoxville in August 2004. Her research interest includes Reconfigurable Power Amplifier design for multi-service wireless equipments, MMIC design, microwave circuit design and reconfigurable antenna design. She finished her Ph. D education in August 2009.